Pardee Reservoir

Pardee Outlet Tower Seismic Evaluation

September 2013

EAST BAY MUNICIPAL UTILITY DISTRICT

Prepared by:

JACOBS ASSOCIATES
Engineers/Consultants

Jacobs Associates
49 Stevenson Street, 3rd Floor
San Francisco, CA 94105

amec

AMEC Environment & Infrastructure, Inc.
2101 Webster Street, 12th Floor
Oakland, CA 94612

QuestStructures

Quest Structures, Inc.
3 Altarinda Road, Suite 203
Orinda, CA 94563

Distribution

To:	Bilgin Atalay East Bay Municipal Utility District 375 Eleventh Street Oakland, CA 94607
From:	Jan Van Greunen, PhD, PE Jacobs Associates
Prepared By:	Jan Van Greunen, PhD, PE Jacobs Associates
	Marc Ryan, PE AMEC Environment & Infrastructure, Inc.
	Todd Crampton, CEG AMEC Environment & Infrastructure, Inc.
	Yusof Ghanaat, PhD, PE Quest Structures, Inc.
Reviewed By:	Michael McRae, DEng, PE, GE Jacobs Associates

Table of Contents

List of Figures

List of Appendices

Executive Summary

This report summarizes the findings of a seismic evaluation performed for the Pardee Outlet Tower subjected to the maximum design earthquake (MDE) ground motion. The MDE was selected by East Bay Municipal Utility District (EBMUD) and approved by the Federal Energy Regulatory Commission (FERC) as a ground motion with a return period of 2,475 years (2% probability of exceedance in 50 years), and having a mean horizontal peak ground acceleration of 0.15g. The seismic evaluation employed finite-element analysis using the response-spectrum mode-superposition method, available facility and material parameters based on as-built drawings and visual inspection, as well as parameter sensitivity with respect to material properties and modeling assumptions.

The Pardee Outlet Tower is a lightly reinforced concrete cylindrical structure built in 1929 with a 19-foot inside diameter and wall thicknesses varying from 1.5 feet at the top to 4.5 feet at the bottom. The tower shaft is approximately 200 feet tall, with 70 feet of its height embedded in rock below the base of the approach channel excavation. A four-span, three-pier truss bridge provides access to a circular gate lift house built atop the tower. The tower can draw water from various levels and transfer it to the tunnel that ties into the base of the tower. There are four levels of inlets above and one at the tunnel elevation.

The tower was modeled as a series of equivalent beam elements distributed from top to bottom with nodal points chosen at elevations of steel reinforcement changes. The embedment in rock was represented by equivalent lateral spring supports. The inside and outside water inertia forces due to earthquake excitation were modeled as additional masses lumped at the submerged nodal points. The seismic response of the tower was evaluated by subjecting the tower to the two horizontal components of the earthquake ground motion. The effect of vertical ground motion was considered to be negligible and was ignored. The model was analyzed for a base condition that incorporated our best estimate of material properties (base model) as well as other cases to assess sensitivity of the results to the concrete strength, cracked section properties, and stiffness magnitude and distribution of the foundation spring supports.

The results for the base model with 5,000-psi concrete and uncracked section properties indicate that the EM 1110-2-2400 (USACE, 2003) acceptance criteria for moment and shear demand capacity ratios (DCRs) and brittle failure modes are satisfied. The moment DCRs do not exceed 2, while shear DCRs remain less than 1 except at one location within the rock embedment. However, sensitivity analyses indicate that the actual shear demand at this location is expected to be lower than that obtained from the base model for the following reasons:

- The use of cracked section properties reduces seismic moment and shear demands.
- Reducing the foundation spring spacing to simulate continuous support decreases the maximum shear and moment demands.
- Reducing the magnitude of the spring constants to account for rock fractures near the surface further decreases shear demands. This also increases moment demands within the embedded region, but it is not a problem since moments in this region are small.

For the above reasons, the actual maximum shear demands are expected to be less than the shear capacity, and additionally, the maximum shear demand occurs at a section where the tower is fully supported by the surrounding rock. Consequently, the use of a moment reduction factor of 2 is fully justified. Further, all other brittle failure modes were also checked and found to meet the EM 1110-2-2400 (USACE, 2003)

requirements. Only the nominal to cracking moment ratios of the tower do not meet the criteria, but the follow-up displacement-based analysis indicates that the tower meets the required deformation capacity.

Therefore, it is concluded that the seismic performance of the tower for the postulated ground motion would be satisfactory and the tower is not subject to collapse under the design ground motions. Concrete cracking and steel yielding could be expected at one or more locations, but reinforcing steel would remain intact and the overall stability of the tower would be maintained. If concrete cracking and steel yielding are concentrated at a single location, it could result in minor permanent tilting of the tower. It is believed such tilting would not be large enough to impede operation of the tower. However, repair and strengthening of the tower may be required to maintain its long-term functionality if the tower experiences a design level event and if a permanent deformation is observed.

1 Introduction

Jacobs Associates was retained by East Bay Municipal Utility District (EBMUD) to perform a seismic evaluation of the Pardee Reservoir's Outlet Tower. The team included AMEC Environment & Infrastructure Inc. and Quest Structures Inc. The first phase of the work consisted of assessing the existing tower and foundation conditions, establishing the level of seismic hazard, and then analyzing the tower's seismic performance when subject to the design event. If the tower was found to be in need of retrofit, the second phase of the work would consist of developing conceptual retrofit alternatives, including construction cost estimates. This report presents the background information, analysis results, and conclusions of this seismic evaluation. Because the tower performance was deemed satisfactory no retrofit alternatives were developed.

AMEC performed a review of the geotechnical conditions at the tower based on the existing information available for the Pardee Reservoir area as summarized in Technical Memorandum No. 1, attached as Appendix A. AMEC also performed a seismic hazard analysis, summarized in Technical Memorandum No. 4, attached as Appendix B. Jacobs Associates and Quest Structures reviewed available historical documentation, including the original as-built drawings, construction photographs, and the preliminary seismic analysis and structural design reports prepared in 1987 and 1998 (Dames and Moore, 1987; HDR, 1998). In addition, Jacobs Associates and Mead & Hunt performed a visual and remote operated vehicle (ROV) inspection of the inside and all accessible areas of the outside of the tower as documented in the Pardee Outlet Tower Condition Assessment Report (Jacobs Associates, 2013). Quest Structures used the information gathered to perform a detail evaluation of the seismic performance of the Outlet Tower, as presented in their seismic structural evaluation report, attached as Appendix C.

2 Tower Description

The Pardee Dam and Reservoir are located on the Mokelumne River in the foothills of the Sierra Nevada Mountains, near the town of Valley Springs in Calaveras County, California. Water is diverted from the Pardee Reservoir through the Pardee Outlet Tower and Tunnel. The Pardee Outlet Tower and tunnel are located about 0.75 mile southeast of Pardee Dam. The dam was completed in 1929, and the tunnel and Outlet Tower were constructed during the same time period. The relationship of the dam, the reservoir, and the outlet tower is shown in Figure 1. Photographs of the Outlet Tower are shown in Figures 2 and 3.

The Outlet Tower is located along the reservoir's western shore, approximately 840 feet from the tunnel's eastern portal. The Outlet Tower is 226 feet tall from its foundation at approximately El. 380 feet to the top of the gate house at El. 606 feet. The tower is a partially submerged reinforced concrete structure which is accessed from the shoreline by a footbridge.

The 317-foot-long footbridge connects the tower's operating floor (the gate lift house floor) at El. 585 feet, with the shoreline. The bridge, approximately 5 feet wide, consists of four spans supported by intermediate piers. The span closest to the shore consists of a reinforced concrete deck about 46 feet long. The three other spans are steel trusses, each about 90 feet long. The pier closest to the shore is reinforced concrete, while the two other piers are of steel construction.

The Outlet Tower shaft extends from approximately El. 380 feet to El. 583 feet, and supports the gate lift house. The tower shaft is surrounded by rock below El. 479 feet and is freestanding from El. 479 to El. 583 feet.

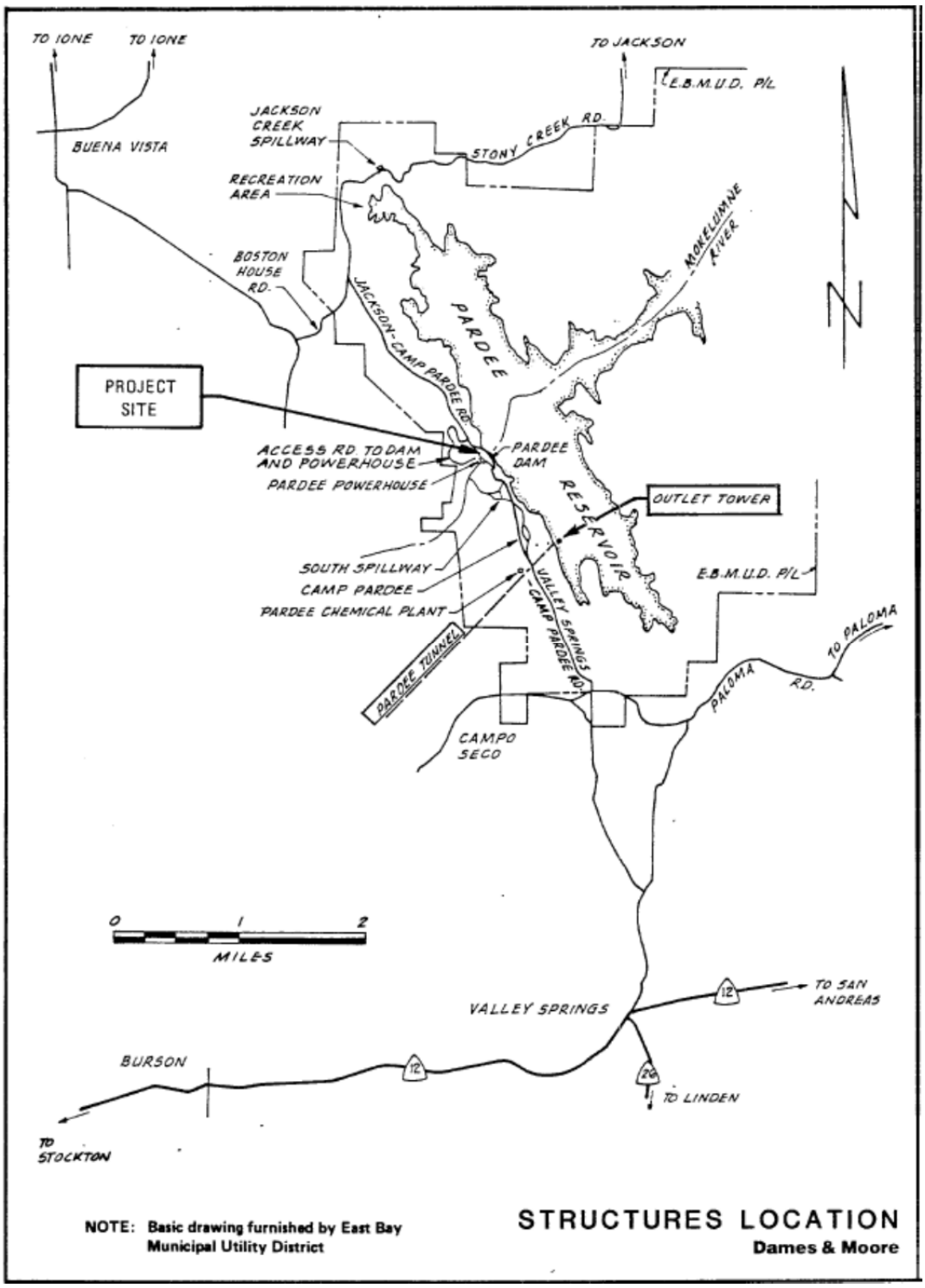

Figure 1. Location of Pardee Dam

Figure 2. Outlet Structure during a Drought

Figure 3. Outlet Structure with Normal Reservoir Level

3 Evaluation of Geologic/Geotechnical Conditions

AMEC reviewed the available geologic and geotechnical information of the Pardee Reservoir and surrounding area, as summarized in Technical Memorandum No. 1 and attached as Appendix A. AMEC also provided recommendations for the stiffness of the rock springs at the tower base to serve as input for the Outlet Tower analysis as documented in the report.

4 Tower Material Properties

The shaft is circular in cross section, and its overall diameter varies from a maximum of 28 feet at the bottom to 23 feet immediately below the gate lift house. The inside diameter of the tower shaft is constant at 19 feet. The shaft wall thickness is 54 inches from the base to El. 421 feet and then tapers from 48 inches at El. 421 feet to 18 inches at the gate lift house floor. The 30-foot inside diameter gate lift house consists of a 12-inch-thick operating floor with 12-inch-thick walls. The tower is embedded below the base of the reservoir from about El. 479 feet with an intake structure in the form of a screening chamber extending down to El. 450 feet (see Figures 1-2, 1-3, and 2-1 in Appendix C). The tower shaft includes four levels of 30- by 36-inch inlets, with centerline elevations of 550, 520, 490, and 460 feet, respectively.

There are three inlet openings per level, regularly distributed around the shaft perimeter. The gate lift house has nine windows and one door.

The interior and exterior surfaces of the Outlet Tower were visually inspected during the site visit on June 19, 2012. A walk-around was performed to assess the condition of the tower gate lift house and the interior and exterior walls above the water line. In addition, an assessment of the Outlet Tower and screening chamber below the water line was conducted using an ROV on November 28, 2012, as described in the Pardee Outlet Tower Condition Assessment Report (Jacobs Associates, 2013).

Both the Outlet Tower and the screening chamber appear to be in excellent condition. The visual inspections did not identify any visible indicators of concrete deterioration, efflorescence, or reinforcement corrosion. There were no signs of structural distress or cracking on the observed surfaces of concrete. Hairline cracks were observed at construction joints between concrete pours. All mechanical and structural anchorages to the concrete walls were intact and showed no signs of wear or corrosion.

The following structural and mechanical features were not inspected:

- The tower's gate lift house roof
- The access bridge truss and its supports

The available information regarding the tower material properties and the values assumed for the seismic analysis are summarized in Section 2 of the Quest Structures Final Report, attached as Appendix C.

5 Earthquake Hazard Assessment

AMEC performed a site-specific ground motion study to assess the deterministic and probabilistic seismic hazard for future earthquakes in the region. This hazard analysis is documented in Technical Memorandum No. 4 and attached as Appendix B.

The deterministic median peak ground acceleration (PGA) for the moment magnitude, M_W 6.4 earthquake on the Waters Peak fault (which is the controlling deterministic event) is estimated to be 0.43g. The probabilistic site hazard analysis resulted in a PGA of 0.15g for an approximately 2,500 year return period event. Because the tower is 0.75 mile away from the dam, it is not essential for dam safety, and the reservoir level is controlled by the outlet works at the dam, EBMUD informed FERC that it was planning to use the lower probabilistic ground motion PGA of 0.15g for evaluation of the tower in a letter dated September 19, 2012. FERC confirmed its acceptance of this approach in its response dated March 18, 2013.

6 Tower Seismic Structural Analysis

Quest Structures modeled the Pardee Outlet Tower using the geometry presented in the as-built drawings for the recommended probabilistic seismic PGA of 0.15g. The tower was modeled as a series of equivalent beam elements distributed from top to bottom with nodal points chosen at elevations of steel reinforcement changes. The embedment in rock was represented by equivalent lateral spring supports.

The inside and outside water inertia forces due to earthquake excitation were modeled as additional masses lumped at the submerged nodal points. The seismic response of the tower was evaluated by subjecting the tower to the two horizontal components of the earthquake ground motion. The effect of vertical ground motion was considered to be negligible and was ignored. The model was analyzed for a base condition that incorporated our best estimate of material properties (base model) as well as other cases to assess sensitivity of the results to the concrete strength, cracked section properties, and stiffness magnitude and distribution of the foundation spring supports.

The detailed discussion of its analysis and the results are documented in the Quest structural seismic evaluation report, attached as Appendix C.

7 Conclusions

Overall, the Pardee Reservoir Outlet Tower appears to be in good condition. The visual inspection of the Outlet Tower and inlet channel on November 28, 2012 (Jacobs Associates, 2013) did not identify any major structural or mechanical deficiencies affecting the outlet's continued reliability.

The results for the base model with 5,000-psi concrete and uncracked section properties indicate that the EM 1110-2-2400 (USACE, 2003) acceptance criteria for moment and shear DCRs and brittle failure modes are satisfied. The moment DCRs do not exceed 2, while shear DCRs remain less than 1 except at one location within the rock embedment. However, sensitivity analyses indicate that the actual shear demand at this location is expected to be lower than that obtained from the base model for the following reasons:

- The use of cracked section properties reduces seismic moment and shear demands.
- Reducing the foundation spring spacing to simulate continuous support decreases the maximum shear and moment demands.
- Reducing the magnitude of the spring constants to account for rock fractures near the surface further decreases shear demands. This also increases moment demands within the embedded region, but it is not a problem since moments in this region are small.

For the above reasons, the actual maximum shear demands are expected to be less than the shear capacity, and additionally, the maximum shear demand occurs at a section where the tower is fully supported by the surrounding rock. Consequently, the use of a moment reduction factor of 2 is fully justified. Further, all other brittle failure modes were also checked and found to meet the EM 1110-2-2400 (USACE, 2003) requirements. Only the nominal to cracking moment ratios of the tower do not meet the criteria, but the follow-up displacement-based analysis indicates that the tower meets the required deformation capacity.

Therefore, it is concluded that the seismic performance of the tower for the postulated ground motion would be satisfactory and the tower is not subject to collapse under the design ground motions. Concrete cracking and steel yielding could be expected at one or more locations, but reinforcing steel would remain intact and the overall stability of the tower would be maintained. If concrete cracking and steel yielding are concentrated at a single location, it could result in minor permanent tilting of the tower. It is believed such tilting would not be large enough to impede operation of the tower. However, repair and strengthening of the tower may be required to maintain its long-term functionality if the tower experiences a design level event and if a permanent deformation is observed.

8 References

Dames and Moore. 1987. Final Report Preliminary Seismic Evaluation Pardee Outlet Tower and Tunnel. San Francisco, CA.

EBMUD letter to FERC, dated September 11, 2012.

FERC letter to EBMUD, dated March 18, 2013.

HDR. 1998. Pardee Reservoir Raised Intake Tower Preliminary Seismic Analysis & Structural Design. Vol. 14. Oakland, CA.

Jacobs Associates. 2013. Pardee Outlet Tower Condition Assessment. Prepared for EBMUD.

US Army Corps of Engineers (USACE). 2003. *Engineering and Design—Structural Design and Evaluation of Outlet Works. EM 1110-2-2400*. Washington, DC: Department of the Army.

9 Revision Log

Revision No.	Date	Revision Description
0	September 3, 2013	Draft Issued for Review and Comment
1	September 12, 2013	Final Report

Appendix A

Technical Memorandum No. 1: Summary of Geologic/ Geotechnical Site Conditions and Recommendations for Foundation Properties and Rock Springs

AMEC Environment & Infrastructure Inc., August 2012

Technical Memorandum No. 1

To:	Bilgin Atalay, East Bay Municipal Utility District	Project:	OD12163180
From:	Todd Crampton and Marc Ryan	cc:	Jan Van Greunen, PE Jacobs Associates
Tel:	(510) 663-4100		
Fax:	(510) 663-4141		
Date:	August 7, 2012		

Subject: Summary of Geologic/Geotechnical Site Conditions and Recommendations for Foundation Properties and Rock Springs
Pardee Reservoir Outlet Tower Evaluation
Calaveras County, California

This Technical Memorandum (TM) summarizes relevant existing geologic and geotechnical information that was reviewed by AMEC Environment & Infrastructure, Inc. (AMEC) as part of the Pardee Reservoir Outlet Tower project (Project). This TM also provides a geological characterization of the outlet tower site based on the review of existing information, and provides recommendations for the foundation properties and for horizontal and vertical rock springs, to be used by the Project team in the outlet tower seismic evaluation.

SOURCES OF EXISTING INFORMATION

Existing reports and drawings related to the Pardee Reservoir Outlet Tower, Pardee Dam, and Pardee Spillway were obtained from Mr. Bilgin Atalay, Project Manager for the East Bay Municipal Utility District (EBMUD). AMEC reviewed these reports to identify the information relevant to characterizing the geologic and geotechnical conditions at the Outlet Tower site. In addition, AMEC reviewed available published geologic maps of the Project area and participated in a site visit with members of the Project team. A complete list of the references used to prepare this TM is provided in References section.

GEOLOGIC AND GEOTECHNICAL SITE CONDITIONS

Pardee Reservoir is in the western foothills of the Sierra Nevada, within a northwest-trending belt of metamorphic rocks known as the foothills metamorphic belt, or the western metamorphic belt. This metamorphic belt consists of several distinct, northwest-trending fault-bounded bands of Mesozoic and Paleozoic metamorphic rocks that extend for over 240 miles along the western foothills of the north-central Sierra Nevada. In the vicinity of Pardee Dam and the outlet tower, these rocks consist of the Jurassic-age Gopher Ridge Volcanics and Salt Springs Slate. The Salt Springs Slate stratigraphically overlies and interfingers with the Gopher Ridge Volcanics. On a regional scale, the volcanics typically form resistant ridges with the weaker, interbedded slates forming narrow valleys throughout the foothills. Locally (at the outcrop scale), thin (≤ 50 feet thick) beds of slate occur within the metavolcanic rocks.

AMEC Environment & Infrastructure, Inc.
2101 Webster Street, 12th Floor
Oakland, California 94612-3066
USA
Tel (510) 663-4100
Fax (510) 663-4141
amec.com

The available information indicates the dam and spillway are directly underlain by metavolcanic rocks of the Gopher Ridge Volcanics, whereas the outlet tower is founded in Salt Springs Slate. Both of these formations have a pervasive foliation that strikes northwest and dips moderately to steeply to the east. The existing geologic mapping of the dam, spillway, and outlet tower area shows the Gopher Ridge Volcanics form an approximately 1,400-foot-wide, northwest-trending band that is bounded on both the east and west by metasedimentary rocks of the Salt Springs Slate. The western contact between these formations is marked by the Waters Peak fault, approximately 1,600 feet southwest of the outlet tower. The conformable (i.e., non-faulted) eastern contact is mapped within about 400 feet southwest of the outlet tower, generally near the western shoreline of Pardee Reservoir.

The geologic and geotechnical characteristics of the Salt Springs Slate have been documented from geologic mapping of outcrops near the dam and spillway; however, little subsurface information for this formation exists, primarily because the dam and spillway are founded on the Gopher Ridge Volcanics. The Salt Springs Slate is described primarily as sericite (micaceous) slate with a black color resulting from abundant organic material. The formation also contains lesser amounts of metagraywacke (sandstone), metavolcaniclastic, and metaconglomerate, the latter of which contains beds of small, well-rounded pebbles. As previously mentioned, the slate has a pervasive metamorphic foliation and typically is thinly bedded and laminated. The rock breaks readily along cleavage (foliation) planes that typically are 0.1 to 0.2 foot apart. Geologic mapping of the Gopher Ridge Volcanics and Salt Springs Slate near the outlet tower indicates the average foliation in this vicinity strikes about N19°W and dips 62° to the east. Numerous joints that cross-cut the foliation also have been mapped in the vicinity of the outlet tower. These measurements suggest an approximately east-west-striking joint set, with steep dips to both the north and south. Other randomly oriented joints occur in this area as well.

Few exploratory borings in the vicinity of the outlet tower have encountered the Salt Springs Slate. One boring near the left abutment of Pardee Dam encountered a thin slate bed within the Gopher Ridge Volcanics from a depth of about 51 to 58 feet. The slate was described as closely fractured, hard, and strong to very strong. Several borings at the Jackson Creek Dam site, located near the northern end of Pardee Reservoir about 2 miles north of the outlet tower, encountered Salt Springs Slate. These borings indicate that weathering typically extends to depths ranging from about 12 to 50 feet. Fractures that cross cut the metamorphic foliation are often healed with quartz, or coated with iron oxide.

Laboratory tests performed on selected rock core samples of the Salt Springs Slate indicate the unconfined compressive strength ranges from about 375 psi to 8,310 psi, and averages about 3,080 psi (7 samples). As a comparison, unconfined compressive strength tests performed on rock core samples of the Gopher Ridge Volcanics range from about 450 psi to 14,600 psi and average about 7,645 psi (15 samples).

Downhole P- and S-wave measurements have been obtained from three borings at the Pardee Dam site, all within the Gopher Ridge Volcanics. There are no such measurements for the Salt Springs Slate. Based on the existing measurements, the shear wave velocity of the Gopher

Ridge Volcanics increases with depth and ranges from about 1220 feet per second (fps) to 9510 fps, and averages about 4288 fps over a total depth of about 127 feet.

RECOMMENDED FOUNDATION PROPERTIES

It is our understanding that the structural evaluation of the tower requires the initial shear wave velocity, shear modulus, bulk modulus, unit weight, and Poison's ratio for the foundation rock. As discussed above, no direct measurements of the shear wave velocity are available for the Salt Springs Slate. In lieu of these data, the shear wave velocity was estimated assuming the shear modulus values of the formations are directly correlated with the unconfined compressive strengths. The average unconfined compressive strength, and therefore the shear modulus, of the Salt Springs Slate is about 40 percent of that of the Gopher Ridge Volcanics; therefore the shear wave velocity of the Salt Springs Slate is about 65 percent of the shear wave velocity of the Gopher Ridge Volcanics. The recommended geotechnical properties for the Salt Springs Slate are:

Shear Wave Velocity	2,800 fps
Shear Modulus	3.41×10^7 psf
Bulk Modulus	1.59×10^8 psf
Unit Weight	140 pcf
Poisson's Ratio	0.40

Using these properties and a closed-form solution developed by Novak et al (1978), frequency-dependent values of the lateral and vertical foundation springs were computed as shown in Table 1. The closed-form solution provides complex stiffness functions per unit length for an embedded cylinder with a radius of 13 ft. The stiffness per unit length was obtained at a range of frequencies from 0.10 to 100 Hz. These stiffness values can be multiplied by the tributary area of each foundation node to obtain the spring constant at that location.

LIMITATIONS

The information summarized in this letter report is based on a review of available data and information, and a limited field reconnaissance. No subsurface exploration or laboratory testing was performed for this study. The information summarized in this report is intended only for Jacobs Associates' usage to support the Pardee Outlet Tower Project. Unanticipated site conditions, which cannot be disclosed fully by limited field reconnaissance and data review, are commonly encountered and frequently require additional expenditures and effort to attain a properly designed and constructed project.

In the performance of its professional services, AMEC, its employees, and its agents comply with the standards of care and skill ordinarily exercised by members of our profession practicing in the same or similar localities. No warranty, either express or implied, is made or intended in connection with the work performed by us, or by the proposal for consulting or other services, or by the furnishing of oral or written reports or findings. In the event conclusions based on these

data are made by others, such conclusions are not our responsibility unless we have been given an opportunity to review and concur with such conclusions in writing.

CLOSURE

AMEC appreciates this opportunity to work with Jacobs Associates on this project. Please contact either of the undersigned if you have any questions about this letter report or if we can be of further service.

Sincerely yours,
AMEC Environment & Infrastructure, Inc.

Todd Crampton, CEG
Senior Geologist
Direct Tel.: (510) 663-4272
E-mail: todd.crampton@amec.com

Marc Ryan, PE (CA)
Principal Engineer
Direct Tel.: (510) 663-4207
E-mail: marc.ryan@amec.com

tac/mjr/ldu
\\Oad-fs1\doc_safe\16300s\163180\3000\Pardee Tower Tech Memo No. 1\1 txt\Pardee_Tower Tech Memo No. 1__Rev_1.docx

Attachments: References
Table 1 – Rock Spring Values for Seismic Evaluation

REFERENCES

REFERENCES

BCA Geophysics, Inc., 1991, Geophysical Surveys Performed at Pardee Dam, California: unpublished consulting report prepared for Geo/Resource Consultants and Dames & Moore, January 1991.

Dames & Moore, 1987, Preliminary Seismic Evaluation, Pardee Outlet Tower and Tunnel: unpublished consulting report prepared for East Bay Municipal Utility District, June 1992.

Earth Sciences Associates and Geo/Resource Consultants, 1992, Raised Pardee Dam Additional Storage Alternative Geotechnical Investigation (Volumes 1 through 4): unpublished consulting report prepared for East Bay Municipal Utility District, June 1992.

HCG, 1998, Pardee Reservoir Enlargement Project, Preliminary Design Report, Volume 4, Conceptual Design Report: unpublished consulting report prepared for East Bay Municipal Utility District, June 1988.

HCG, 1998, Pardee Reservoir Enlargement Project, Preliminary Design Report, Volume 9, Jackson Creek Saddle Dams Site Geology and Geotechnical Report: unpublished consulting report prepared for East Bay Municipal Utility District, June 1988.

HCG, 1998, Pardee Reservoir Enlargement Project, Preliminary Design Report, Volume 10, Downstream Dam Site Geology and Geotechnical Report: unpublished consulting report prepared for East Bay Municipal Utility District, June 1988.

Novak, M., Nogami, T., Aboul-Ella, F., 1978, Dynamic Soil Reaction for Plane Strain Case, Journal of Engineering Mechanics Division, Vol. 104, No. EM4, August 1978.

Portola Geophysics, 1991, Geophysical Investigation, Pardee Dam Raise, Amador County, California: unpublished consulting report prepared for Earth Sciences Associates, March 1991.

Woodward-Clyde Consultants, 1993, Geotechnical Report, Jackson Creek Spillway, Pardee Dam, Amador County, California: unpublished consulting report prepared for East Bay Municipal Utility District, January 1993.

Woodward-Clyde Consultants, 1993, Geotechnical Report, South Spillway, Pardee Dam, Amador County, California: unpublished consulting report prepared for East Bay Municipal Utility District, March 1993.

Woodward-Clyde Consultants, 1988, Pardee Dam South Spillway Geological Investigation: unpublished consulting report prepared for East Bay Municipal Utility District, February 1988.

TABLE

TABLE 1

ROCK SPRING VALUES FOR SEISMIC EVALUATION

Pardee Reservoir Outlet Tower
Amador County, California

1a. Frequency-Dependant Lateral Soil Springs

Frequency (hz)	K*= Re(K*) + i·Im(K*)	
	Re(K*)	Im(K*)
	(kips/ft/ft)	(kips/ft/ft)
99.99	136643	1084711
33.32	136643	359501
19.98	136643	229672
14.29	133216	175739
11.11	128990	145493
10.01	126997	135007
3.33	103546	67435
1.99	93492	51475
1.44	87786	44091
1.10	83349	39004
0.99	81825	37372
0.34	67821	24713
0.21	62478	20814
0.14	58746	18347
0.10	56335	16858

1b. Frequency-Dependant Vertical Soil Springs

Frequency (hz)	K*= Re(K*) + i·Im(K*)	
	Re(K*)	Im(K*)
	(kips/ft/ft)	(kips/ft/ft)
99.99	91420	637005
33.32	91420	227665
19.98	86423	146917
14.29	82199	112365
11.11	78747	92812
10.01	77287	86015
3.33	62167	42257
1.99	56010	32019
1.44	52535	27311
1.10	49838	24082
0.99	48912	23049
0.34	40419	15087
0.21	37186	12658
0.14	34930	11127
0.10	33475	10206

Appendix B

Technical Memorandum No. 4: Earthquake Ground Motion Assessment

AMEC Environment & Infrastructure, Inc., August 2012

Technical Memorandum No. 4

To:	Bilgin Atalay, East Bay Municipal Utility District	Project:	OD12163180
From:	Debra Gilkerson and Marc Ryan	cc:	Jan Van Gruenen, PE Jacobs Associates
Tel:	(510) 663-4100		
Fax:	(510) 663-4141		
Date:	August 27, 2012		

Subject: Earthquake Ground Motion Assessment
Pardee Reservoir Outlet Tower Evaluation
Calaveras County, California

This Technical Memorandum (TM) summarizes a ground motion study performed by AMEC Environment & Infrastructure, Inc. (AMEC) as part of the Pardee Reservoir Outlet Tower project (Project). The primary objective of this assessment is to characterize the site-specific probabilistic and deterministic ground motion hazard for possible future earthquakes in the region, represented in terms of peak horizontal ground acceleration and response spectral ordinates.

TECTONIC AND SEISMIC SETTING

The site (Figure 1) is located within the Sierra Nevada (or Sierran) Microplate, a westward-tilted, relatively rigid crustal block that includes the Sierra Nevada Range and the crust beneath the adjacent Sacramento and San Joaquin valleys to the west. The microplate is bounded to the west by faults of the San Andreas fault system, and to the east by the Walker Lane Belt, which makes up the western part of the Basin and Range Province. Motion of the Sierran Microplate relative to surrounding tectonic provinces is accommodated primarily by active faulting and deformation around its margins, which are characterized by moderate to high levels of seismic activity. The interior of the Sierran Microplate, on the other hand, is a region of low historical seismicity. Deformation within the interior of the microplate generally is attributed to reactivation of optimally oriented sections of the Sierra Nevada Foothills fault system, an ancient Mesozoic subduction zone. Late Cenozoic deformation rates of these structures are very low, ranging from about 0.001 to 0.01 mm/yr.

GEOLOGIC SETTING

Pardee Reservoir is in the western foothills of the Sierra Nevada, within a northwest-trending belt of metamorphic rocks known as the foothills metamorphic belt, or the western metamorphic belt. This metamorphic belt consists of several distinct, northwest-trending fault-bounded bands of Mesozoic and Paleozoic metamorphic rocks that extend for over 240 miles along the western foothills of the north-central Sierra Nevada. The Foothills fault system typically juxtaposes the different metamorphic terrains in the region, and several Quaternary-active faults of the Foothills fault system are mapped near the site (Figure 2).

AMEC Environment & Infrastructure, Inc.
2101 Webster Street, 12th Floor
Oakland, California 94612-3066
USA
Tel (510) 663-4100
Fax (510) 663-4141
amec.com

In the vicinity of Pardee Dam and the outlet tower, the metamorphic bedrock consists of the Jurassic-age Gopher Ridge Volcanics and Salt Springs Slate. Available information indicates the dam and spillway are directly underlain by metavolcanic rocks of the Gopher Ridge Volcanics, whereas the outlet tower is founded in Salt Springs Slate. Both of these formations have a pervasive foliation that strikes northwest and dips moderately to steeply to the east (subparallel to the Foothills fault system). The existing geologic mapping of the dam, spillway, and outlet tower area shows the Gopher Ridge Volcanics form an approximately 1,400-foot-wide, northwest-trending band that is bounded on both the east and west by metasedimentary rocks of the Salt Springs Slate. The western contact between these formations is marked by the Waters Peak fault, approximately 1,600 feet southwest of the outlet tower. The conformable (i.e., non-faulted) eastern contact is mapped within about 400 feet southwest of the outlet tower, generally near the western shoreline of Pardee Reservoir.

For a more complete description of the geologic setting of the site, refer to Technical Memorandum No. 1 (AMEC, 2012).

GROUND MOTION HAZARD ANALYSIS

The ground motion hazard assessment included probabilistic and deterministic seismic hazard analysis (PSHA and DSHA, respectively) to characterize earthquake ground shaking that may occur at the site during future seismic events in the region. The PSHA was conducted to estimate the probability of exceedance of peak horizontal ground acceleration (PGA) and response spectral accelerations (Sa) at the site. Median deterministic ground motions were also estimated for maximum credible earthquakes on the significant fault sources contributing to the ground motion hazard at the site.

Seismic Source Characterization

The Foothills fault system can be modeled as either individual faults sources, or as areal source zones (not associated with specific faults) that account for the overall seismicity of the region with gridded seismicity data. This study modeled the Foothills fault system as an areal source zone in the PSHA, and as individual fault sources in the DSHA.

The seismic source model used for the PSHA study was obtained from the fault source documentation for the USGS National Seismic Hazard Mapping Program (Petersen et al., 2008). This source model uses gridded seismicity to model the Foothills fault system, and individual fault sources to model the larger, more active faults of the Bay Area (San Andreas, Calaveras, and Hayward faults). The USGS Quaternary fault and fold database (http://earthquake.usgs.gov/hazards/qfaults/) was used as a basis for developing the National Seismic Hazard Map faults. This latter database is the most comprehensive source of information on Quaternary (past 1.6 million years) faulting for the region.

The fault source parameters used for this study are based on a review of existing reports and information, including Pacific Gas and Electric Company (PG&E, 2007), Petersen et al. (2008), and HCG (1998). The assessment of maximum magnitudes and earthquake recurrence rates for the sources, as applicable, are described below.

Areal Source Zones

The Foothills fault system was modeled as an areal source zone in the PSHA. The areal source zone is used to model all of the known and postulated seismic sources within the fault zone by using gridded seismicity values to estimate the seismic hazard. The Foothills fault system is modeled as having a maximum magnitude of 7.6 (Petersen et al., 2008).

Fault Sources

All of the identified local faults in the vicinity of the Pardee Tower are part of the Foothills fault system (Figure 2). The local faults were not included as sources in the PSHA, but were used in the DSHA. The closest Quaternary fault to the project site is the Waters Peak fault, a normal-oblique fault located approximately 0.5 km west of the site that is reported to be capable of earthquakes as large as magnitude 6.4 (HCG, 1998). A summary of the other local fault sources used in the DSHA are shown in Table 1.

Other larger and distant fault sources located west of the site (e.g. San Andreas, Calaveras, and Hayward faults), were included in both the PSHA and DSHA. These faults are typically better characterized and have higher slip rates and shorter recurrence intervals. As an example, the parameters for the San Andreas fault are included in Table 1.

Table 1 – Fault Source Parameters

Fault Name	Type	Dip	Distance (km)	M_{max}	Slip-rate (mm/yr)
Waters Peak[1]	Normal-Oblique	75	0.5	6.4	0.02
Ione[1]	Normal-Oblique	75	1.9	6.4	0.03
Youngs Creek[2]	Normal-Oblique	75	3.7	6.5	0.0003 to 0.0015
San Andreas[3]	Strike-Slip	90	155	8.0	24

1. Slip type, Mmax, and slip rate from HCG (1998).
2. Slip type, Mmax, and slip rate from PG&E (2007).
3. Slip type, Mmax, and slip rate from Petersen et al. (2008).

Attenuation Relationships

Attenuation relationships appropriate for ground motions produced by crustal seismic sources were selected and used in the PSHA and DSHA. For all of the seismic sources, the Next Generation Attenuation (NGA) models were used to determine the ground motion hazard at the project site. The five NGA models for the randomly-oriented average horizontal component of ground motions are those of Abrahamson and Silva (2008), Boore and Atkinson (2008), Campbell and Bozorgnia (2008), Chiou and Youngs (2008), and Idriss (2008).

Deterministic Ground Motions

Median deterministic ground motions were estimated for the fault sources using the NGA attenuations described above. Based on AMEC (2012), Pardee Tower is founded in the Salt Springs Slate with an average shear wave velocity in the upper 30 meters (V_{S30}) of 2,800 fps (860 m/s). The average PGA and spectral accelerations were calculated using an equal weight for each of the five attenuation relationships and a V_{S30} of 2,800 fps (860 m/s) . The average median PGA and spectral acceleration (S_a) at 20 spectral periods for the faults in Table 1 are shown on Figure 3. As shown on Figure 3, the median PGA for the moment magnitude, M_w 6.4 earthquake on the Waters Peak fault (which is the controlling deterministic event) is estimated to be approximately 0.43g.

Probabilistic Ground Motions

A probabilistic seismic hazard analysis (PSHA) was also performed for the project site. The PSHA was performed using the commercially available program EZ-FRISK™ 7.62 (Risk Engineering, 2011). The PSHA is based on an assessment of the recurrence of earthquakes on potential seismic sources in the region of the project site. The PSHA was performed using the same attenuation relationships that were used for the deterministic evaluation described above. Results of the PSHA are expressed in terms of the relationship between amplitude of peak ground acceleration or spectral acceleration, and the associated annual rate of recurrence or return period.

The seismic source model used in the PSHA included the areal source zones and active fault sources from Petersen et al. (2008). The analysis included all fault sources within 200 km of the project site and gridded background seismic sources used to capture the background seismicity (Petersen et al., 2008).

The results of the PSHA showing the mean uniform hazard response spectra (UHRS) for the horizontal component of ground motions are presented on Figure 4 along with the controlling deterministic scenario event for the local source, and a scenario for a large magnitude event on the distant San Andreas fault. The UHRS for return periods 975, 2,475 and 9,975 years are shown on Figure 4. As shown on Figure 4, for a return period of about 2,500 years (approximately 2% probability of exceedance [P_E] in 50 years) the PGA is estimated to be 0.14g. The PSHA results were checked using the USGS website. The PGA for a 2,475 year return period using the USGS website was also 0.14g.

Recommended Ground Motions for Analysis

As shown on Figure 4, the median deterministic response spectrum for the local Waters Peak fault is significantly higher than the 2,500 year UHRS below a period of 2 seconds, but the two are similar above 2 seconds. This is because the low slip rate (<0.01 mm/yr) of the local faults are associated with a long recurrence interval for large earthquakes. At periods above 2 seconds, the UHRS has more contribution from the larger magnitude San Andreas fault which has a much higher slip rate (~24 mm/yr), and therefore a much shorter recurrence interval for large earthquakes.

The Pardee Outlet tower is located several kilometers from the Pardee Dam site and is founded about 85 feet into bedrock. The tower operates as one of two intakes for releasing water from Pardee reservoir. The other outlet is through the low-level outlet at the dam site. Based on discussions with EBMUD and the project team, the tower is not considered a critical structure relative to dam safety, because it is not part of a high-hazard project (i.e. it is not located at the dam site) and failure of the tower would not result in loss of life, only in operational constraints. For these reasons, we recommend that the Maximum Design Earthquake (MDE) generally be based on the level of ground motion with a 2 percent chance of exceedance in 50 years (or a return period of about 2,500 years). However, because the PGA associated with the 2,500 year return period is only 0.14g, we recommend scaling up the UHRS slightly to a PGA of 0.15g to be consistent with the California Department of Water Resources, Division of Safety of Dams (DSOD) minimum PGA of 0.15g for seismic environments similar to that of the Pardee Reservoir Outlet Tower.

Because of its close proximity to the Foothills fault system, ground motions at the tower caused by earthquakes occurring on this source could exhibit two kinds of near-fault effects (at periods longer than 0.5 second). For fault rupture propagating towards the site, the first effect, termed the forward directivity, produces a large velocity pulse at the beginning of strong shaking and a resulting enhancement of the long-period horizontal spectral accelerations. However, for fault ruptures propagating away from the site, a de-amplification of long-period spectral acceleration is expected.

It is not clear at present whether these directivity effects are adequately accounted for in current empirical attenuation relationships. This study assumed that directivity effects are not adequately included in current empirical attenuation relationships, and the relationship developed by Spudich and Chiou (2008) were used to account for such effects. Spudich and Chiou (2008) present period-dependant modification factors that were applied to the scaled UHRS.

The second near-field effect, called the fault-normal/fault-parallel effect, produces unequal long-period (> 0.5 second) spectral accelerations between the two horizontal components. Empirical observations, as well as theoretical considerations, suggest that in the near-field of an earthquake rupture (as is potentially the case for the site), longer-period ground motion amplitudes (e.g., > 0.5-second-period response spectral ordinates, and peak ground velocity) tend to be systematically stronger in the direction normal to the fault strike than in the direction parallel to the fault (as shown by Somerville et al., 1997). At short periods of vibration (i.e., <0.5 second and including peak ground acceleration), there is no systematic tendency for one horizontal component to be stronger than the other. Accordingly, using procedures developed by Somerville et al. (1997) and Abrahamson (2000), adjustments to average horizontal-component spectra were made to increase response spectral values at longer periods for the fault-normal direction.

For normal-oblique faults, the DSOD (Fraser and Howard, 2002) suggests that the percentage of fault length that ruptures towards the site be taken as 85 percent of the total fault rupture, when considering modification to the fault-normal (FN) component of ground motion. The guidelines also suggest that the standard response spectra be used to represent the fault-parallel (FP) component. These guidelines were followed in developing the fault-normal and fault-parallel components in this study.

The recommended FN and FP spectra for the tower were developed by considering the near-field directivity effects and the fault-normal/fault-parallel effects. The FN component of the target spectra includes the directivity effects of Spudich and Chiou (2008), and the fault-normal factors from Somerville et al., (1997), as modified by Abrahamson (2000). The FP component was assumed to be the scaled UHRS. The recommended spectra (FN and FP) for the tower evaluation are shown on Figure 5, along with the median deterministic spectrum for the Waters Peak fault. It is noted that the median deterministic spectrum shown does not include directivity and is analogous to the FP component of the UHRS. If the deterministic results were to be used as the basis for the recommended spectra, they would also have to be factored up to account for directivity.

The PGA and spectral values for the recommended horizontal MDE are presented in Table 2.

LIMITATIONS

The information summarized in this letter report is based on a review of available data and information. No subsurface exploration or laboratory testing was performed for this study. The information summarized in this report is intended only for East Bay Municipal Utility District's and Jacobs Associates' usage to support the Pardee Outlet Tower Project. Unanticipated site conditions, which cannot be disclosed fully by limited field reconnaissance and data review, are commonly encountered and frequently require additional expenditures and effort to attain a properly designed and constructed project.

In the performance of its professional services, AMEC, its employees, and its agents comply with the standards of care and skill ordinarily exercised by members of our profession practicing in the same or similar localities. No warranty, either express or implied, is made or intended in connection with the work performed by us, or by the proposal for consulting or other services, or by the furnishing of oral or written reports or findings. In the event conclusions based on these data are made by others, such conclusions are not our responsibility unless we have been given an opportunity to review and concur with such conclusions in writing.

CLOSURE

AMEC appreciates this opportunity to work with Jacobs Associates and East Bay Municipal Utility District on this project. Please contact either of the undersigned if you have any questions about this letter report or if we can be of further service.

Sincerely yours,
AMEC Environment & Infrastructure, Inc.

Debra Gilkerson, PE (CA)
Project Engineer
Direct Tel.: (510) 663-4284
E-mail: debra.gilkerson@amec.com

Marc Ryan, PE (CA)
Principal Engineer
Direct Tel.: (510) 663-4207
E-mail: marc.ryan@amec.com

tac/mjr/ldu
\\Oad-fs1\doc_safe\16300s\163180\3000\PSHA Memo\1 Txt\TM No 4_Pardee Tower_082712.docx

Attachments: References
- Table 2: Uniform Hazard Spectra for ($V_{s,30}$ = 860 m/sec) Site Conditions for the Maximum Design Earthquake
- Figure 1: Site Location and Regional Tectonic Map
- Figure 2: Local Fault Sources
- Figure 3: Comparison of Median Deterministic Response Spectra
- Figure 4: Comparison of Uniform Hazard Spectra for 975, 2,475, 9,975-Year Return Periods and Deterministic Response Spectra
- Figure 5: Recommended UHRS for 2,475-Year Return Period

REFERENCES

REFERENCES

Abrahamson, N., and Silva, W., 2008, Summary of the Abrahamson & Silva NGA Ground Motion Relations: Earthquake Spectra, v. 24, no. 1, p. 67-97.

Abrahamson, N., 2000, Effects of Rupture Directivity on Probabilistic Seismic Hazard Analysis: Proceedings of the 6th International Conference on Seismic Zonation, Palm Springs California.

AMEC, 2012 [Draft], Technical Memorandum No. 1 - Summary of Geologic/Geotechnical Site Conditions and Recommendations for Foundation Properties and Rock Springs, Pardee Reservoir Outlet Tower Evaluation Amador County, California.

Boore, D.M. and Atkinson, G.M., 2008, Ground-Motion Prediction Equations for the Average Horizontal Component of PGA, PGV, and 5%-Damped PSA at Spectral Periods between 0.01 s and 10.0 s, Earthquake Spectra, vol. 24, No. 1, p 99-138, February.

Campbell, K.W., and Bozorgnia. Y, 2008, NGA Ground Motion Model for the Geometric Mean Horizontal Component of PGA, PGV, PGD and 5% Damped Linear Elastic Response Spectra for Periods Ranging from 0.01 to 10.0 s, Earthquake Spectra, vol. 24, No. 1, p 139-171, February.

Chiou, B. S.-J. and Youngs, R.R., 2008, An NGA Model for the Average Horizontal Component of Peak Ground Motion and Response Spectra, Earthquake Spectra, vol. 24, No. 1, p 173-215, February.

Fraser, W.A., and Howard, J.K., 2002, Guidelines for use of the Consequence-Hazard Matrix and selection of ground motion parameters, Division of Safety of Dams, Department of Water Resources, the State of California, October.

HCG, 1998, Pardee Reservoir Enlargement Project, Summary Technical Report, Volume 1, Conceptual Design Report: unpublished consulting report prepared for East Bay Municipal Utility District, June 1988.

Idriss, I.M., 2008, An NGA empirical model for estimating the horizontal spectral values generated by shallow crustal earthquakes, Earthquake Spectra, v. 24, no. 1, p. 217-242.

Jennings, C.W., and Bryant, W.A., 2010, 2010 fault activity map of California: California Geological Survey, Geologic Data Map No. 6.

Pacific Gas and Electric Company, 2007, Regional geology, seismicity, and general ground motion considerations for the Mokelumne and Stanislaus hydroelectric systems, Alpine, Amador, Calaveras, and Tuolumne Counties, California, FERC projects 137, 1061, and 2130, October 2007.

Petersen, M.D., Frankel, A.D, Harmsen, S.C., Mueller, C.S., Haller, K. M., Wheeler, R.L., Wesson, R.L., Zeng, Y., Boyd, O.S., Perkins, D.M., Luco, N., Field, E.H., Wills, C.J., and Rukstales, K.S., 2008, Documentation for the 2008 Update of the United states National Seismic Hazard Maps, USGS Open File Report 2008-1128, 61p.

Somerville, P., Smith, N., Graves, R., and Abrahamson, N., 1997, Modification of Empirical Strong Ground Motion Attenuation Relations to Include the Amplitude and Duration Effects of Rupture Directivity: Seismological Research Letters. v. 68, pp. 199-222.

Spudich, P., and Chiou, B., 2008, Directivity in NGA Earthquake Ground Motion: Analysis Using Isochrone Theory: Earthquake Spectra, v. 24, no. 1, p. 279-298.

Risk Engineering Inc., 2011, EZ-FRISK™- Software for Earthquake Ground Motion Estimation, V7.62.

Wakabayashi, J. and Sawyer, T.L., 2001, Stream incision, tectonics, uplift, and evolution of topography of the Sierra Nevada, California: Journal of Geology, vol. 109, p. 539-562.

TABLE

TABLE 2

UNIFORM HAZARD SPECTRA FOR (V_{S30} = 860 M/S) SITE CONDITIONS FOR THE MAXIMUM DESIGN EARTHQUAKE

Pardee Reservoir Outlet Tower
Calaveras County, California

Period (seconds)	Spectral Accelerations (g)	
	Fault Normal Maximum Design Earthquake (Scaled 2,475-Year Return Period)	Fault Parallel Maximum Design Earthquake (Scaled 2,475-Year Return Period)
0.01	0.150	0.150
0.02	0.153	0.153
0.03	0.163	0.163
0.05	0.194	0.194
0.08	0.246	0.246
0.10	0.289	0.289
0.15	0.352	0.352
0.20	0.375	0.375
0.25	0.375	0.375
0.30	0.368	0.368
0.40	0.337	0.337
0.50	0.300	0.300
0.75	0.253	0.234
1.00	0.223	0.193
1.50	0.184	0.143
2.00	0.148	0.107
3.00	0.097	0.058
4.00	0.065	0.034
5.00	0.052	0.027
7.50	0.034	0.018
10.00	0.023	0.012

Note:

Response spectra are five-percent damped.

FIGURES

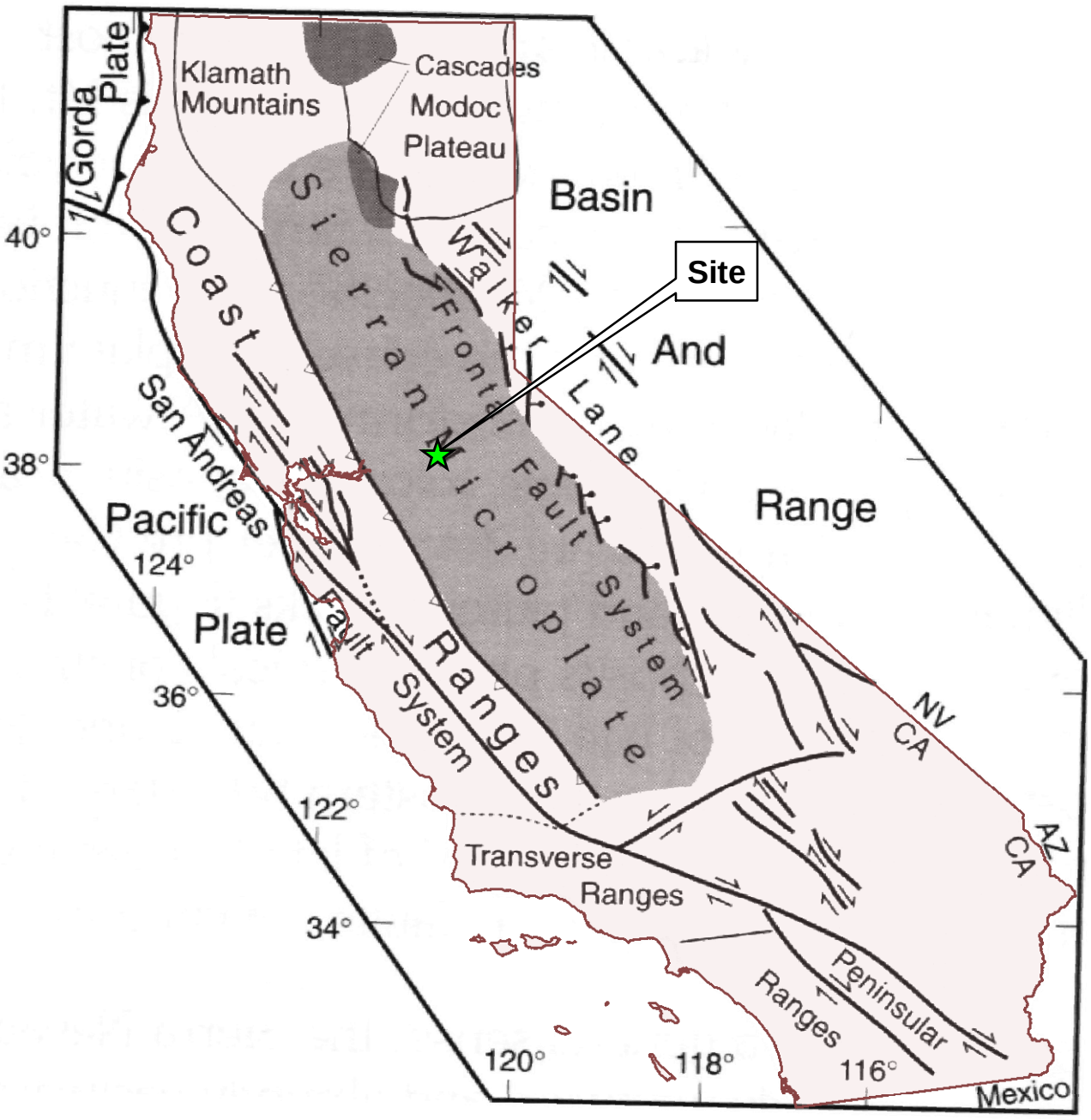

From Wakabayashi and Sawyer (2001).

SITE LOCATION AND REGIONIAL TECTONIC MAP
Pardee Reservoir Outlet Tower Evaluation
Calaveras County, California

By: _____	Date: 08/02/2012	Project No. OD12163180.B.02
amec		Figure 1

S:\OD12\163180\163180.b\task_2\12_0801_psha_fig_01.mxd

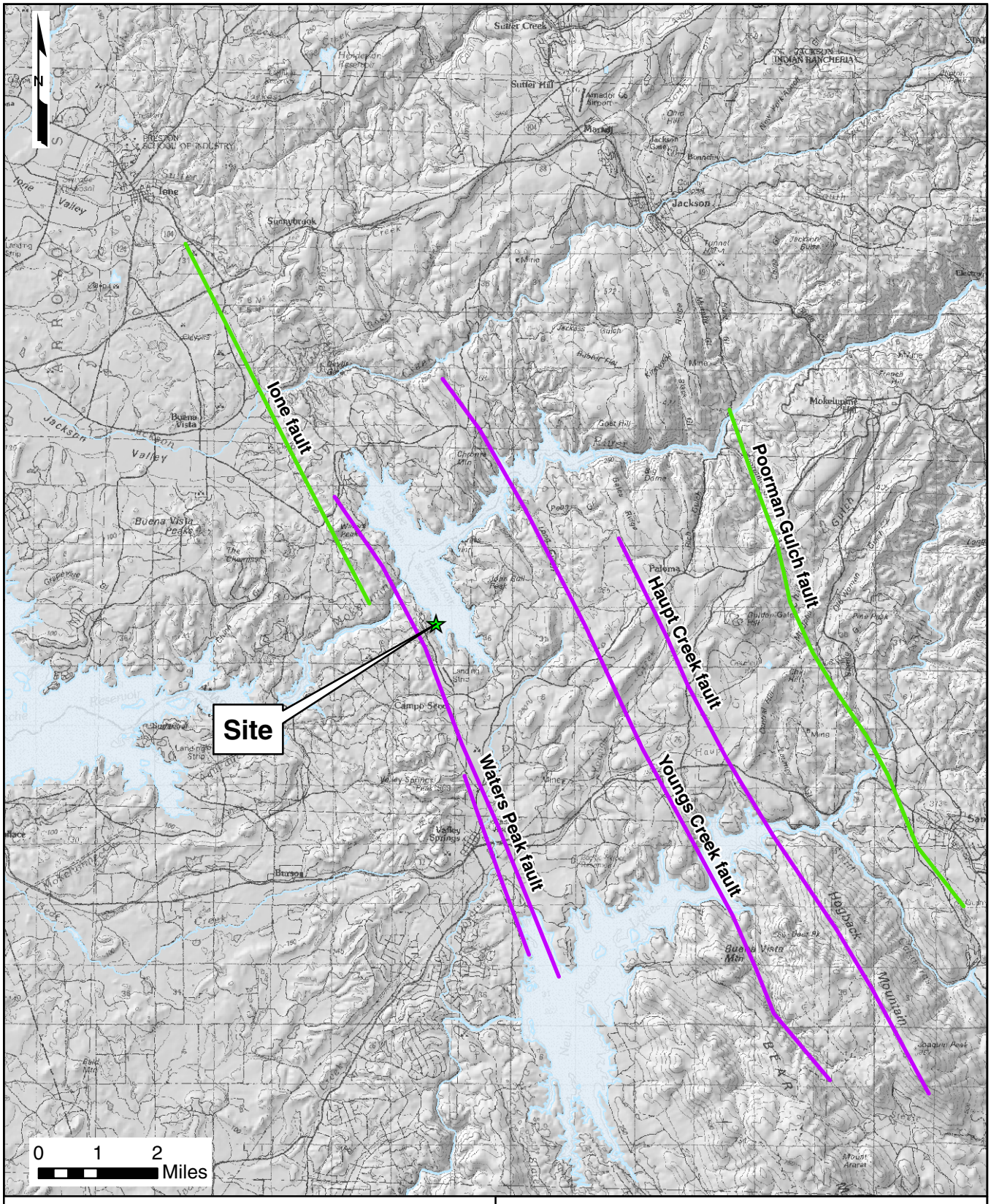

Explanation

Late Quaternary displacement

Quaternary displacement (age undifferentiated)

Faults from Jennings and Bryant (2010).

LOCAL FAULT SOURCES
Pardee Reservoir Outlet Tower Evaluation
Calaveras County, California

By: _____	Date: 08/06/2012	Project No. OD12163180.B.02
amec		Figure 2

S:\OD12\163180\163180.b\task_2\12_0801_pshа_fig_02.mxd

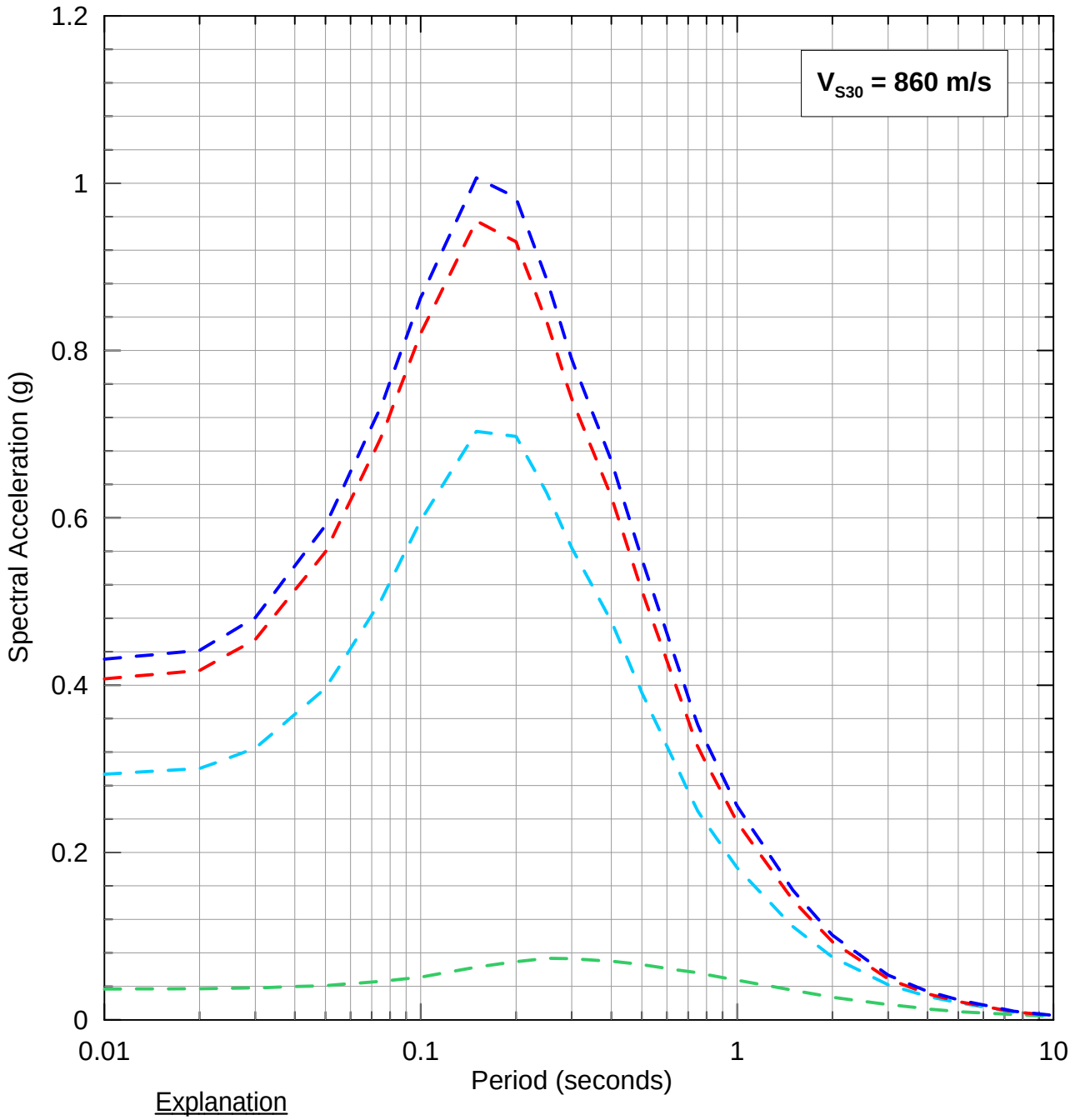

Explanation

- Median Deterministic (Waters Peak Fault) Mw = 6.4 at 0.5 km
- Median Deterministic (Ione Fault) Mw = 6.4 at 1.9 km
- Median Deterministic (Youngs Creek Fault) Mw = 6.5 at 3.7 km
- Median Deterministic (San Andreas) Mw = 8.0 at 155 km

Notes:
1. Spectra are five-percent damped.

COMPARISON OF MEDIAN DETERMINISTIC RESPONSE SPECTRA
Pardee Reservoir Outlet Tower Evaluation
Calaveras County, California

By: DG	Date: 7/26/2012	Project No. OD12163180
amec		Figure 3

I:\Project\163001\63180_Pardee_Tower\12000_CALCS_EVALS\Figures

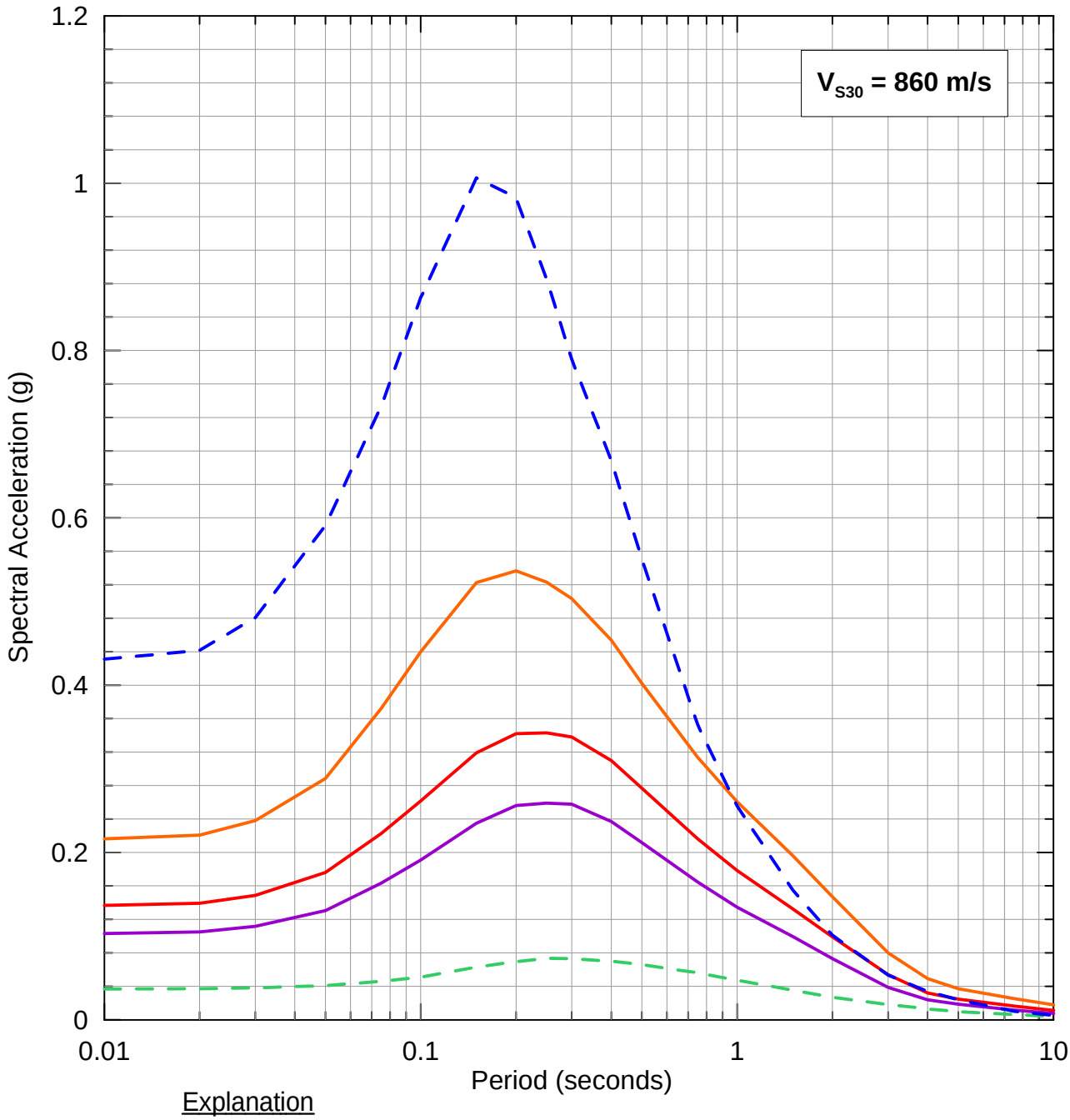

Explanation

- 975 RP - 5% PE in 50 Years
- 2,475 RP - 2% PE in 50 Years
- 9,975 RP - 0.5% PE in 50 Years
- Median Deterministic (San Andreas) Mw = 8.0 at 155 km
- Median Deterministic (Waters Peak Fault) Mw = 6.4 at 0.5 km

Notes:
1. Spectra are five-percent damped.
2. RP is return period; PE is probability of exceedance.

COMPARISON OF UNIFORM HAZARD SPECTRA FOR THE 975, 2,475- AND 9,975-YEAR RETURN PERIODS AND DETERMINISTIC RESPONSE SPECTRA
Pardee Reservoir Outlet Tower Evaluation
Calaveras County, California

By: DG	Date: 7/26/2012	Project No. OD12163180
amec		Figure 4

I:\Project\163001\63180_Pardee_Tower\12000_CALCS_EVALS\Figures

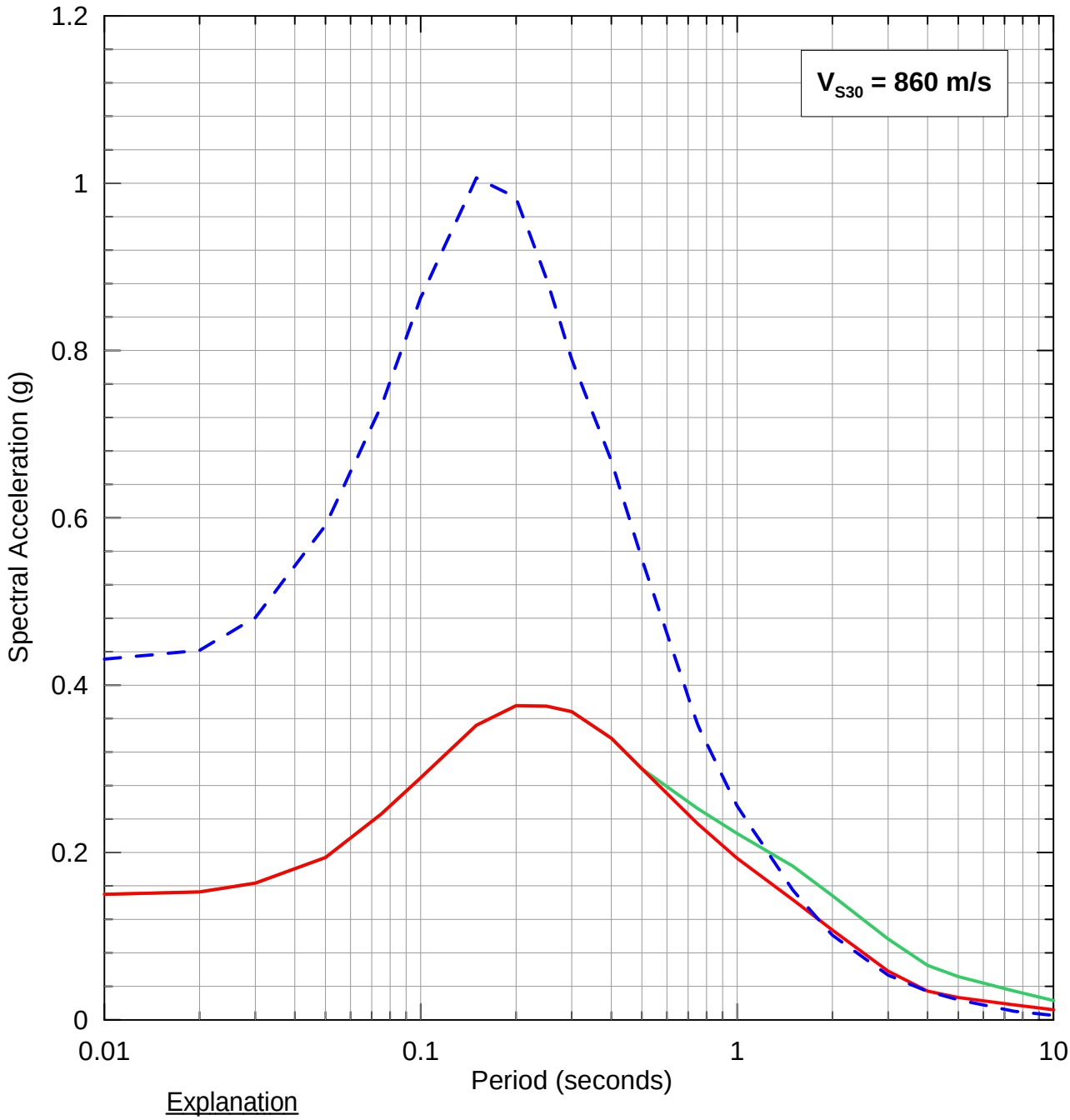

Explanation

- 2,475 RP - 2% PE in 50 Years Fault Normal
- 2,475 RP - 2% PE in 50 Years Fault Parallel
- Median Deterministic (Waters Peak Fault) Mw = 6.4 at 0.5 km

Notes:
1. Spectra are five-percent damped.
2. RP is return period; PE is probability of exceedance.

RECOMMENDED UNIFORM HAZARD RESPONSE SPECTRA FOR THE 2,475-YEAR RETURN PERIOD
Pardee Reservoir Outlet Tower Evaluation
Calaveras County, California

By: DG	Date: 7/26/2012	Project No. OD12163180
amec		Figure 5

I:\Project\163001\63180_Pardee_Tower\12000_CALCS_EVALS\Figures

Appendix C

Seismic Structural Evaluation of Pardee Outlet Tower—Final Report

Quest Structures, Inc., August 2013

Seismic Structural Evaluation of Pardee Outlet Tower

Final Report

Prepared for:

Jacob Associates
49 Stevenson Street, 3rd Floor
San Francisco, CA 94105-2950

Prepared by:

Quest Structures, Inc.
3 Altarinda Road, Suite 203
Orinda, CA 94563

Quest Project 2012011
Report No. 2012011.01

QuestStructures

August 20, 2013

Seismic Structural Evaluation of Pardee Outlet Tower

Final Report

Prepared for:

Jacob Associates
49 Stevenson Street, 3rd Floor
San Francisco, CA 94105-2950

Prepared by:

Quest Structures, Inc.
3 Altarinda Road, Suite 203
Orinda, CA 94563

August 20, 2013

Report No. 2012011.01 **Quest Project 2012011**

Table of Contents

List of Figures

List of Tables

SEISMIC STRUCTURAL EVALUATION OF PARDEE OUTLET TOWER

EXECUTIVE SUMMARY

This report summarizes the findings of a seismic evaluation performed for the Pardee Outlet Tower subjected to the maximum design earthquake (MDE) ground motion. The MDE was selected by EBMUD and approved by the FERC as a ground motion with a return period of 2,475 years (2% probability of exceedance in 50 years) having a mean horizontal peak ground acceleration of 0.15g. The seismic evaluation employed finite-element analysis using the response-spectrum mode-superposition method, available material parameters based on as-built drawings, as well as parameter sensitivity with respect to materials and modeling assumptions.

The Pardee Outlet Tower is a lightly reinforced concrete cylindrical structure built in 1929 with 19 ft inside diameter and wall thicknesses varying from 1.5 ft at the top to 4.5 ft at the bottom. The tower is 190 ft tall with 70 ft of its length immersed below the grade of the reservoir bottom. A four-span three-pier truss bridge provides access to a round gatehouse built atop the tower. The tower can draw water from various levels and transfer it to the tunnel located at the bottom of the tower. There are three inlets above grade, one below and one at the tunnel level.

The tower was modeled as a group of equivalent beam elements distributed from top to bottom with nodal points chosen at elevations of steel reinforcement changes. The embedment in rock was represented by equivalent lateral spring supports. The inside and outside water inertia forces due to earthquake excitation were modeled as additional masses lumped at the submerged nodal points. The seismic response of the tower was evaluated by subjecting the tower to two horizontal components of the earthquake ground motion. The effect of vertical ground motion was considered to be negligible and was ignored. The model was analyzed for a basic condition with best estimate material properties (base model) as well as other conditions to assess sensitivity of results to the concrete strength, cracked section properties, stiffness magnitude and distribution of foundation spring supports.

The results for the base model with 5000-psi concrete and uncracked section properties indicate that the EM 1110-2-2400 [4] acceptance criteria for moment and shear DCRs and brittle failure modes are met. The moment DCRs do not exceed 2 while shear DCRs remain less than 1 except at one location within the rock embedment. However, sensitivity analyses indicate that the actual shear demand at this location is expected to be lower than that obtained from the base model for the following reasons:

- An increase in compressive strength of the concrete increases the shear strength more than the shear and moment demands (Section 7.1). The actual compressive strength of the concrete is expected to be higher than 5000-psi concrete, which would result in shear capacity being very close or greater than the maximum shear demand.

- The use of cracked section properties reduces seismic moment and shear demands (Section 7.2).
- Reducing the foundation spring spacing to simulate continuous support decreases the maximum shear and moment demands (Section 7.3).
- Reducing magnitude of the spring constants to account for rock fractures near the surface further decreases shear demands (Section 7.3). This also increases moment demands within the embedded region, but it is not a problem since moments in this region are small.

For the above reasons the actual maximum shear demands is expected to be less than the shear capacity and besides the maximum shear occurs where the tower is fully supported by the surrounding rock. Consequently, the use of a moment reduction factor of 2 is fully justified. Further, all other brittle failure modes were also checked and found to meet the EM 1110-2-2400 requirements (Section 8). Only the nominal to cracking moment ratios of the tower do not meet the criteria, but the follow up displacement-based analysis indicates that the tower meets the deformation capacity.

Therefore, it is concluded that the seismic performance of the tower for the postulated ground motion would be satisfactory without collapse. Concrete cracking and steel yielding could be expected at one or more sections, but reinforcing steel would remain intact and the overall stability of the tower would be maintained. If cracking and steel yielding is concentrated in a single section, it can result in some permanent tilting of the tower. It is believed such tilting is not large enough to impede operation of the tower, but may require repair and strengthening for the long term functionality if the tower experiences such an event and if a permanent deformation is observed.

1. DESCRIPTION OF TOWER

The Pardee Outlet Tower is located on the Mokelumne River near Valley Springs, Amador County, California. It is a lightly reinforced concrete structure with 19 ft internal diameter. It is 190 ft tall with 70 ft of its length immersed below the grade of the bottom of the reservoir. A round gate house with conical roof is atop the cylindrical tower. The gate house is accessible using a four-span, three-pier truss bridge. One of the piers is reinforced concrete while the other two are metal trusses. The tower can draw water from various levels and transfer it to the tunnel located at the bottom of the tower. There are three inlets above grade, one below and one at the tunnel level.

The tower was finished in 1929, the same year as the rest of the complex which includes the Pardee Dam and an outlet tunnel. Location of the tower with respect to the dam can be seen in Figure 1-1. Selected profile and cross-section drawings of the tower are shown in Figures 1-2 and 1-3.

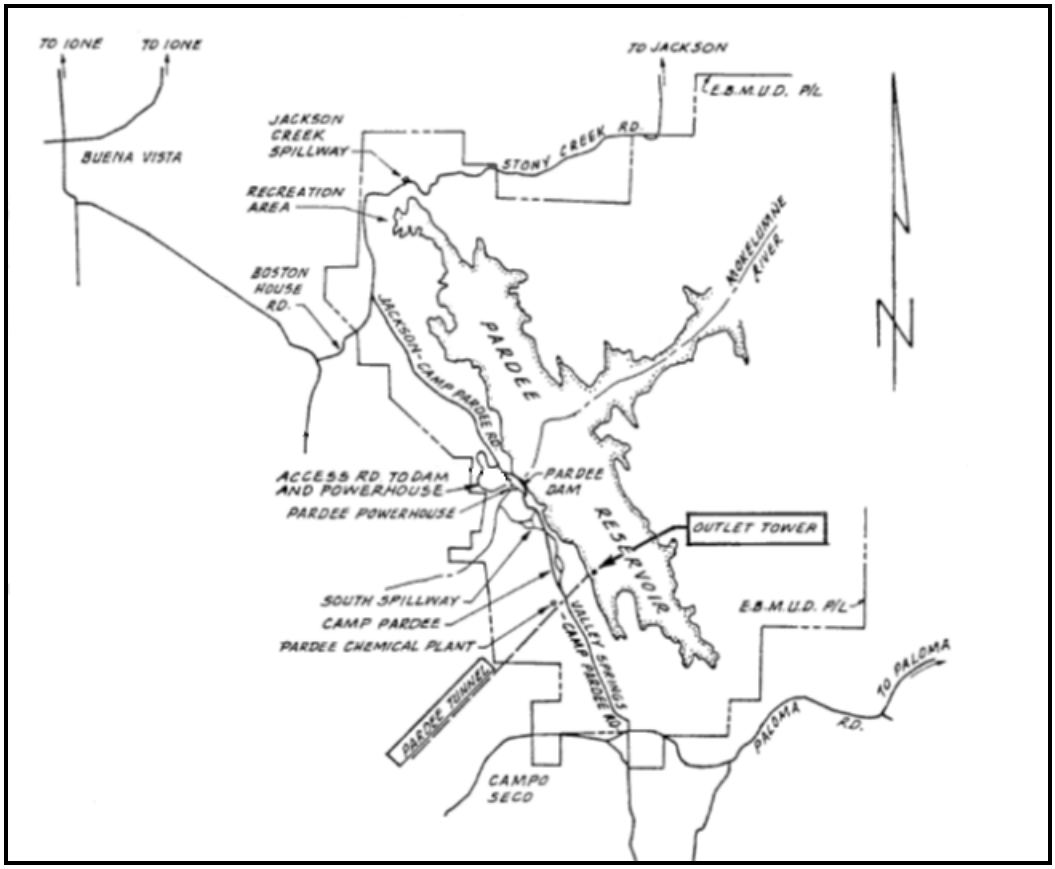

Figure 1-1. Location of Pardee Dam and Outlet Tower.

(source: Preliminary report-1987, Plate No.2)

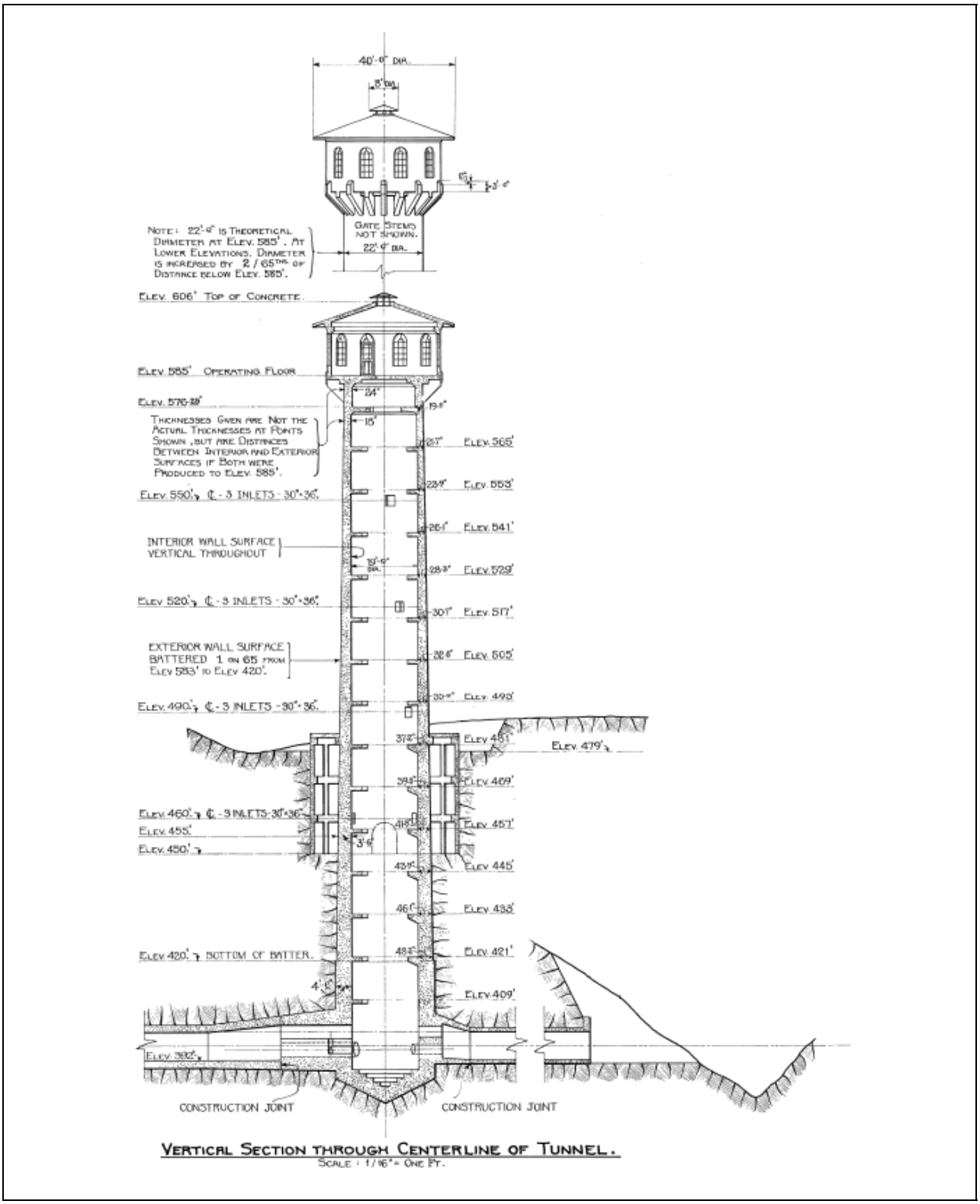

Figure 1-2. Vertical section through centerline of tunnel.

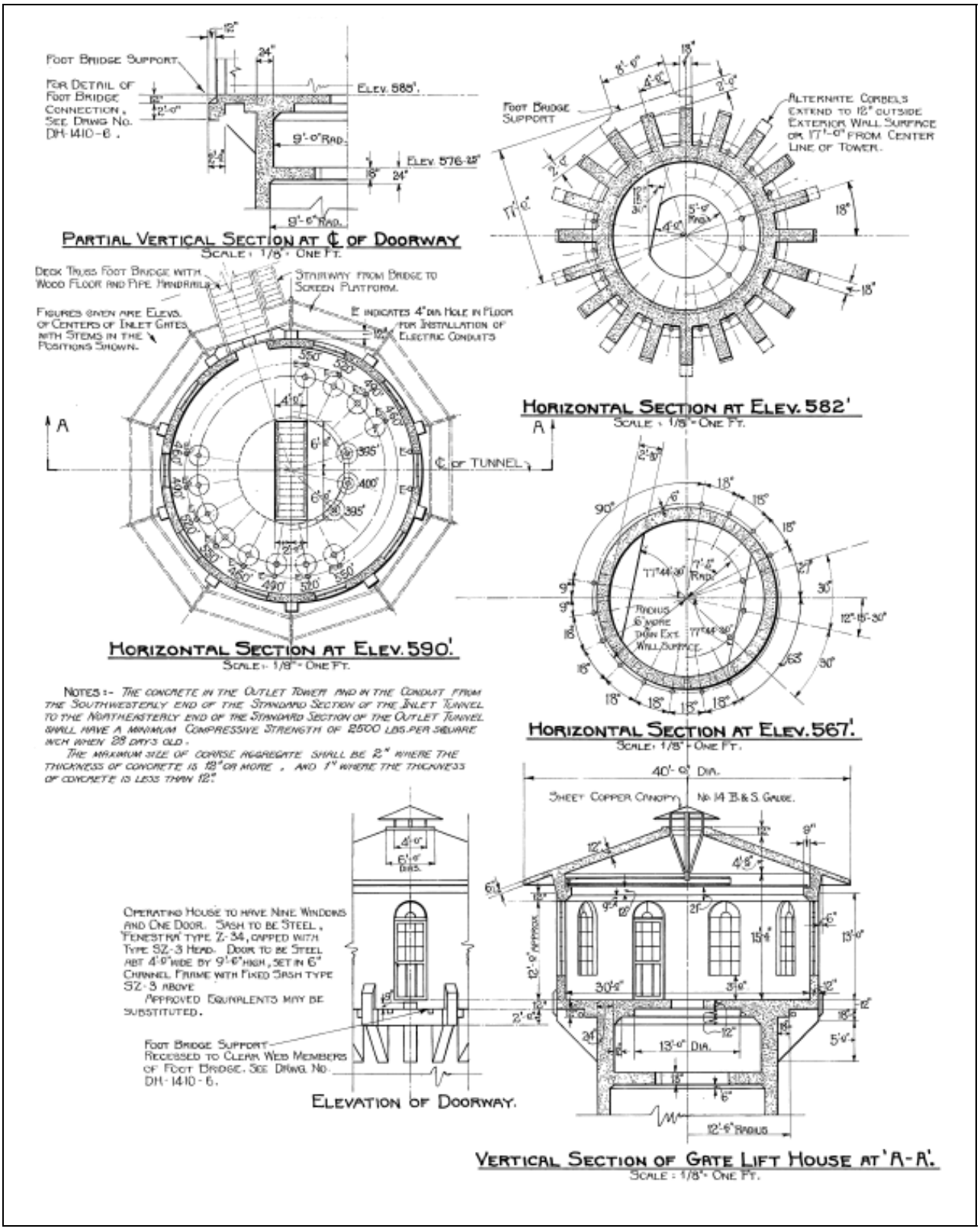

Figure 1-3. Horizontal sections with vertical section of gate lift house.

2. MATERIAL PROPERTIES

2.1 Concrete Properties

The concrete for the outlet tower was specified to have a minimum compressive strength of 2,500 psi at 28 days (Drawing No. DH-1350-6). In view of the observed excellent condition of the concrete and its likelihood of gaining strength with age, the current compressive strength of the concrete is believed to be significantly higher than 2,500 psi. However, in the absence of measured data an average value of 5,000 psi is used to account for the aging and rapid rate of seismic loading. In the analysis, the concrete strength is varied ± 25% to assess the effects that the compressive strength might have on the results. A constant Poisson's ratio of 0.2 and a unit weight of 150 pcf were assumed for the concrete. Values of the concrete modulus of elasticity and modulus of rupture were estimated in accordance with ACI -318.

$$E_c = 57000\sqrt{f'c}$$

$$f_r = 7.5\sqrt{f'c}$$

Concrete Nominal Properties

f'_c	=	5,000 psi	Compressive strength
f_r	=	530 psi	Modulus of rupture
E_c	=	4,000,000 psi	Rounded modulus of elasticity

Concrete Lower Bound properties

f'_c	=	3,750 psi	Compressive strength
f_r	=	495 psi	Modulus of rupture
E_c	=	3,500,000 psi	Rounded modulus of elasticity

Concrete Upper Bound properties

f'_c	=	6,250 psi	Compressive strength
f_r	=	593 psi	Modulus of rupture
E_c	=	4,500,000 psi	Rounded modulus of elasticity

2.2 Reinforcing Steel Properties

The following properties of reinforcing steel were used in the earlier report on the seismic performance of the Pardee tower by Dames & Moore in 1986 [1]:

f_y	=	45 ksi	Yield strength of steel
E_s	=	29,000 ksi	Modulus of elasticity
f_u	=	64 ksi	Ultimate tensile strength

The yield strength of 45ksi was considered high for vintage 1920's reinforcing steel without coupon tests support. In this study a lower value of 40ksi was considered to be more appropriate and thus was used in the analysis.

2.3 Foundation Stiffness Properties

Flexibility of the foundation rock and its effects on seismic response of the tower were represented by equivalent linear spring supports along the depth of embedment. Frequency dependent spring properties for the foundation rock were provided by AMEC [2] and are presented in Table 2-1. The real part of the stiffness vector corresponding to the fundamental frequency of the structure is used in the calculations. Since the fundamental frequency of the structure is dependent on the stiffness of the springs, the final stiffness values of the foundation spring is obtained by an iterative process. The iteration begins with a spring constant at an assumed frequency value. The initial spring constant is used in the model to compute the tower frequency, which then is employed to obtain an improved estimate of the spring constant (see Section 3.2). This process continues until differences between consecutive spring constants or frequencies are negligible. The final spring values are presented below in the units of kip/ft/ft. These values are multiplied by their respective tributary lengths to arrive at the spring stiffness values lumped at the tower embedded nodal points between elevations 392 ft and 450 ft, except that the bottom node at 392 ft is fixed.

Between El. 450 ft and 479 ft, the outlet tower is surrounded by a screening chamber as shown in the Figure 2-1 with a cross section at El. 460 ft. The tower is connected to the perimeter of the chamber via a 1-foot-thick slab with negligible lateral resistance. Thus, no foundation spring supports were included between El. 450 to 479 ft. The 1987 Dames & Moore [1] seismic evaluation did not incorporate foundation stiffness in the analysis, instead the tower was analyzed for two limiting cases, first fixing the tower at El. 479 ft and then at El. 421 ft, or 58 ft below the ground surface.

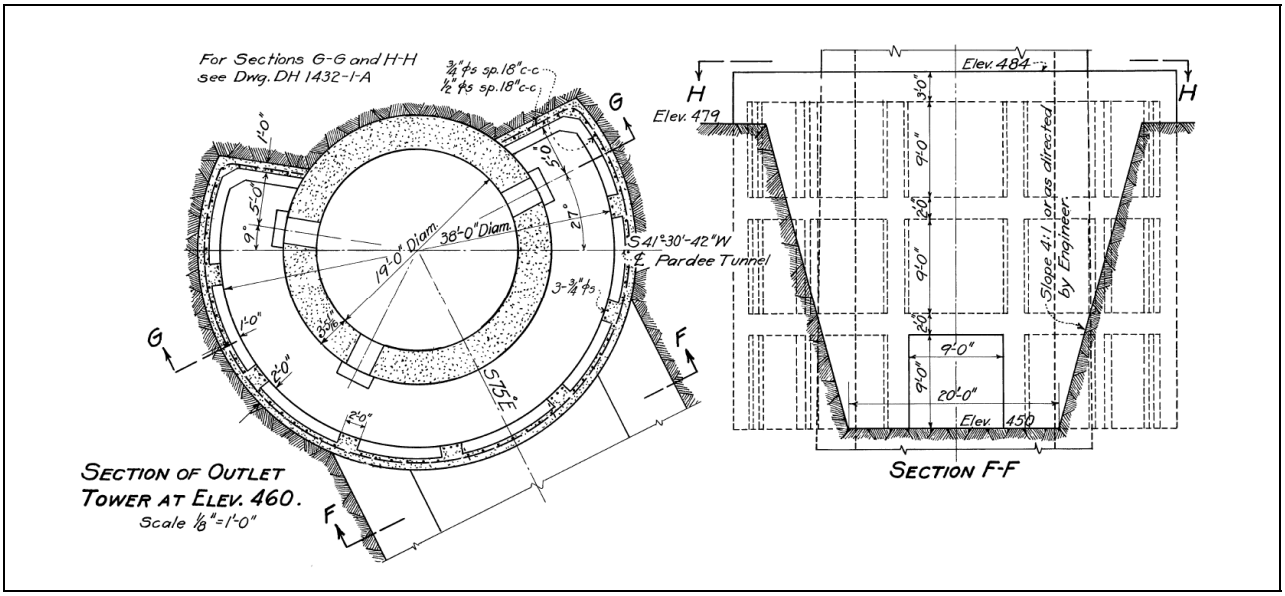

Figure 2-1. Section of outlet tower at elev. 460 ft with profile between elev. 450 ft and 479 ft.

Table 2-1. Stiffness properties of foundation springs.

Lateral soil springs		
Frequency (Hz)	K*=Re(K*)+i.im(K*)	
	Re(K*) (kips/ft/ft)	Im(k*) (kips/ft/ft)
99.99	136,643	1,084,711
33.32	136,643	359,501
19.98	136,643	229,672
14.29	133,216	175,739
11.11	128,990	145,493
10.01	126,997	135,007
3.33	103,546	67,435
1.99	93,492	51,475
1.44	87,786	44,091
1.1	83,349	39,004
0.99	81,825	37,372
0.34	67,821	24,713
0.21	62,478	20,814
0.14	58,746	18,347
0.1	56,335	16,858

Vertical Soil springs		
Frequency (Hz)	K*=Re(K*)+i.im(K*)	
	Re(K*) (kips/ft/ft)	Im(k*) (kips/ft/ft)
99.99	91,420	637,005
33.32	91,420	227,665
19.98	86,423	146,917
14.29	82,199	112,365
11.11	78,747	92,812
10.01	77,287	86,015
3.33	62,167	42,257
1.99	56,010	32,019
1.44	52,535	27,311
1.1	49,838	24,082
0.99	48,912	23,049
0.34	40,419	15,087
0.21	37,186	12,658
0.14	34,930	11,127
0.1	33,475	10,206

3. FINITE-ELEMENT MODEL

3.1 Model Description

The tower was modeled as a group of beam elements. Table 3-1 below lists relevant elevations of the model:

Table 3-1. Relevant elevations of the FEM model.

Tower bottom elevation	392 ft
Tower top elevation	606 ft
Water pool elevation	565 ft
Top of rock elevation	479 ft
Elevation at which the tower is assumed to be fixed	392 ft
Elevations at which lateral springs are applied	409 ft - 450 ft

There are 23 nodes making up 22 beam elements along the height of the tower. Elevations and height of the nodes from the bottom are listed in Table 3-2 and shown graphically in Figure 3-1. Each element is assumed to have homogenous material properties. Except for Element 22, which is conical, all the other frame sections are cylindrical non-prismatic sections. Although the inner diameter remains constant, the outer diameter of the tower varies with height. The thickness at the mid-section of each element is assigned to the entire element. Nodes were chosen at elevations where the steel reinforcement changes. The mass of the conical roof of the operating house is equally distributed between Nodes 22

and 23 at El. 598.75 ft and 606 ft, respectively. The 20 concrete brackets supporting the operating floor between El. 576.25 ft and 585 ft add considerable mass to the structure and hence are included in the model. Their weight is distributed equally to Nodes 20 and 21 at El. 576.25 ft and 585 ft, respectively. Masses of all the remaining elements are distributed equally among the respective nodes making the element. To account for the 9 windows and one door openings in the operating house, only 80% of the total mass associated with the solid wall sections of the cylinder is assigned to the nodes at El. 585 ft and 598.75 ft. Appendix A provides data used to calculate the of mass of brackets and operating house.

Table 3-2. Elevation of finite-element nodes.

Node	Elevation(ft)	Height (ft)	Node	Elevation(ft)	Height (ft)
1	392	0	13	510	118
2	409	17	14	517	125
3	421	29	15	520	128
4	433	41	16	529	137
5	445	53	17	541	149
6	457	65	18	553	161
7	470.5	78.5	19	565	173
8	479	87	20	576.25	184.25
9	490	98	21	585	193
10	493	101	22	598.75	206.75
11	500	108	23	606	214
12	505	113			

3.2 Foundation Springs

The foundation springs were lumped at Nodes 2, 3, 4, and 5 using a tributary length of 14.5 ft for Node 2, and 12 ft for Nodes 3, 4, and 5 (Figures 3-1 and 3-2). The spring stiffness values were initially picked from Table 2-1 at the fundamental frequency of the tower without the springs (f_0). They were then used in the model to obtain the fundamental frequency of the tower with the springs (f_1). The frequency f_1 was used to update the spring stiffness and input to the model to obtain an improved fundamental frequency for the tower (f_1'). This process was repeated for couple of iterations until the changes in the fundamental frequency of the tower were negligible. The following spring stiffness values corresponding to the fundamental frequency of 1.60 Hz (0.624 sec) were achieved:

K_h= 89,466 kip/ft/ft

K_v=53,558 kip/ft/ft

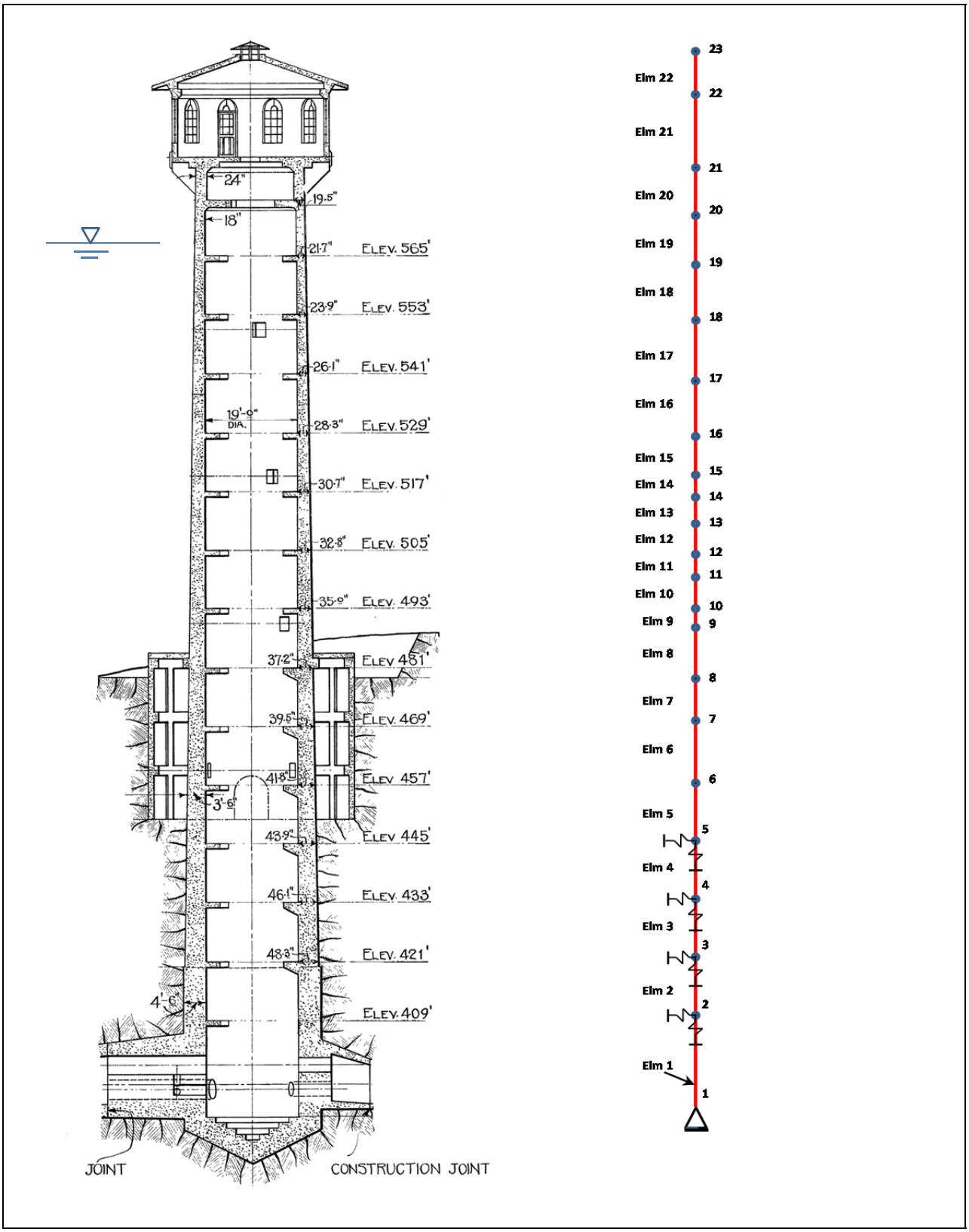

Figure 3-1. Tower and finite-element model side by side.

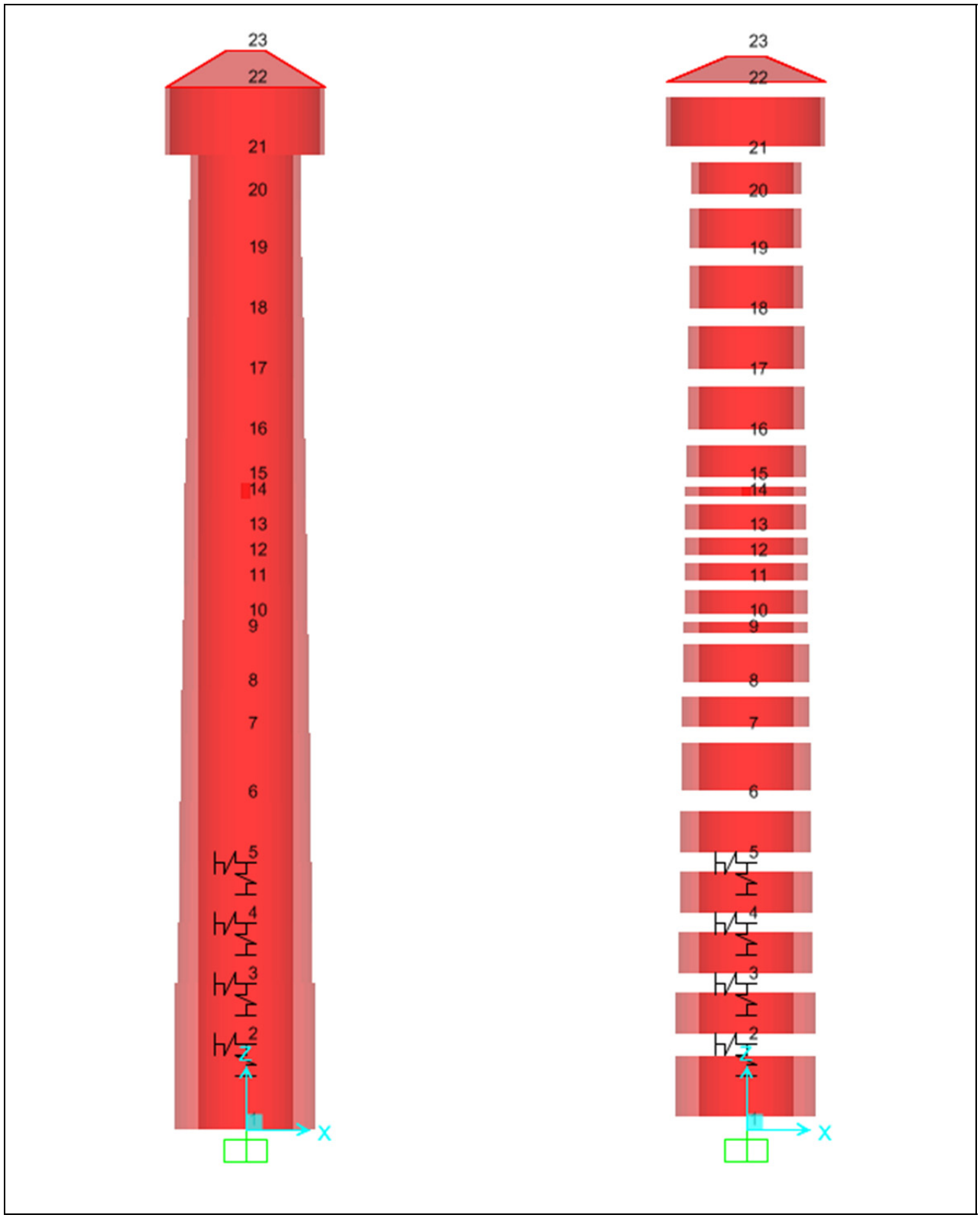

Figure 3-2. Sap2000 model of tower with foundation springs distributed at 12 feet.

3.3 Weight of Gate Operating Equipment

Weight of the gate operating equipment is also taken into account in the calculations. Table 3-3 summarizes the weight of the equipment, the elevation at which they are present and the nodes at which the associated mass values are lumped in the SAP 2000 model.

Table 3-3. Mass of operational equipment.

Elevation	Weight (lb)	Mass (kip.s2/ft)	Node
550	1500	0.047	18
520	1500	0.047	15
490	1500	0.047	9
460	1500	0.047	6
390	750	0.023	1

Finally, Table 3-4 provides a summary of the complete model data including the element dimensions, section properties, and structural nodal masses. The hydrodynamic added mass values for the inside and outside water are computed in Section 3.4.

3.4 Added Mass of Water

The inertial effects of the inside and outside water due to earthquake excitation were represented by added-mass terms using the procedure developed by Goyal and Chopra [3]. With the rock surface at El. 479 ft and water level at 565 ft, the nodes 8 to 19 have added mass contributions from both the water present inside and outside the tower. Nodes 1 to 7 have added mass contributions from the water inside the tower. Between El. 450 ft and 479 ft, the screening chamber is immediately surrounded by the rock and there is no added-mass contribution from the water around the tower between these elevations.

According to Goyal and Chopra [3], added mass terms for a particular section are dependent on the ratio of the radius of the section to the total submerged height of the tower (r_i/H_i for inside water, and r_o/H_o for outside water), ratio of mid-section depth to total submerged depth (z/H). Using r_i/H_i = 0.05 for inside water and r_o/H_o = 0.07 for outside water, the value of normalized mass is read off the chart presented below in Figure 3-3. These values can be seen in Columns 6 and 7 of Table 3-5 for the outside and inside added mass, respectively. The term $m_i(z)/\rho A$ is multiplied by ρA to get inside mass and $m_o(z)/m_o(\infty)$ by $m_o(\infty)$ to obtain outside mass. The term $m_o(\infty)$ represents the added mass for infinitely long tower associated with outside water. For circular sections, $\frac{m_o(\infty)}{\rho A}$ = 1, i.e. $m_o(\infty) = \rho A$. Here, ρ is the density of water and A is the area of cross-section. Such calculations for all the sections are presented below in the Table 3-5. The sections being symmetric, the x and y components of the added mass are the same.

Table 3-4. Dimensions, section properties and structural nodal masses.

Node	Element No.	Element Length (ft)	Inside Radius (in)	Mid-Section Elevation (ft)	Mid-Section Height (ft)	Wall Thickness (in)	Outside Radius (in)	Gross Area (in^2)	Ix-Iy (in^4) x10^8	Mass ($Kip.s^2/ft$)	Nodal Mass ($kip.s^2/ft$)
1											13.18
	1	17	114	400.5	8.5	54.00	168.00	47,840.17	4.93	26.31	
2											22.44
	2	12	114	415	23	54.00	168.00	47,840.17	4.93	18.57	
3											17.20
	3	12	114	427	35	47.19	161.19	40,799.74	3.98	15.84	
4											15.41
	4	12	114	439	47	44.98	158.98	38,571.41	3.69	14.97	
5											14.55
	5	12	114	451	59	42.76	156.76	36,373.93	3.42	14.12	
6											14.52
	6	13.5	114	463.75	71.75	40.27	154.27	33,938.61	3.12	14.82	
7											11.87
	7	8.5	114	474.75	82.75	38.70	152.70	32,425.29	2.94	8.92	
8											9.88
	8	11	114	484.5	92.5	36.67	150.67	30,489.84	2.72	10.85	
9											6.93
	9	3	114	491.5	99.5	36.12	150.12	29,966.49	2.66	2.91	
10											4.71
	10	7	114	496.5	104.5	34.82	148.82	28,752.82	2.53	6.51	
11											5.51
	11	5	114	502.5	110.5	33.90	147.90	27,892.35	2.43	4.51	
12											4.44
	12	5	114	507.5	115.5	32.98	146.98	27,037.22	2.34	4.37	
13											5.11
	13	7	114	513.5	121.5	31.68	145.68	25,849.05	2.21	5.85	
14											4.16
	14	3	114	518.5	126.5	31.13	145.13	25,343.04	2.16	2.46	
15											4.75
	15	9	114	524.5	132.5	29.47	143.47	23,836.58	2.00	6.94	
16											7.71
	16	12	114	535	143	27.25	141.25	21,854.96	1.80	8.48	
17											8.11
	17	12	114	547	155	25.04	139.04	19,904.17	1.61	7.73	
18											7.40
	18	12	114	559	167	22.82	136.82	17,984.22	1.43	6.98	
19											6.44
	19	11.25	114	570.625	178.625	20.75	134.75	16,212.27	1.26	5.90	
20											5.91
	20	8.75	114	580.625	188.625	19.13	133.13	14,852.83	1.14	4.20	
21											6.32
	21	13.75	180	591.875	199.875	12.0	192	14,024.07	2.43	6.24	
22											3.60
	22	7.25	varies	602.375	210.375	12.0	varies	varies	varies	1.66	
23											0.55

Table 3-5. Added Mass Calculations.

Node No.	Element No.	Length (ft)	ri/H	ro/H	Z/H	$m_o(z)/m_o(\infty)$	$m_i(z)/\rho A$	$m_o(z)$ kips-s^2/ft/ft	$m_i(z)$ kips-s^2/ft/ft	$m_i(z)+m_o(z)$ kips-s^2/ft/ft	Total Added-mass kips-s^2/ft	Nodal Added-mass kips-s^2/ft
1												4.67
	1	17	0.05	0.08	0.05	0.99	1	0	0.55	0.55	9.34	
2												7.97
	2	12	0.05	0.08	0.13	0.99	1	0	0.55	0.55	6.59	
3												6.59
	3	12	0.05	0.08	0.20	0.98	1	0	0.55	0.55	6.59	
4												6.59
	4	12	0.05	0.08	0.27	0.98	1	0	0.55	0.55	6.59	
5												6.59
	5	12	0.05	0.08	0.34	0.98	1	0	0.55	0.55	6.59	
6												7.01
	6	13.5	0.05	0.07	0.41	0.98	1	0	0.55	0.55	7.42	
7												6.04
	7	8.5	0.05	0.07	0.48	0.98	1	0	0.55	0.55	4.67	
8												10.53
	8	11	0.05	0.07	0.53	0.98	1	0.94	0.55	1.49	16.39	
9												10.39
	9	3	0.05	0.07	0.58	0.96	1	0.91	0.55	1.46	4.39	
10												7.27
	10	7	0.05	0.07	0.60	0.96	1	0.90	0.55	1.45	10.14	
11												8.66
	11	5	0.05	0.07	0.64	0.96	1	0.89	0.55	1.44	7.19	
12												7.16
	12	5	0.05	0.07	0.67	0.96	1	0.88	0.55	1.43	7.13	
13												8.45
	13	7	0.05	0.07	0.70	0.95	0.99	0.85	0.54	1.40	9.77	
14												6.95
	14	3	0.05	0.07	0.73	0.93	0.99	0.83	0.54	1.37	4.12	
15												8.11
	15	9	0.05	0.07	0.77	0.92	0.99	0.80	0.54	1.34	12.10	
16												13.74
	16	12	0.05	0.07	0.83	0.88	0.98	0.74	0.54	1.28	15.37	
17												14.79
	17	12	0.05	0.07	0.90	0.79	0.98	0.65	0.54	1.18	14.21	
18												11.69
	18	12	0.05	0.07	0.97	0.48	0.7	0.38	0.38	0.76	9.17	
19												4.59

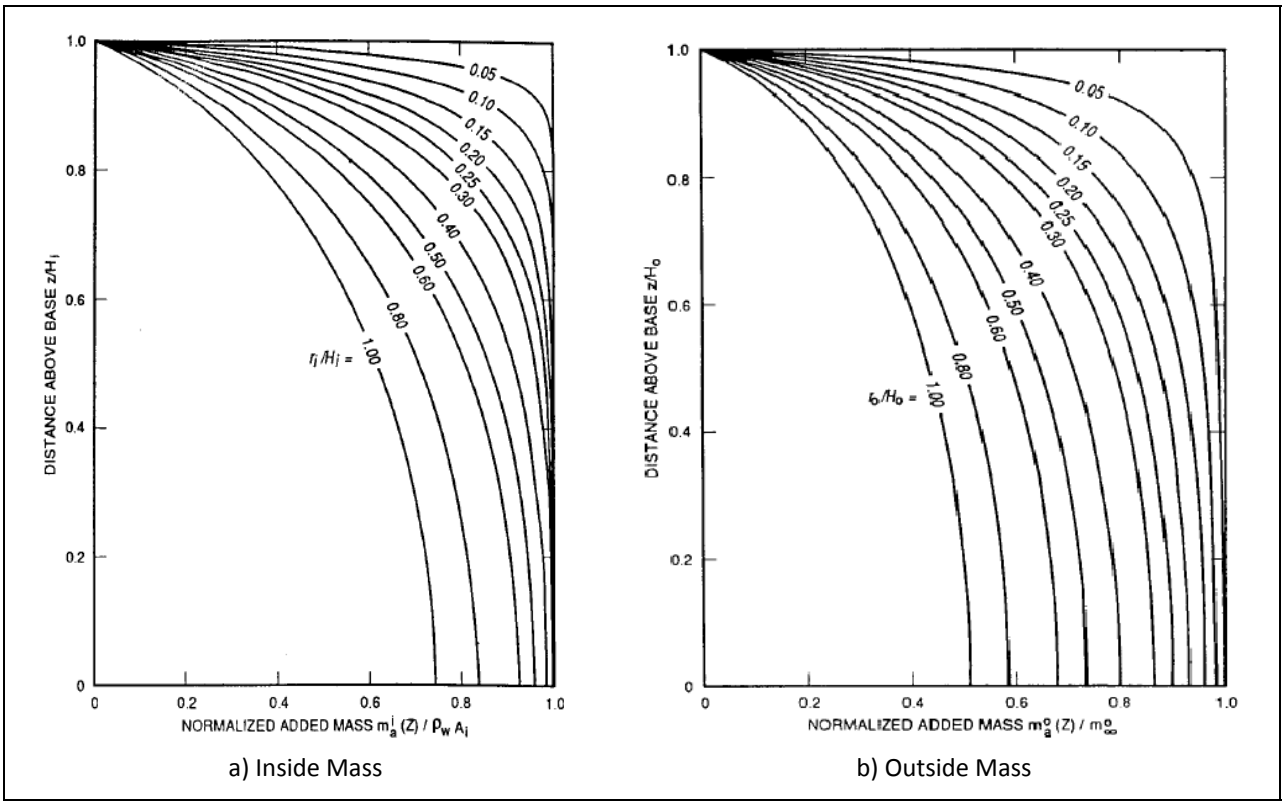

a) Inside Mass

b) Outside Mass

Figure 3-3. Normalized added mass vs. Distance above base.

4. RESPONSE-SPECTRUM ANALYSIS

The response-spectrum mode-superposition method was used to evaluate the seismic response of the Pardee Outlet Tower. The maximum seismic response of the tower was obtained by combining the maximum responses from individual modes of vibration and multiple components of the earthquake ground motion. The complete quadratic combination (CQC) was used to combine modal responses and the square-root-of-the-sum-of-the-squares (SRSS) to combine directional effects of two horizontal components of the ground motion. The analysis was carried out using SAP2000 Version 15. A total of seven mode shapes were required to achieve approximately 90% modal participation in the horizontal direction.

4.1 Vibration Periods and Mode Shapes

Table 4-1 below summarizes estimated vibration periods and corresponding modal mass participation factors for the lowest seven modes of vibration of the tower. The periods vary from 0.624 sec to 0.022 sec with mass participation factors varying from 51% for the first mode to 89% for all seven modes.

The tower deflected shapes for Modes 1 to 5 are displayed in Figure 4-1. The mode shapes and modal participations clearly show that Modes 1, 2, 3, 5, and 6 (not shown) represent bending modes and that Modes 4 and 7 (not shown) with main contribution to vertical mass participation are axial or vertical modes.

Table 4-1. Modal periods, frequencies and mass participation factors.

Mode	Period (sec)	Frequency(hz)	SumUX	SumUY	SumUZ
1	0.624	1.6019	0.5099	0.5099	0
2	0.139	7.165	0.6726	0.6726	0
3	0.059	16.793	0.7339	0.7339	0
4	0.054	18.352	0.7339	0.7339	0.6932
5	0.035	28.133	0.7945	0.7945	0.6932
6	0.025	38.666	0.8879	0.8879	0.6932
7	0.022	44.409	0.8879	0.8879	0.8468

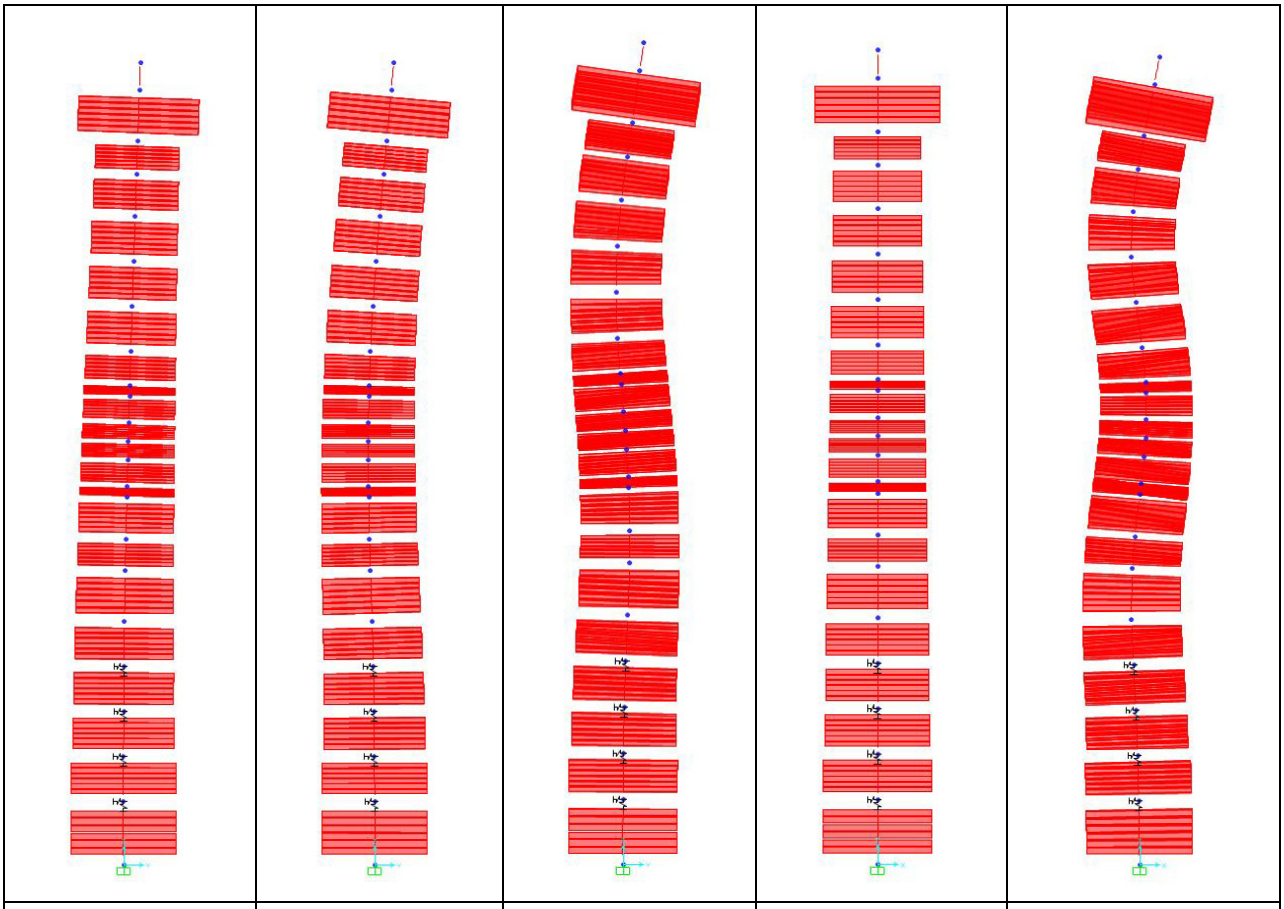

Figure 4-1. Mode shapes 1 to 5.

4.2 Seismic Load

The seismic hazard assessment at the Pardee Outlet Tower included both probabilistic and deterministic analyses (AMEC, 2012 [2]). The median peak ground acceleration (PGA) for the controlling deterministic event with the magnitude, M_w 6.4 earthquake on the Waters Peak fault is approximately 0.43g. The mean horizontal PGA for the probabilistic estimate of the ground motion for a return period of 2,475 years (2% probability of exceedance in 50 years) was found to be 0.15g. Since the Pardee Outlet Tower is located several kilometers from the Pardee Dam site and its failure would not affect dam safety, EBMUD in a letter to FERC proposed that the tower be evaluated for a 2,475-year maximum design earthquake (MDE) ground motion. In its response letter dated 18 March 2013, the FERC accepted the proposed 2,475-year MDE for the seismic evaluation of the tower.

The seismic load for evaluation of Pardee Outlet Tower consists of two horizontal components of the 2,475-year MDE ground motion. The 5%-damped fault-normal and fault-parallel response-spectra of the 2,475-year MDE ground motion are shown in Figure 4-2. Also shown on this figure are the seven lowest vibration periods of the tower, indicating that spectral accelerations for the critical first and second modes of vibration are 0.275g and 0.34g, respectively.

The load combination for the seismic assessment of the tower consisted of the gravity plus seismic loads due to two horizontal components of ground motion combined as follows (EM1110-2-2400 [4]):

$$Q = Q_D \pm \sqrt{Q_{EX}^2 + Q_{EY}^2}$$

Where,

- Q = Peak value of forces and moments due to dead and seismic load
- Q_D = Effects resulting from dead load
- Q_{EX} = Effects resulting from horizontal response spectra in X-direction
- Q_{EY} = Effects resulting from horizontal response spectra in Y-direction

The vertical component of the ground motion was ignored, because its effects are negligible.

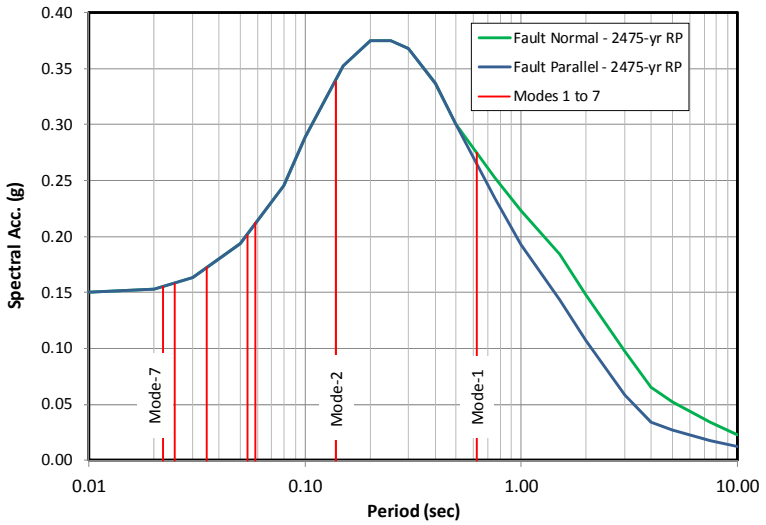

Figure 4-2. 5%-damped response spectra used as the seismic input.

5. SECTION CAPACITY

5.1 Moment Capacity

The axial force-moment or P-M interaction diagrams for the tower reinforced concrete sections were generated using the "Section Designer" feature of SAP2000. Reinforcement details for the outlet tower at different heights as provided in Drawings "Reinforcement Details Sheet A of job 52244" and "Arrangement of reinforced steel" (Drawing DH-1365-6) are used in the calculations of different section capacities (Table 5-1).

Twenty one (21) different sections are present in the model. Table 5-2 matches the element numbers with the corresponding section names used in SAP2000 model.

Table 5-1. Arrangement of reinforcement steel.

REINFORCING STEEL IN TOWER SHELL					
ZONE		STEEL IN EACH OF 2 ROWS			
ELEV. AT TOP	ELEV. AT BASE	HORIZONTAL RING BARS.		VERTICAL BARS.	
		SIZE	SPACING	SIZE	SPACING
585	576	1" ϕ	6"	¾" ϕ	18"
576	520	¾" ϕ	18"	"	"
520	510	"	15"	"	"
510	500	"	12"	"	12"
500	490	1" ϕ	18"	1" ϕ	18"
490	480	"	"	"	12"
480	470	"	"	1-¼" ϕ	18"
470	460	"	16"	"	"
460	450	"	14"	"	16"
450	440	"	13"	"	14"
440	430	"	12"	"	12"
430	420	"	"	"	"
420	410	"	"	"	"
410	400	"	"	"	"
400	BOTTOM	"	"	"	"

Table 5-2. Elevations and sections of elements.

Elevation (ft)	Element No.	Section Name	Elevation (ft)	Element No.	Section Name
392'-409'	1	FSEC1	505'-510'	12	FSEC11
409'-421'	2	FSEC1	510'-517'	13	FSEC12
421'-433'	3	FSEC2	517'-520'	14	FSEC13
433'-445'	4	FSEC3	520'-529'	15	FSEC14
445'-457'	5	FSEC4	529'-541'	16	FSEC15
457'-470.5'	6	FSEC5	541'-553'	17	FSEC16
470.5'-479'	7	FSEC6	553'-565'	18	FSEC17
479'-490'	8	FSEC7	565'-576.2'	19	FSEC18
490'-493'	9	FSEC8	576.2'-585'	20	FSEC19
493'-500'	10	FSEC9	585'-598.7'	21	FSEC20
500'-505'	11	FSEC10	598.7'-606'	22	CONE

The strength reduction factors (ϕ) for the calculation of P-M diagrams were used in accordance with Section 9.3.2 of ACI 318-11. The material properties discussed in Sections 2.1 and 2.2 were employed.

$$\phi_c = \begin{cases} \phi_c & \text{if } \varepsilon_t \le \varepsilon_y \\ \phi_t - (\phi_t - \phi_c)\left(\dfrac{0.005 - \varepsilon_t}{0.005 - \varepsilon_y}\right) & \text{if } \varepsilon_y < \varepsilon_t \le 0.005, \\ \phi & \text{if } \varepsilon_t \ge 0.005, \text{where} \end{cases} \qquad \text{(ACI 9.3.2)}$$

ϕ_t = ϕ for tension controlled sections, which is 0.90 by default (ACI 9.3.2.1)

ϕ_c = ϕ for compression controlled sections

= 0.70 (by default) for column sections with spiral reinforcement (ACI 9.3.2.2a)

= 0.65 (by default) for column sections with tied reinforcement

ε_t = Tensile strain in reinforcing steel

ε_y = Yield strain of reinforcing steel

The P-M interaction diagrams for Sections FSEC1 and FSEC18 with two different cross-section area and reinforcement details are shown in Figures 5-1 and 5-2, respectively. P-M interaction diagrams for the remaining sections can be found in Appendix B.

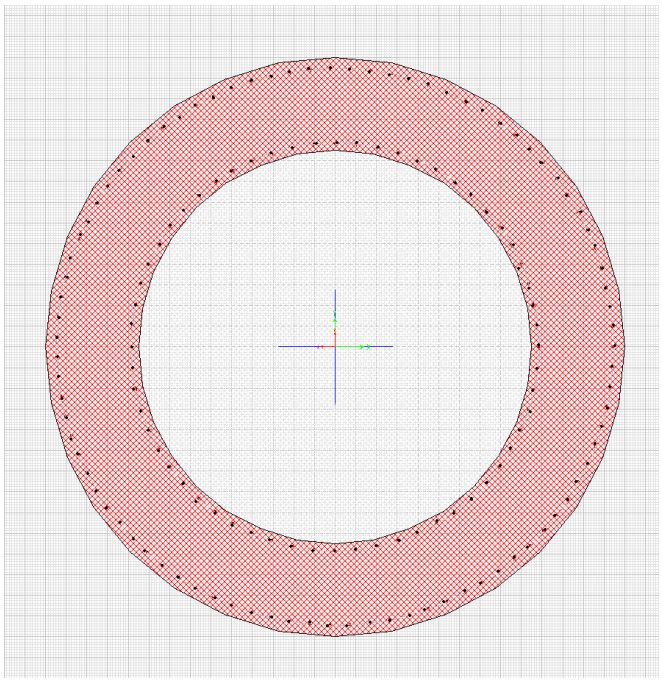

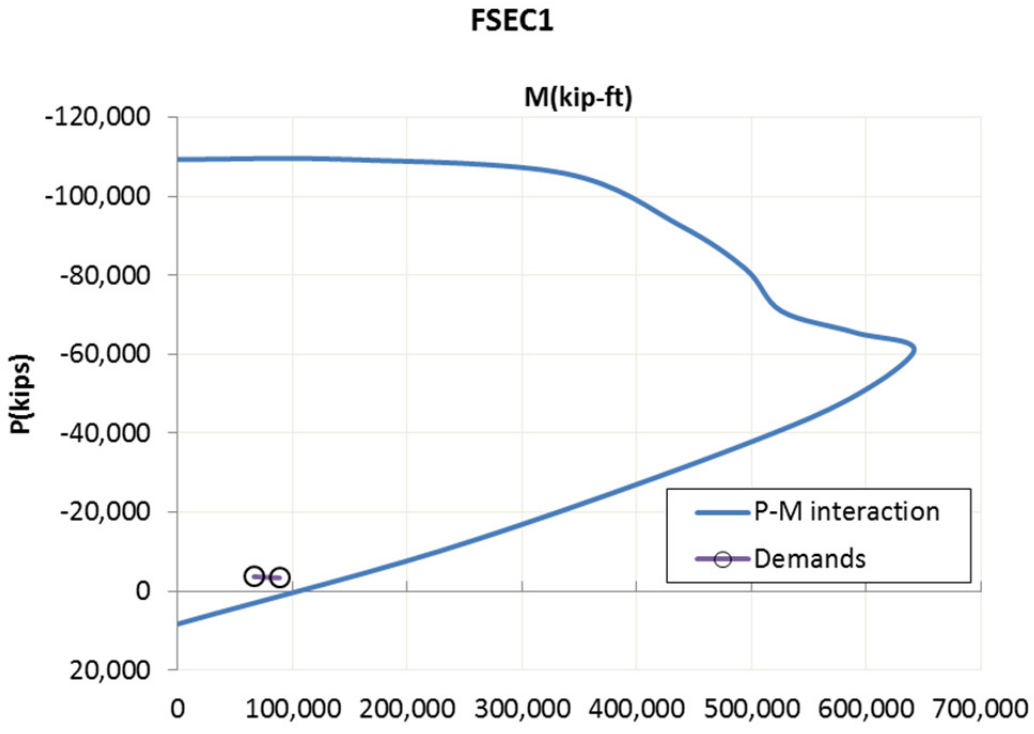

Figure 5-1. Axial force-moment diagram and reinforcement arrangements for Section FSEC1.

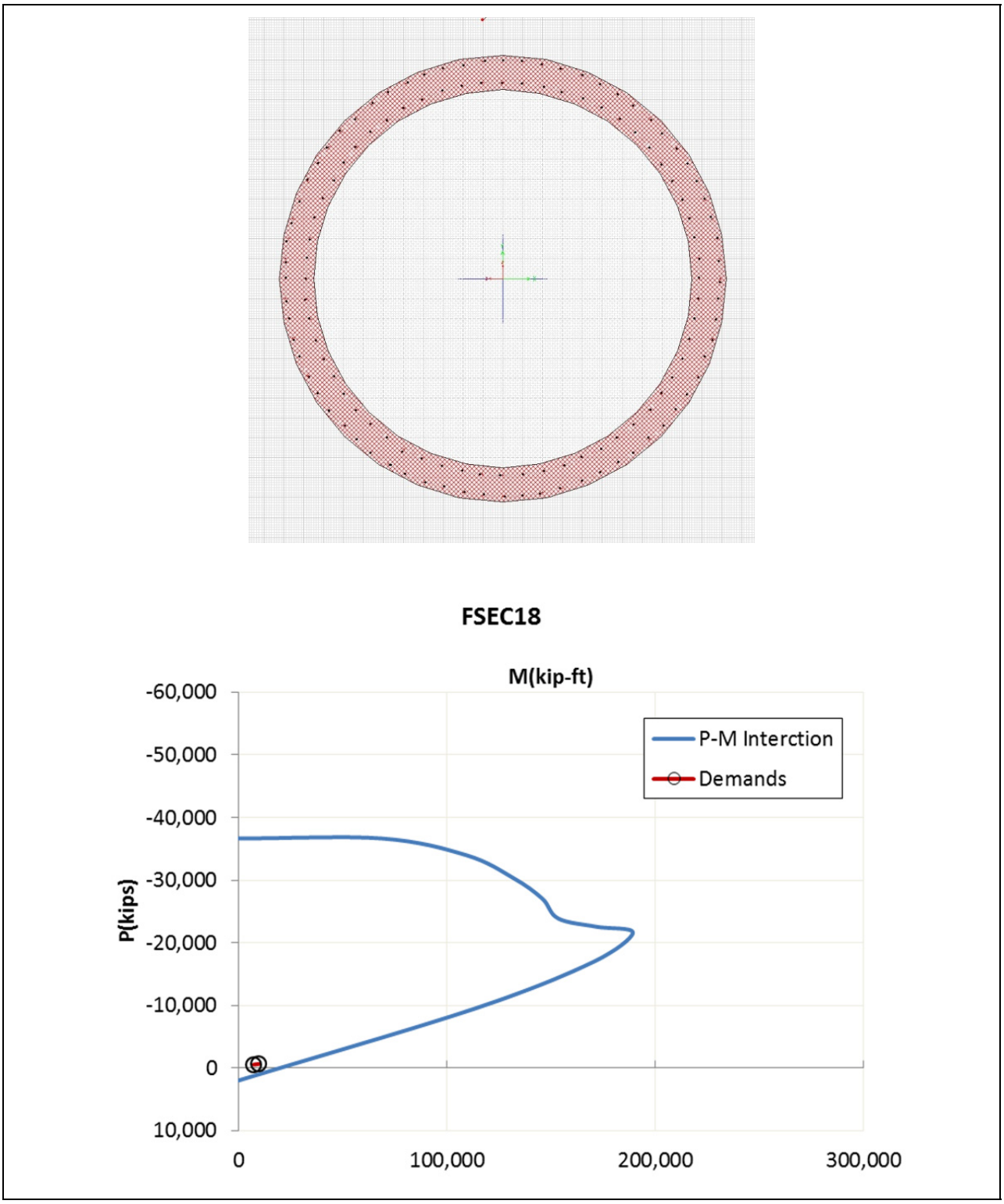

Figure 5-2. Axial force-moment diagram and reinforcement reinforcements for Section FSEC18.

5.2 Shear Capacity

Shear capacity of the tower section was calculated in accordance with Section 4.2 of the US Army Corps of Engineers Manual EM 1110-2-2400. The formula is expressed as:

$$V_U = 0.85(V_C + V_S)$$

where V_C is the shear contribution from the concrete and V_S is the shear contribution from the reinforcing steel. The concrete contribution to shear is given by:

$$V_c = 2\left[K + \frac{P}{2000A_g}\right]\sqrt{f'_{CA}}A_E$$

where

K = $\begin{cases} 1 \ for \ Rm = 1 \\ 0.5 \ for \ Rm = 2 \end{cases}$

P = Axial load on the section

f_{CA}' = Actual concrete compressive strength (typically $f_{cA}' \geq 1.5f_c'$)

A_E = 0.8 A_{gross}

In this report, K =0.5 and K=1 were used to determine whether flexure or shear would govern.

The reinforcing steel contribution to shear is obtained from:

$$V_S = \frac{\pi \, Ah \, (fy)(0.8 \, d)}{2s}$$

where

A_h = Horizontal reinforcement cross-section area

d = Outside diameter of the tower

f_y = Steel yield strength, 40 ksi

s = Spacing of reinforcement.

Shear capacities for K = 0.5 and 1 were calculated using the above method. The shear capacity results for all sections for the dead plus seismic load case are presented in Tables 6-2 and 6-3 with computed shear demands. The results show that K = 0.5 controls.

6. RESULTS: ESTIMATED FORCES/MOMENTS & DCR RATIOS

6.1 Moment Demands

With more than one station along the length of each element, multiple moment demands are obtained from the SAP2000 analysis along the height of tower. Table 6-1 summarizes moment demands computed at multiple locations and compares them with corresponding moment capacities. Also presented are the values of DCR (Demand Capacity Ratio) at each of these locations. Moment capacity of a section for a particular axial load is read off from its corresponding P-M interaction curve such as those shown in Figures 5-1 and 5-2. Moment demands listed in the table are for the combined effects of the dead load plus the SRSS combination of the seismic moments in the horizontal X and Y directions.

The tabulated results in Table 6-1 show that the moment demands exceed moment capacities at 15 different Sections FSEC2 to FSEC16. The peak moment reaches 194,942 kip-ft at El. 445 ft, 5 ft within the embedment. The moment DCR at the location of maximum moment is 1.68, which is not the largest. The largest moment DCR of 2.02 occurs at El. 510 ft, about 30 ft above the ground surface within the freestanding length of the tower. The same results are illustrated graphically in Figure 6-1, showing that moment demands exceed moment capacities over a length of about 125 ft from El. 425 ft to 545 ft.

6.2 Shear Demands

Table 6-2 summarizes shear demands computed at multiple locations and compares them with factored shear capacities estimated for an Rm=2 and K=0.5 in accordance with Section 5.2. Also included in the table are the shear DCR values. The shear demands and capacities are also compared graphically in Figure 6-2 along the height of tower. The results show that the seismic shear demands generally remain below the shear capacities, except within the embedded region between El. 421 to 427 ft where the tower is fully supported by the surrounding rock. The results for Rm=1 and K=1 are listed in Table 6-3, indicating shear demands are well within the shear capacities; thus K=1 does not control.

6.3 Demand Capacity Ratios

Demand capacity ratios for Rm =2 and K=0.5 are plotted in Figure 6-3 and for Rm =1 and K=1 in Figure 6-4 to facilitate assessment of the seismic performance. According to EM 1110-2-2400 specifications, a moment reduction factor of 2 (Rm=2) is applicable in the absence of brittle mode of failure such a shear. On this basis the seismic performance of the tower is acceptable if moment DCR is not exceeding 2 while shear DCR remains below unity. Figure 6-3 indicates that the moment DCR remains below 2 at all locations and reaches 2 at one location (El. 510 ft) where the corresponding shear DCR is 0.79. In fact, for all moment DCRs greater than 1.2 the corresponding shear demand-capacity ratios are less than unity or well within unity. In other words moment DCRs do not exceed 2 and those moment DCRs exceeding 1 correspond to shear demands well within the corresponding section shear capacities. Further, the slightly higher than unity shear DCR occurs locally and within the embedded portion of the tower with ample rock support. Thus it can be concluded that the results meet both the flexural and shear requirements of EM 1110-2-2400 and the tower would survive the postulated 2,475-year ground motion with some damage involving concrete cracking and steel yielding. The tower may experience some permanent displacement due to concrete cracking and steel yielding leading to small dislocation

and tilting, but it is unlikely that it would completely fail and overturn as indicated by displacement based analysis discussed later in Section 8.1.2.

Table 6-1. Moment capacities and uncracked-section moment demands

(*Rm* = 2, *K*=0.5: f_c' = 5 ksi, f_y = 40ksi).

Section Name	Elev. (ft)	Demand (kip-ft)	Capacity (kip-ft)	Moment DCR
FSEC1	392.0	15,545	155,298	0.10
	400.5	40,870	150,179	0.27
	409.0	66,322	145,475	0.46
	415.0	88,647	141,861	0.62
FSEC2	421.0	110,980	128,004	0.87
	427.0	135,320	125,051	1.08
FSEC3	433.0	159,668	125,893	1.27
	439.0	177,296	123,229	1.44
FSEC4	445.0	194,942	116,115	1.68
	451.0	181,865	113,555	1.60
FSEC5	457.0	168,892	100,447	1.68
	463.8	154,626	97,801	1.58
FSEC6	470.5	140,532	87,377	1.61
	474.8	131,926	85,802	1.54
FSEC7	479.0	123,405	73,183	1.69
	484.5	112,807	71,288	1.58
FSEC8	490.0	102,365	53,405	1.92
	491.5	99,635	52,899	1.88
FSEC9	493.0	96,917	52,545	1.84
	496.5	90,763	51,423	1.77
FSEC10	500.0	84,669	43,939	1.93
	502.5	80,497	43,166	1.86
FSEC11	505.0	76,355	39,616	1.93
	507.5	72,369	38,871	1.86
FSEC12	510.0	68,411	33,939	2.02
	513.5	63,143	32,950	1.92
FSEC13	517.0	57,927	31,841	1.82
	518.5	55,800	31,427	1.78
FSEC14	520.0	53,682	30,494	1.76
	524.5	47,707	29,340	1.63
FSEC15	529.0	41,803	27,641	1.51
	535.0	34,937	26,249	1.33
FSEC16	541.0	28,168	24,527	1.15
	547.0	22,793	23,276	0.98
FSEC17	553.0	17,484	21,562	0.81
	559.0	13,673	20,446	0.67
FSEC18	565.0	9,889	26,117	0.38
	570.6	7,398	25,186	0.29
FSEC19	576.3	4,914	16,645	0.30
	580.6	3,549	15,988	0.22
FSEC20	585.0	2,187	23,477	0.09
	591.9	1,188	22,324	0.05
	598.8	190	21,170	0.01

Table 6-2. Uncracked-section shear demand and shear capacity

(*Rm* = 2, *K*=0.5: f_c'=5 ksi, f_y = 40ksi).

Section Name	Elevation (ft)	Shear Capacity V_u (kips)	Shear Demand V_d (kips)	Shear DCR
FSEC1	392.0	4,022	2,999	0.75
	400.5	4,009	2,999	0.75
	409.0	3,993	3,362	0.84
	415.0	3,980	3,724	0.94
FSEC2	421.0	3,747	3,892	1.04
	427.0	3,515	4,061	1.16
FSEC3	433.0	3,445	3,507	1.02
	439.0	3,375	2,954	0.88
FSEC4	445.0	3,276	2,621	0.80
	451.0	3,176	2,289	0.72
FSEC5	457.0	3,012	2,262	0.75
	463.8	2,847	2,236	0.79
FSEC6	470.5	2,748	2,199	0.80
	474.8	2,653	2,162	0.82
FSEC7	479.0	2,584	2,111	0.82
	484.5	2,514	2,059	0.82
FSEC8	490.0	2,488	2,004	0.81
	491.5	2,466	1,950	0.79
FSEC9	493.0	2,424	1,912	0.79
	496.5	2,380	1,874	0.79
FSEC10	500.0	2,304	1,824	0.79
	502.5	2,229	1,775	0.80
FSEC11	505.0	2,198	1,732	0.79
	507.5	2,167	1,689	0.78
FSEC12	510.0	2,081	1,637	0.79
	513.5	1,994	1,584	0.79
FSEC13	517.0	1,973	1,537	0.78
	518.5	1,954	1,490	0.76
FSEC14	520.0	1,875	1,436	0.77
	524.5	1,794	1,381	0.77
FSEC15	529.0	1,727	1,279	0.74
	535.0	1,659	1,177	0.71
FSEC16	541.0	1,592	1,045	0.66
	547.0	1,524	914	0.60
FSEC17	553.0	1,457	777	0.53
	559.0	1,391	641	0.46
FSEC18	565.0	1,330	543	0.41
	570.6	1,270	444	0.35
FSEC19	576.3	1,151	363	0.32
	580.6	1,046	313	0.30
FSEC20	585.0	954	227	0.24
	591.9	836	145	0.17

Table 6-3. Uncracked-section shear demand and shear capacity

(*Rm* = 1, *K*=1: f_c'=5 ksi, f_y = 40ksi).

Section Name	Elevation (ft)	Shear Capacity V_u (kips)	Shear Demand V_d (kips)	Shear DCR
FSEC1	3390.9	6,839	2,999	0.44
	3390.9	6,827	2,999	0.44
	4116.2	6,810	3,362	0.49
	4116.2	6,797	3,724	0.55
FSEC2	4452.7	6,357	3,892	0.61
	4452.7	5,918	4,061	0.69
FSEC3	3345.6	5,782	3,507	0.61
	3345.6	5,647	2,954	0.52
FSEC4	2680.5	5,482	2,621	0.48
	2680.5	5,318	2,289	0.43
FSEC5	2627.9	5,082	2,262	0.45
	2627.9	4,845	2,236	0.46
FSEC6	2554.3	4,702	2,199	0.47
	2554.3	4,563	2,162	0.47
FSEC7	2451.1	4,436	2,111	0.48
	2451.1	4,309	2,059	0.48
FSEC8	2341.8	4,268	2,004	0.47
	2341.8	4,231	1,950	0.46
FSEC9	2265.9	4,153	1,912	0.46
	2265.9	4,073	1,874	0.46
FSEC10	2166.6	3,972	1,824	0.46
	2166.6	3,871	1,775	0.46
FSEC11	2081.2	3,815	1,732	0.45
	2081.2	3,759	1,689	0.45
FSEC12	1976.4	3,638	1,637	0.45
	1976.4	3,516	1,584	0.45
FSEC13	1882.1	3,481	1,537	0.44
	1882.1	3,447	1,490	0.43
FSEC14	1772.9	3,323	1,436	0.43
	1772.9	3,198	1,381	0.43
FSEC15	1569.0	3,072	1,279	0.42
	1569.0	2,946	1,177	0.40
FSEC16	1305.9	2,821	1,045	0.37
	1305.9	2,697	914	0.34
FSEC17	1032.9	2,573	777	0.30
	1032.9	2,450	641	0.26
FSEC18	836.3	2,337	543	0.23
	836.3	2,224	444	0.20
FSEC19	704.7	2,071	363	0.18
	704.7	1,935	313	0.16
FSEC20	537.2	1,815	227	0.12
	537.2	1,662	145	0.09

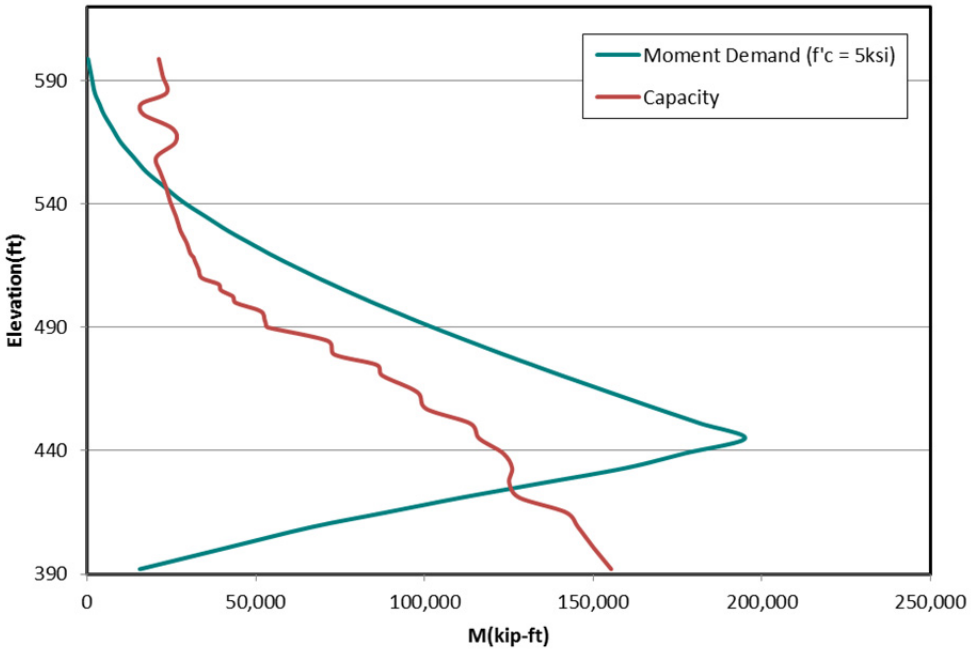

Figure 6-1. Comparison of bending moment demands and capacities (fc'=5 ksi, fy=40 ksi).

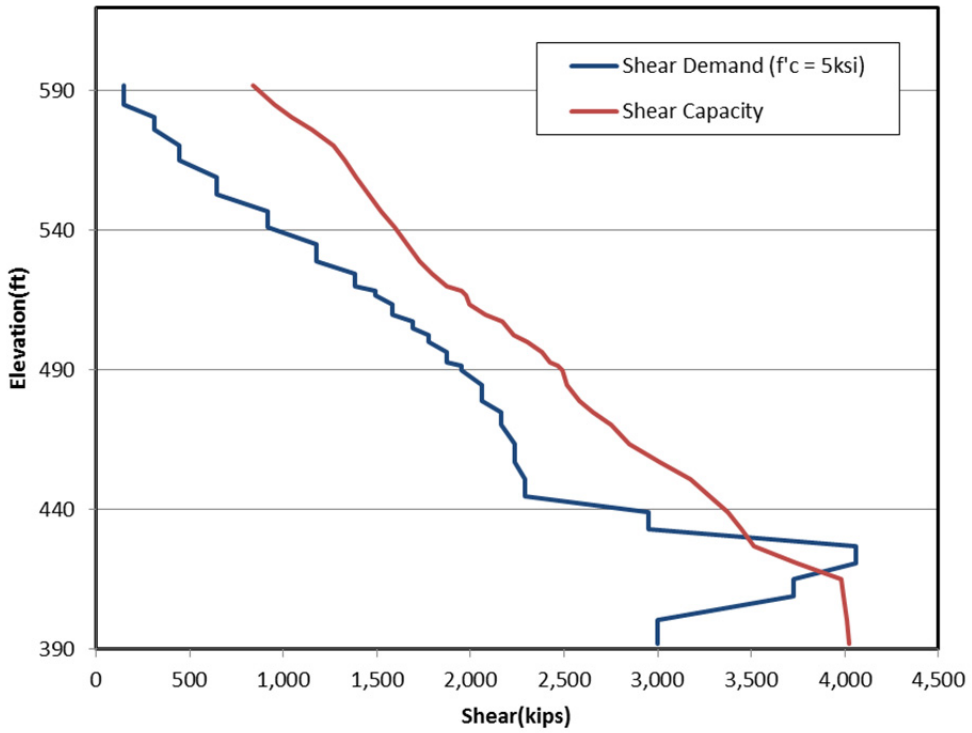

Figure 6-2. Comparison of shear demands and capacities (*Rm*=2, *K*=0.5: fc'=5 ksi, fy = 40 ksi).

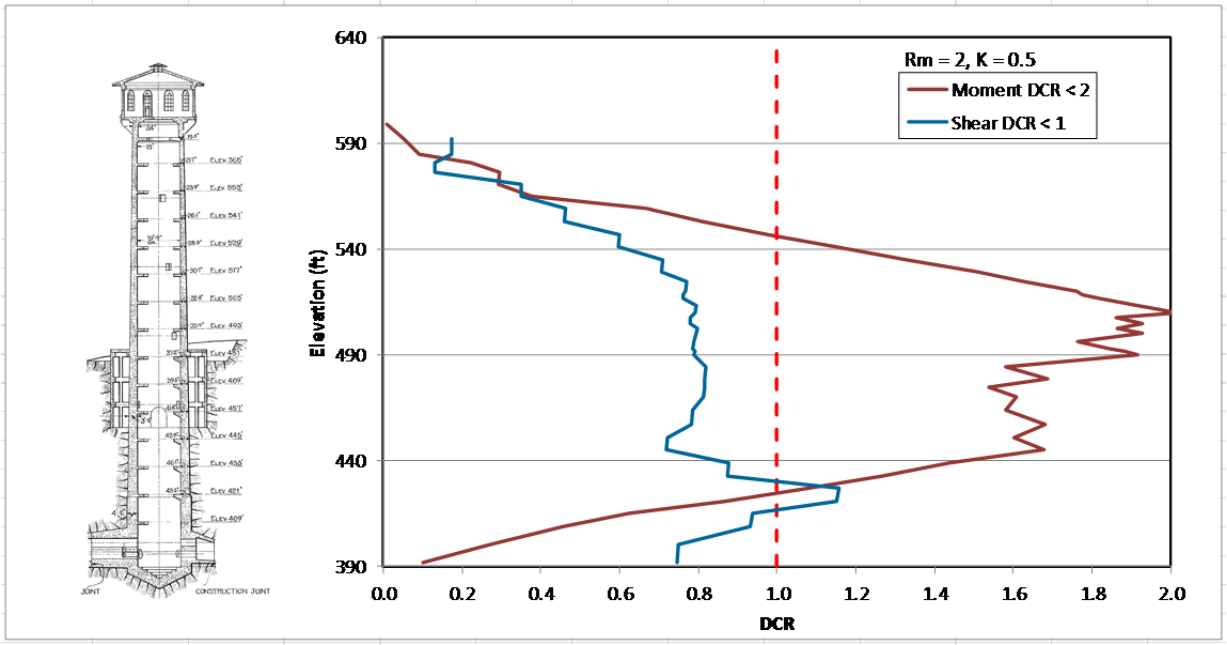

Figure 6-3. Moment and shear demand-capacity ratios for *Rm*=2 and *K*=0.5.

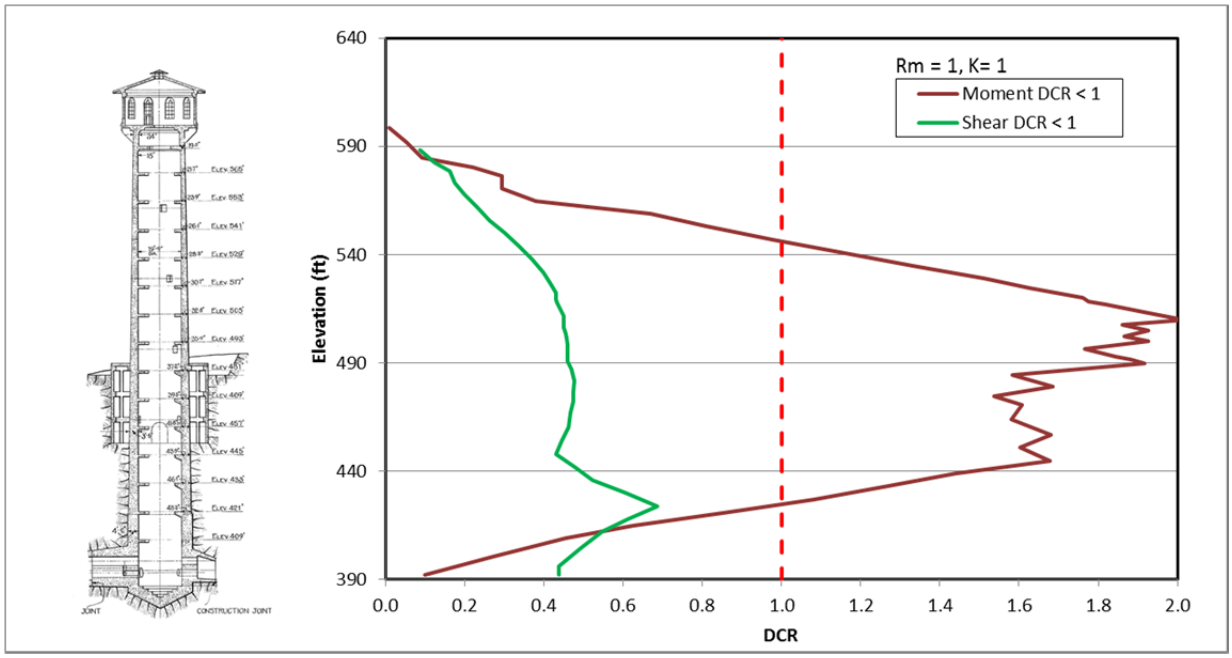

Figure 6-4. Moment and shear demand-capacity ratios for *Rm*=1 and *K*=1.

7. SENSITIVITY ANALYSES

Sensitivity analyses were performed to assess the effects that concrete strength, concrete cracking, and foundation flexibility might have on the seismic response of the tower.

7.1 Effects of Concrete Strength

The section force and moment demands discussed in Section 6 were obtained assuming a nominal compressive strength of 5,000 psi for the concrete. As discussed in Section 2, the concrete strength was varied by ± 25% to investigate the effects of a higher (6,250 psi) and lower (3,750 psi) strength on the moments and shears. The results for these three strength values are summarized in Figures 7-1 and 7-2.

As expected, moment demands and moment capacities are lower for the lower strength and higher for the higher strength concrete. However, variations of demands and capacities are low to modest and noticeable mainly in the regions of maximum demands (El. 445 ft) and maximum capacities (El. 390). From these results it can be concluded that the flexural response is not very sensitive to the concrete strength in the range of 3,750 to 6,250 psi and that the nominal value of 5,000 psi adopted in the analysis is reasonable.

Figure 7-2 shows that variation of concrete strength affects shear capacities more than shear demands. The results indicate a 25% increase in concrete strength would increase shear capacities by about 10% and shear demands by 6%. Inversely, a 25% decrease in concrete strength would decrease shear capacities by about 10% and shear demands by 6%. As such, the higher concrete strength has more positive effects on shear response than the lower concrete strength. In view of the excellent condition of the tower, actual concrete strength more likely is closer to 6,250 psi than the nominal value of 5,000 psi. Thus, the results for the 5,000 psi concrete discussed in Section 6 are somewhat conservative and the actual shear DCR's could be lower.

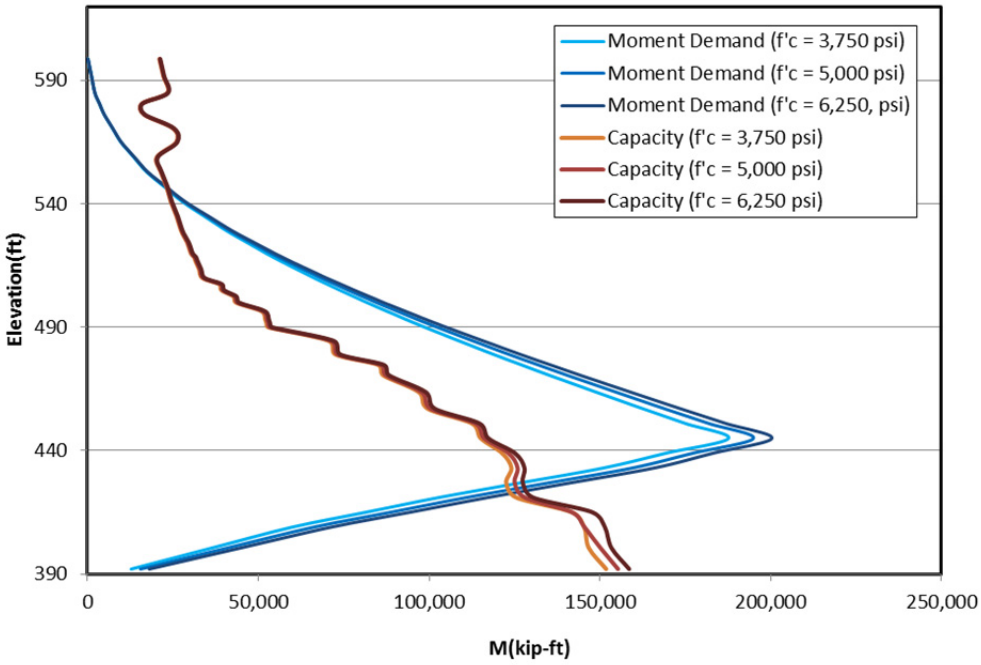

Figure 7-1. Comparison of moment demands with moment capacities for various concrete strengths.

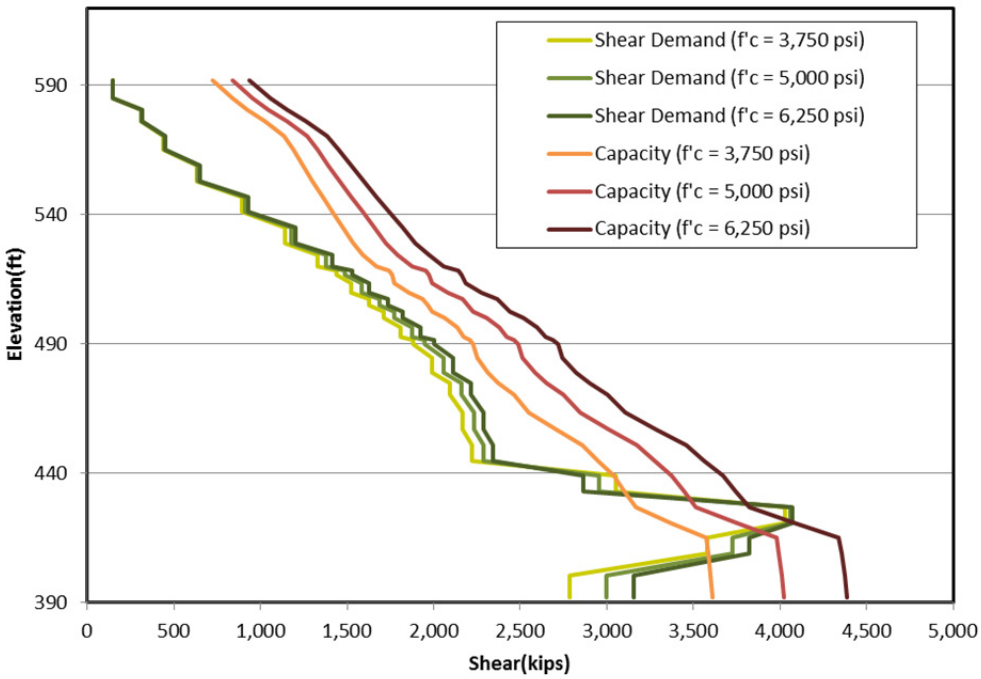

Figure 7-2. Comparison of shear demands with shear capacities for various concrete strengths.

7.2 Effects of Cracking

The results in Section 6 were produced with beam stiffness values using the gross section moment of inertia. If cracking and inelastic action are expected, the linear analysis may be conducted using reduced member stiffness values to reflect the degree of cracking and inelastic action. This is accomplished by replacing the gross moment of inertia with a reduced moment of inertia calculated using the equation provided in EM 1110-2-2400:

$$\frac{I_e}{I_g} = 0.8\text{-}0.9\left|\frac{M_N}{M_{cr}} - 1\right|$$

where, I_e is the moment of inertia of the cracked section, I_g is the moment of inertia of the gross section, M_N is the nominal moment, and M_{cr} is the cracking moment defined in Section 8.1.1.

As discussed in Section 8.1.1, M_N/M_{cr} <1 for all sections because of the light reinforcing, and if those values are substituted in the above equation, it will yield I_e/I_g values which are greater than 1. The EM 1110-2-2400 manual specifies that this ratio should always lie between 0.35 and 0.8. Since the calculated I_e/I_g ratios are greater than 1, the limiting values of 0.8 and 0.35 are used to determine sensitivity of results to the degree of cracking.

Two separate analyses were conducted, one with member stiffnesses reduced to $0.35EI_g$ and another to $0.80EI_g$. As expected, the reduced stiffnesses elongated the fundamental period of vibration and reduced seismic forces, resulting in lower moment and shear demands. The moment and shear demands for the full and reduced stiffnesses are displayed in Figures 7-3 and 7-4 and compared with the moment and shear capacities. Figure 7-5 displays moment and shear DCRs for all three cases.

The results indicate that the maximum moment for the uncracked section (194,942 kip-ft) has dropped 6% for the stiffness reduction of I_e/I_g=0.80 (to 183,470 kip-ft) and 24% for the stiffness reduction of I_e/I_g = 0.35 (to 147,595 kip-ft). The maximum moment DCR occurring at El. 510 ft is 2.0 for the uncracked section, 1.92 for I_e/I_g=0.80, and 1.60 for I_e/I_g = 0.35.

The shear demands in Figure 7-4 show that the maximum shear for uncracked section (4,060 kips) has dropped 2% for I_e/I_g=0.80 (to 3,995 kips) and 23% for I_e/I_g = 0.35 (to 3,140 kips). The maximum shear demand for I_e/I_g = 0.35 is less than the uncracked section shear capacity. It should be noted that the shear capacity is also reduced with cracking and yielding, but according to Paragraph 5-2d(2) of EM 1110-2-6053 [5] the shear capacity will not be less than the values obtained for K = 0.5 and listed in Table 6-2.

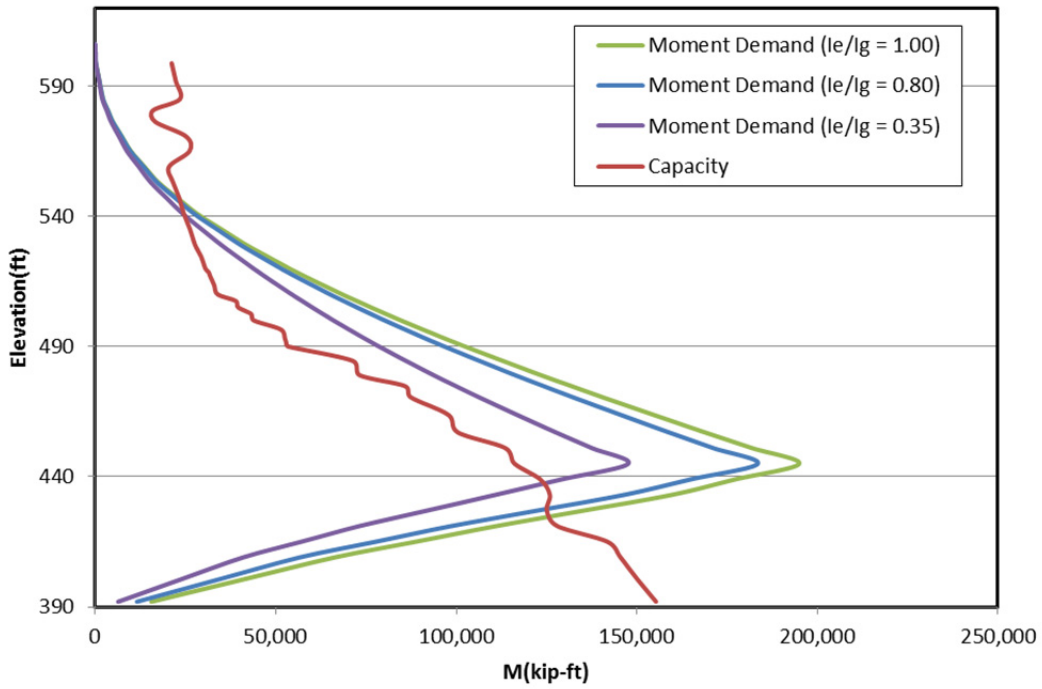

Figure 7-3. Comparison of cracked-section moment demands with moment capacities for various I_e/I_g ratios.

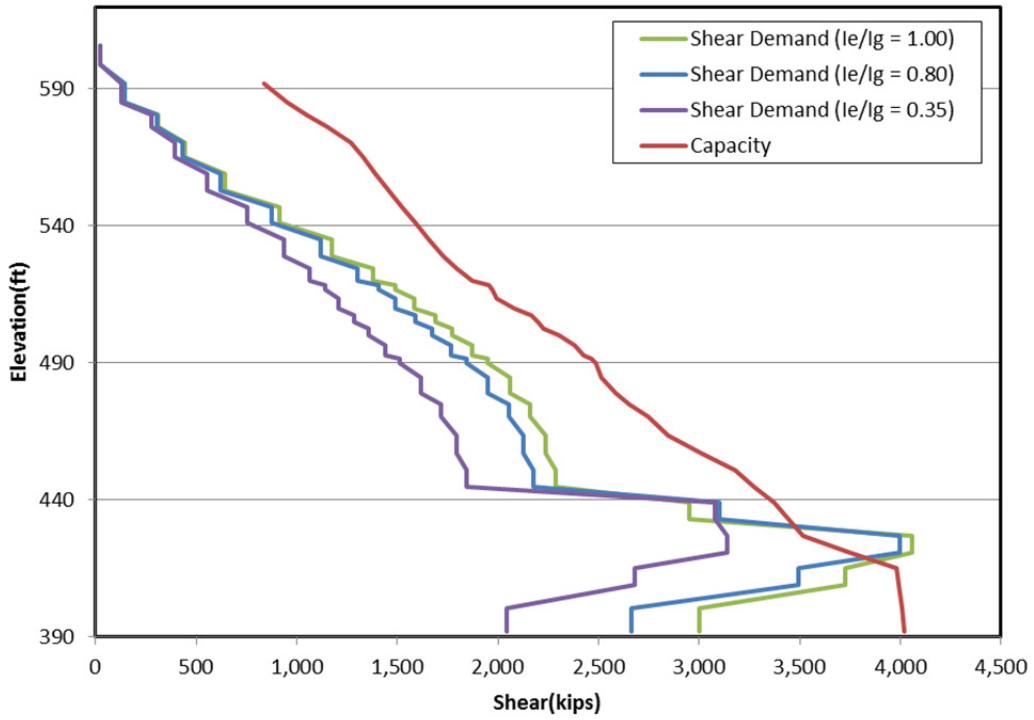

Figure 7-4. Comparison of cracked-section shear demands with shear capacities for various I_e/I_g ratios.

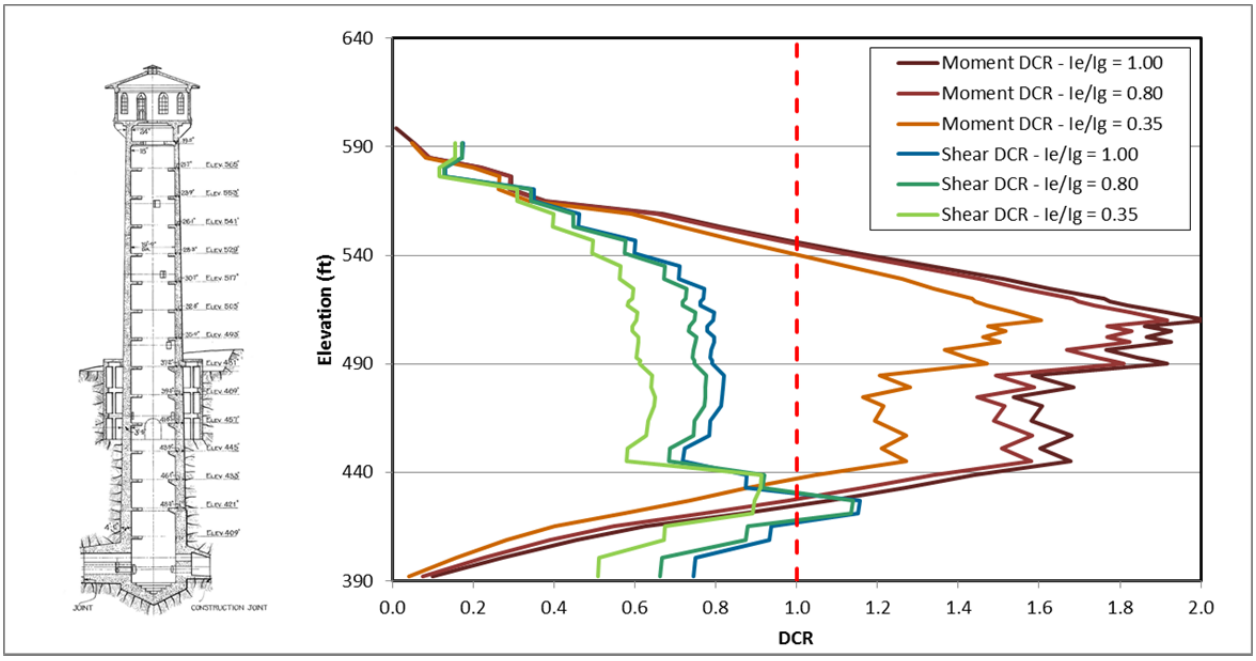

Figure 7-5. Moment and shear DCRs for cracked and uncracked sections.

7.3 Effects of Foundation Flexibility

The basic model discussed in Section 6 employed foundation springs distributed at intervals of 12 feet. To investigate the effects of foundation flexibility on the seismic response of the tower, the basic model was modified to distribute the springs at smaller intervals of 3 ft as well as reducing the spring constants by 50% to account for rock fractures and joints that usually are encountered near the ground surface. The purpose of closely spacing the springs was to better model the embedment in rock that provides a continuous lateral support for the tower and might have some influence on the magnitude and distribution of shear forces. The reason for reducing spring constant by 50% was that the analytical solution used to obtain stiffness values does not account for the lower in-situ rock modulus near the ground surface influenced by fractures and joints.

The modified model with 19 sets of lateral and vertical springs, instead of 4 sets used previously, is shown in Figure 7-6. The modified model was analyzed twice, once directly with the stiffness values provided by AMEC and discussed in Section 2.3, and then with stiffness values reduced by 50%. The moment and shear demands for both cases as well as for the base model are presented and compared with moment and shear capacities in Figures 7-7 and 7-8, respectively.

Figure 7-7 shows that reducing the spring spacing decreases the maximum moment by 4 to 5 percent. Also observed is that reducing the foundation spring stiffness by one-half, increases the moment demands by 1% at El. 445 ft and to 61% at El. 392ft, or mainly within the embedded region. However, this does not change the findings discussed previously for the base model in Section 6, because the

maximum moment changes very little and the maximum moment DCR which occurs at El. 510 remains the same.

Figure 7-8 compares shear demands for the three foundation spring cases with the shear capacities. The results show that decreasing the spring spacing reduces the maximum shear by 4% and that decreasing the foundation spring stiffness by one-half decreases the maximum shear by 16%. In fact the maximum shear demands for the 50% foundation spring stiffness remains below the shear capacity. As discussed previously, the reduced spring stiffness can be justified in the upper rock layer near the ground surface. On this basis the shear DCRs are less than 1, moment DCRs are equal or less than 2, and both meet the acceptance criteria.

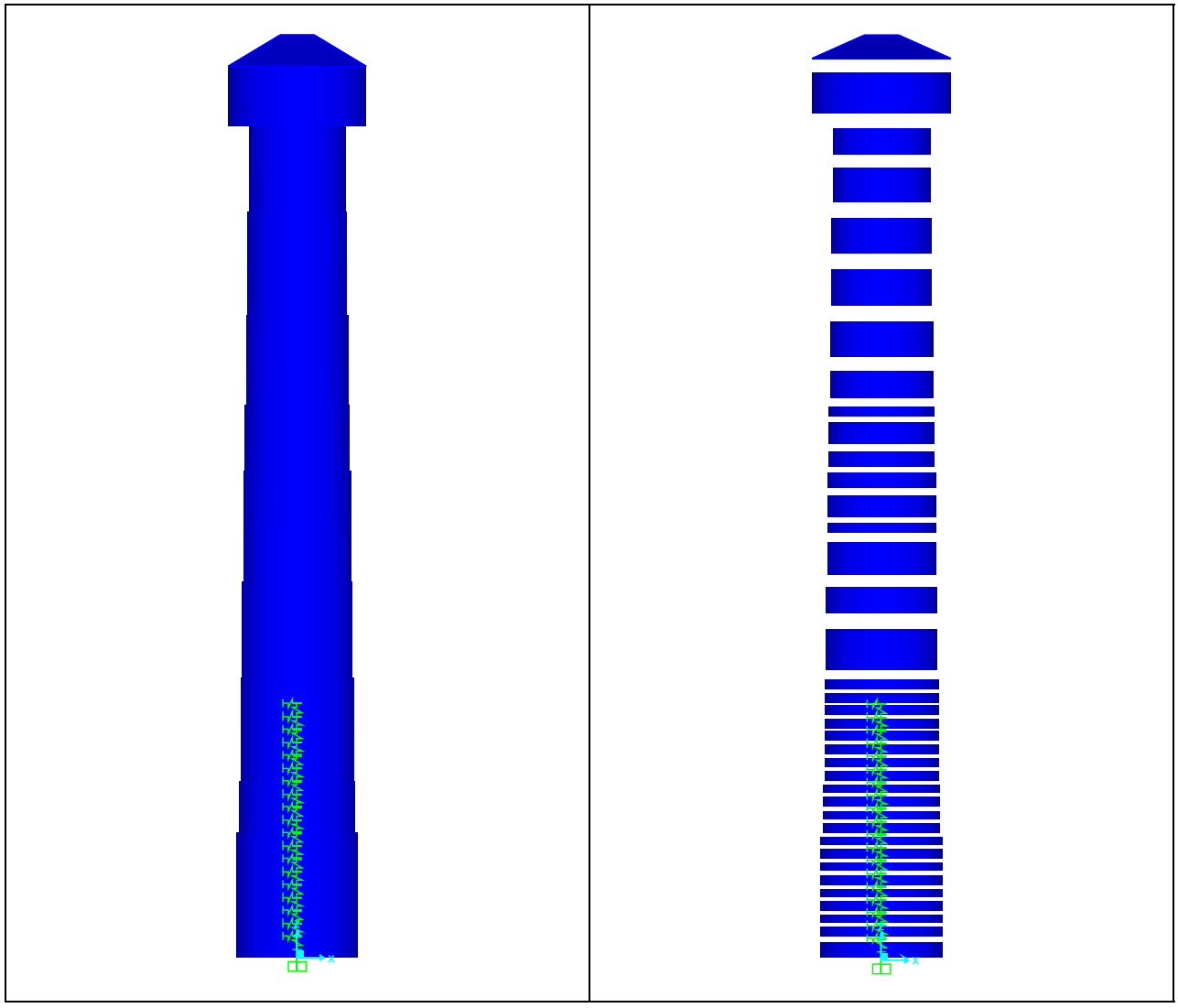

Figure 7-6. Model with foundation springs distributed at 3 feet.

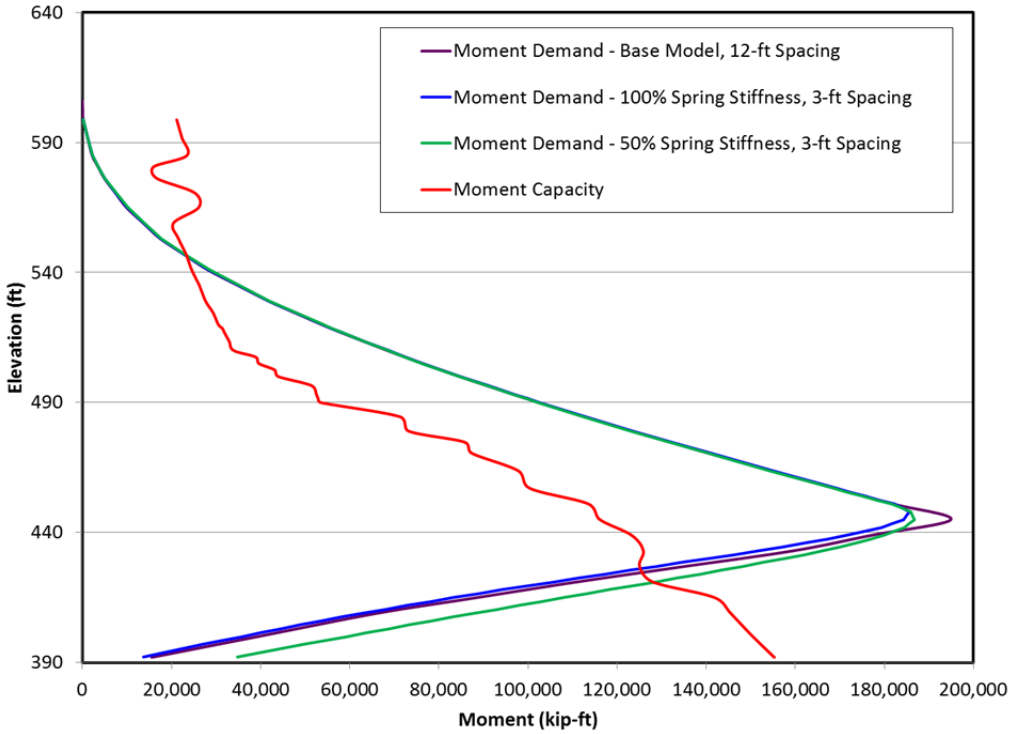

Figure 7-7. Comparison of moment demands for 100% and 50% foundation spring stiffness values with moment capacities.

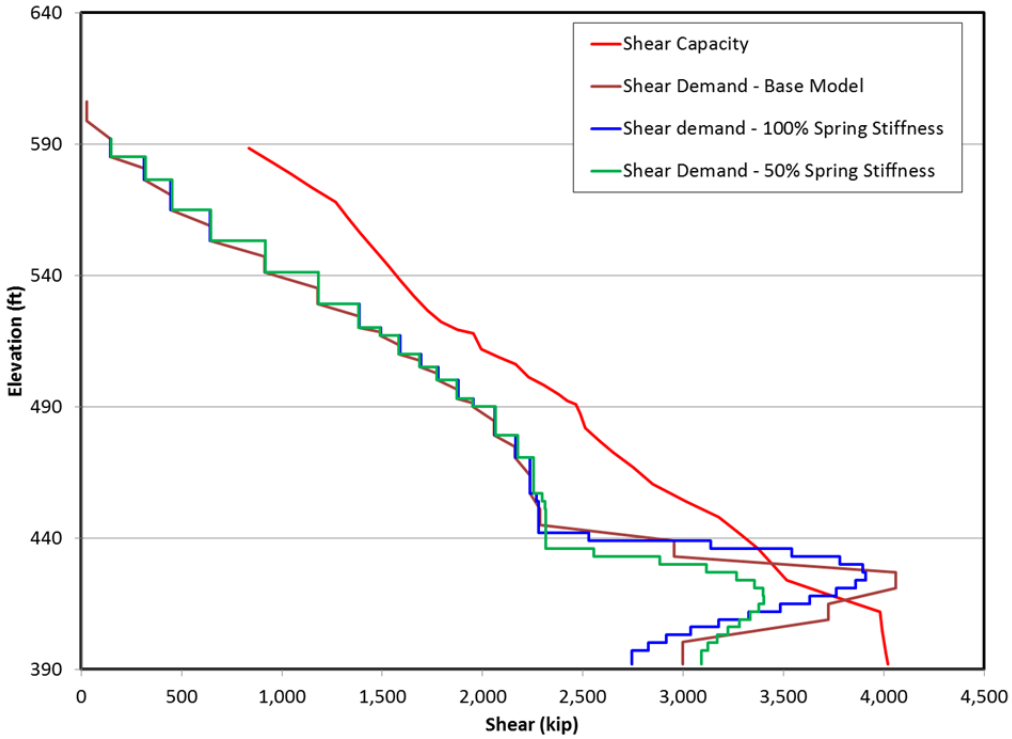

Figure 7-8. Comparison of shear demands for base model and 100% and 50% foundation spring stiffness values

with shear capacities.

8. FAILURE MODE CHECKS

8.1 Flexural Failure

8.1.1 Rupture of Reinforcement

According to EM 1110-2-2400 [4], the tensile reinforcement can fracture suddenly causing a brittle failure if the reinforcement ratio is less than 1% and the tower is subjected to seismic or other lateral loads generating a moment demand that exceeds the tower section moment capacity. To prevent such a failure mechanism, the nominal moment capacity (M_n) should equal or exceed the uncracked moment capacity (M_{cr}) by at least 20%.

M_{cr} is the cracking moment defined by

$$M_{cr} = \left(f_r + \frac{P}{A}\right) S$$

where, f_r is the concrete modulus of rupture, *P* is the axial load, *A* is the cross-section area and *S* is the section modulus of the gross section.

Shown below is a sample calculation of how the cracking moment of Section 'FSEC1' is calculated.

Inside radius (R_i)	=	114 in
Outside radius (R_o)	=	167.47 in
Area (*A*)	=	$\pi * (Ro^2 - Ri^2)$
	=	47,533 in^2
Moment of Inertia (*I*)	=	$\pi * (Ro^4 - Ri^4)/4$
	=	485,164,306 in^4
Section modulus (*S*)	=	*I*/*Ro*
	=	2,896,988 in^3
Concrete strength (f_c')	=	5000 psi
Rupture modulus (f_r)	=	531 psi
Axial load (*P*)	=	4499 kips
Cracking moment (M_{cr})	=	152,684 kip-ft.

Nominal moment (M_n) for the sections was obtained from their respective P-M interaction curves as the moment without strength reduction factor (Φ) at corresponding axial load.

Table 8-1 below presents the results of such calculations for all sections along with their reinforcement ratios. The results show that the nominal moment is less than the cracking moment for all sections except FSEC1 to FSEC4 located in the embedded portion of the tower where 1.25-inch square rebars at 12-inch spacing were used. The general criterion to avoid rupture of tensile reinforcement is to have a nominal moment at least 20% more than the cracking moment. It is noted that all the sections are lightly

reinforced with reinforcement area substantially less than 1% of the gross-section area and that the requirement $M_n/M_{cr} \geq 1.2$ is not met. In situations like this, a displacement based analysis is conducted to insure that the localized cracking and yielding does not result in displacement demands exceeding the ultimate displacement capacity at the top of the tower. Such a displacement based analysis was conducted for the Pardee Outlet Tower, as discussed in Section 8.1.2. The results indicate the tower has sufficient deformation capacity to resist the MDE displacement demand.

Table 8-1. Nominal and cracking capacities.

Section Name	P (kips)	A (in^2)	S (in^3)	M_{cr} (kip-ft)	Mn (kip-ft)	M_n/M_{cr}	Reinforcement ratio (ρ)
FSEC1	4,499	47,840	2,934,482	152,684	157,767	1.03	0.39%
FSEC2	3,724	40,797	2,466,359	127,760	130,068	1.02	0.40%
FSEC3	3,760	38,574	2,321,472	121,452	128,001	1.05	0.42%
FSEC4	4,000	36,372	2,179,288	116,284	117,890	1.01	0.39%
FSEC5	3,547	33,939	2,023,735	107,062	101,988	0.95	0.37%
FSEC6	3,073	32,425	1,927,749	100,420	88,714	0.88	0.34%
FSEC7	2,787	30,491	1,805,992	93,571	83,771	0.90	0.36%
FSEC8	2,439	29,971	1,773,455	90,403	60,444	0.67	0.23%
FSEC9	2,346	28,750	1,697,303	86,553	59,673	0.69	0.25%
FSEC10	2,137	27,892	1,644,046	83,154	49,447	0.59	0.17%
FSEC11	1,993	27,040	1,591,309	80,101	44,444	0.55	0.18%
FSEC12	1,853	25,845	1,517,668	76,140	37,729	0.50	0.15%
FSEC13	1,666	25,342	1,486,818	73,854	35,611	0.48	0.15%
FSEC14	1,586	23,837	1,394,799	69,375	34,159	0.49	0.16%
FSEC15	1,364	21,852	1,274,257	62,943	31,175	0.50	0.17%
FSEC16	1,092	19,906	1,157,055	56,425	27,991	0.50	0.19%
FSEC17	843	17,982	1,042,060	50,124	24,921	0.50	0.22%
FSEC18	620	16,216	937,238	44,407	31,208	0.70	0.35%
FSEC19	403	14,852	856,781	39,802	19,869	0.50	0.26%
FSEC20	213	14,024	1,264,796	57,497	28,646	0.50	0.28%

8.1.2 Displacement Based Analysis

In this method, the structure is assumed to crack at the critical section and rotate about the hinge formed at that location. From Table 6-1, it is evident that the highest moment is observed just below the screening chamber along section FSEC4. For the displacement calculations, it is assumed the tower cracks at El. 445 ft, base of FSEC4 (Figure 3-1). The elastic response of the tower above the crack is thus modeled as a different structure with a rotational spring at the base. The non-linear rotational stiffness is calculated using the moment curvature diagram of the cracked section obtained using "Section Designer" of SAP2000. The curvature values in the moment-curvature diagram are multiplied by the plastic length L_s, defined below, to obtain the moment-rotation diagram shown in Figure 8-2 (blue curve). Procedure laid out in EM 1110-2-2400 Paragraph 4-6e(9)(c)&(d) is followed.

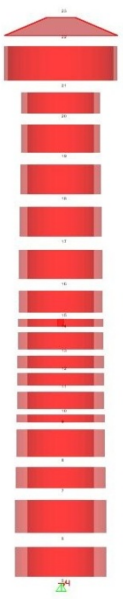

Figure 8-1. Displacement model.

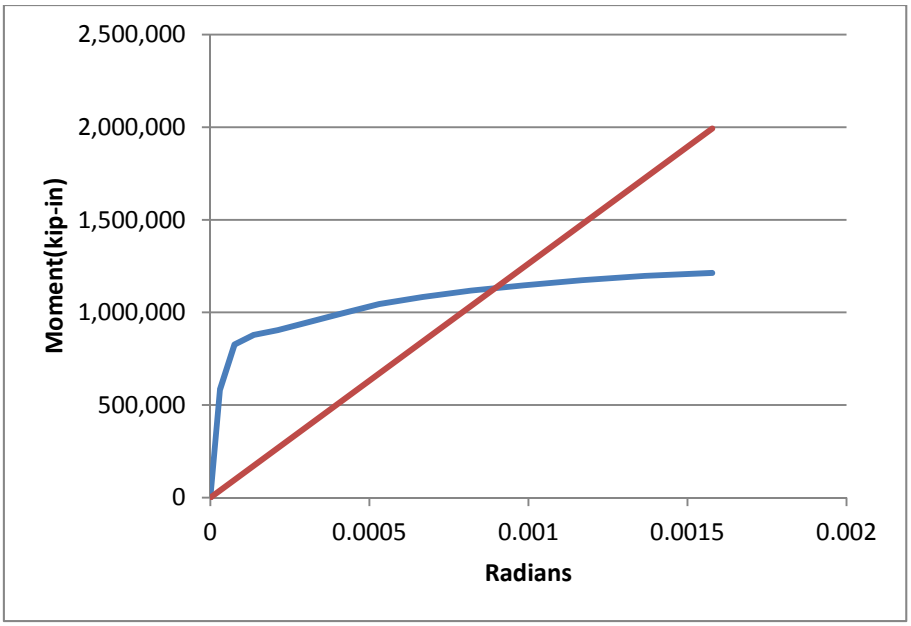

Figure 8-2. Bilinear and equivalent linear moment-rotation relation.

The ultimate crack width at failure is calculated as

C_u= 0.12+ 2.47 ε_u+ 0.312d_b

where,

ε_u = ultimate strain at failure of the bar, taken as 15%
d_b= diameter of the reinforcing in cm.

For #10 vertical reinforcement in FSEC4, C_u= 1.48 cm (0.58 in)

Now, the strain penetration length L_s can be calculated as $L_s = C_u/\varepsilon_u$. Substituting above values, L_s= 3.89 inches is obtained. The curvature values obtained from SAP 2000 are multiplied by L_s to get rotation in radians.

The area under the bilinear moment-rotation curve is calculated from the origin to maximum allowable rotation (1.58E-03 radians) and then a line is drawn from origin to the allowable rotation point so as to encompass the same area as the bilinear curve. The slope of this line then is the equivalent linear stiffness of the rotational spring. Figure 8-2 shows the moment-rotation relation for FSEC4. Figure 8-1 shows the new SAP model with the rotational spring introduced at El. 445 ft (Node 5) and no elements below it.

This new model is now subjected to the same set of ground motions. Note that the section properties of this model are same as the reduced section properties used in the cracked section analysis. The

extracted displacement values for the 'D+X+Y' (dead load+ SRSS combination of two horizontal motions) represent the displacement demands.

From SAP 2000, u_x=2.84 in
u_y=2.50 in

Therefore total displacement demand at the top of tower, $\delta_d = \sqrt{u_x^2 + u_y^2}$ = 3.78 in.

Displacement capacity is calculated as, $\delta_u = \frac{\Phi_E l^2}{3} + l\theta_p$

where,

δ_u = the ultimate displacement capacity
Φ_E= the elastic curvature at cracking = M/EI$_g$
l = the height of the tower above the crack (height of the new model)
θ_p= the plastic rotation at failure = $\frac{C_u}{l_w}$
l_w = depth of section, or in this case outside diameter for FSEC4

Substituting M_{cr} for FSEC4 in this equation, Φ_E= 1.25 x10^{-6}.
With l= 161 ft = 1,932 in, l_w=26 ft = 312 in, δ_u= 4.83 in.

Displacement demand = $\delta_d = 3.78\ in$ < δ_u = 4.83 in (displacement capacity).

This shows that the reinforcing steel will yield but the resulting displacement at the top of the tower caused by such yielding is less than the displacement capacity of the structure. On this basis rupturing of reinforcing steel is unlikely and the tower should survive the postulated ground motion with some concrete cracking and steel yielding that might result in some permanent tilting of the tower. It is believed such tilting would not be large enough to impede operation of the tower, but may require repair and strengthening for the long term functionality of the tower if the tower experiences the postulated MDE event and if a permanent deformation is observed.

8.2 Reinforcing Splice Failure Check

The minimum splice length required for existing towers as specified in section of EM 1110-2-2400 [4] is

$$l = \frac{1860 * db}{\sqrt{f'c}}$$

The calculated minimum splice lengths for the vertical #6, #8, and #10 bars are

$$l = \begin{cases} 19.7\ inches\ \ for\ \#6\ bars \\ 26.3\ inches\ for\ \#8\ bars \\ 32.8\ inches\ for\ \#10\ bars \end{cases}$$

"Drawing reinforcement details sheet A" shows the arrangement of reinforcement and the splice lengths in different parts of the outlet tower. The splice length increases from 3 ft to 5 ft along the height of the tower starting from the base. Minimum provided splicing of 36 inches (3') is more than the minimum required splice (33 in) as derived from the above formula. Hence, the lap splice will not fail.

8.3 Sliding Shear Failure

This failure refers to the potential for sliding along a horizontal crack that could develop within the structure. Nominal sliding shear strength along such a horizontal crack within the tower can be calculated using the equation 4.19 of EM 1110-2-2400 [4].

$$V_{SL}=\mathrm{P}+0.25 f_y A_{VF}$$

where,

V_{SL} = nominal sliding shear strength
P = Axial load on section
f_y = yield strength of reinforcement
A_{VF} = Area of shear friction reinforcement

The above calculated shear strength should be less than $0.01\sqrt{f'c}\ \mathrm{A_g}$ to avoid sliding along all sections.

Table 8-2. Sliding shear strength.

Section Name	V_{SL} (kips)	$0.01\sqrt{f'c}\mathrm{A_g}$ (kips)	V_{SL}< $0.01\sqrt{f'c}\mathrm{A_g}$?	Section Name	V_{SL} (kips)	$0.01\sqrt{f'c}$ $\mathrm{A_g}$ (kips)	V_{SL}< $0.01\sqrt{f'c}\mathrm{A_g}$?
FSEC1	6,367	33,828	OK	FSEC11	2,473	19,118	OK
FSEC2	5,363	28,850	OK	FSEC12	2,232	18,278	OK
FSEC3	5,386	27,274	OK	FSEC13	2,045	17,920	OK
FSEC4	5,410	25,720	OK	FSEC14	1,960	16,855	OK
FSEC5	4,779	23,998	OK	FSEC15	1,734	15,454	OK
FSEC6	4,165	22,928	OK	FSEC16	1,462	14,074	OK
FSEC7	3,867	21,560	OK	FSEC17	1,231	12,717	OK
FSEC8	3,126	21,190	OK	FSEC18	1,184	11,464	OK
FSEC9	3,049	20,331	OK	FSEC19	782	10,503	OK
FSEC10	2,617	19,723	OK	FSEC20	606	9,917	OK

It is clear from the above table that V_{SL}< $0.01\sqrt{f'c}\ \mathrm{A_g}$ for all the tower sections. Hence, sliding shear is not a failure mode for this structure.

8.4 Anchorage Length

The minimum required anchorage length for vertical reinforcement can be calculated using Equation 4.11 of EM 1110-2-2400 [4] as:

$$l_a = \frac{k_s d_b}{\sqrt{f_c'}\left(1+2.5\frac{2}{d_b}\right)} \quad \text{(psi units)}$$

where

l_a = minimum required effective anchorage length in inches.

$k_s = \frac{(f_y - 11000)}{4.8}$ = 6,042 for f_y = 40,000 psi

d_b = nominal bar diameter in inches

Substituting all the values, l_a =21.36 in = 2. 09 ft.

From Drawing "Reinforcement Details Sheet A," the vertical reinforcement starts at elevation 387 ft and provides about 5 ft of anchorage length at the bottom of the tower. Hence, anchorage failure is not one of the failure modes.

8.5 Spalling

According to Paragraph 4-6e(7) of EM 1110-2-2400 [4], compressive spalling failures will not occur at ultimate load conditions if the concrete compressive strains are less than 0.4%, or if the location of neutral axis is less than 15% of the effective depth to the centroid of the reinforcement i.e.,

$$\frac{c}{d} \leq 0.15$$

where

c = distance from extreme compression fiber to the neutral axis, and
d = distance from extreme compression fiber to the centroid of tension reinforcement.

For FSEC4, the critical section in flexure, the neutral axis depth was extracted from the "SpColumn" software as *c* = 27.02 in; and *d* was calculated as the sum of outer radius and average of y-coordinates of the reinforcement bars in tension, *d* = 171.2 in. Thus *c*/*d* = 0.157. The computed *c*/*d* ratio is very close to required value of 0.15, thus it meets the criteria indicating that spalling should not occur.

8.6 Summary of Failure Modes

Table 8-3 summarizes the modes of failure for all the critical sections. It is evident that all the sections are safe against shear, splice failure, and sliding shear. The moment DCRs for several sections exceed one but not two (see Table 6-1), indicating acceptable level of steel yielding. All M_n/M_{cr} ratios are less than the desired value of 1.2, indicating a displacement-based evaluation is needed to check the potential for steel rupture. The displacement-based evaluation is discussed in Section 8.1.2 with the results indicating that the maximum displacement demand is less than the ultimate displacement capacity of the tower. Thus it is concluded that reinforcing steel may experience yielding but would not rupture.

Table 8-3. Failure check for critical sections.

Mode of Failure	Meets Criteria?	Section
Shear	**OK**	**6**
Flexural	**OK ; 1<DCR ≤ 2**, indicates steel yielding	**6**
Rupture of steel	**M_n/M_{cr} < 1.2**; perform displacement-based analysis	**8.1**
Splice	**OK**	**8.2**
Sliding shear	**OK**	**8.3**
Anchorage	**OK**	**8.4**
Spalling	**OK**	**8.5**

9. REFERENCES

[1] Dames & Moore (1987), “Final Report – Preliminary Seismic Evaluation, Pardee Outlet Tower and Tunnel for East Bay Municipal Utility District,” February 12, 1987.

[2] AMEC (2012),”Technical Memorandum No. 1 – Summary of Geologic/Geotechnical Site Conditions and Recommendations for Foundation Properties and Rock Springs,” August 7, 2012.

[3] Goyal, A., and Chopra A.K. (1989), ”Earthquake Analysis and Response of Intake-Outlet Towers,” report No. UCB/EERC-89-04, Earthquake Engineering Research Center, University of California, Berkeley.

[4] EM 1110-2-2400, “Engineering and Design – Structural Design and Evaluation of Outlet Works,” US Army Corps of Engineers, 02 June 2003.

[5] EM 1110-2-6053, “Earthquake Design and Evaluation of Concrete Hydraulic Structures,” US Army Corps of Engineers, 1 May 2007.

Appendix A

Appendix A: Mass calculation of shelves and brackets

Left-side **shelf**

Thickness	12	inches
Maxm width	34	inches

Right-side **shelf**

Minm th	12	inches
Maxm th	27	inches

Area of the triangle	45.12	ft^2
Area of the sector	71.67	ft^2
Area of shelf	26.55	ft^2

Volume of shelf	26.55	ft^3
Weight of shelf	3.9825	kips

Number of **brackets** between elev 576.25ft and 585 ft 20

Area of each bracket	18.5	ft^2
Volume	27.75	ft^3
Weight	4.1625	kips
Total Weight	83.25	kips
Mass	2.59	kips.s^2/ft

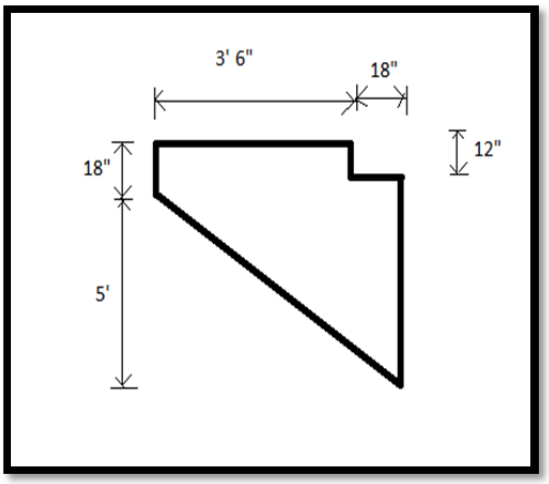

Operating house has 9 windows and 1 door

Approximate size of the window	6.5' x4'	
Approximate size of the door	9.5'x 4'	
Total surface of the operating house	1382.301	
Surface area of Openings	272	
Net Surface area	1110.301	80.32%

APPENDIX B

Appendix B: P-M interaction diagrams for all sections

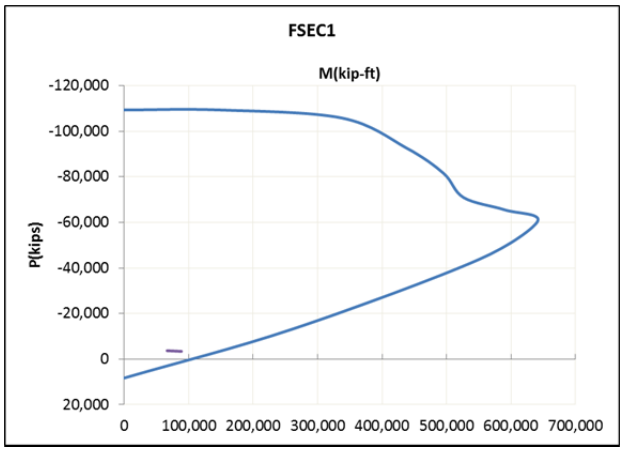

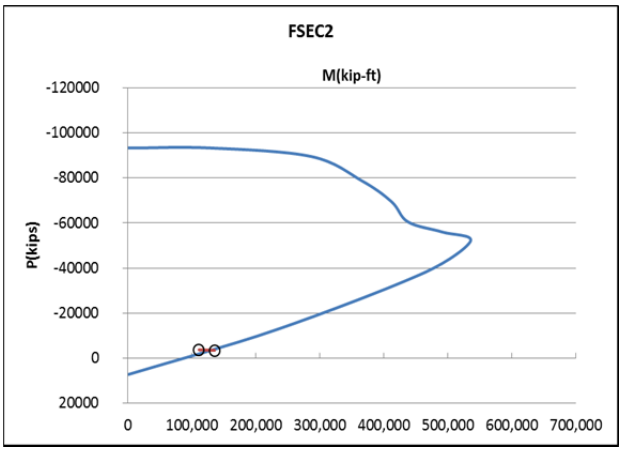

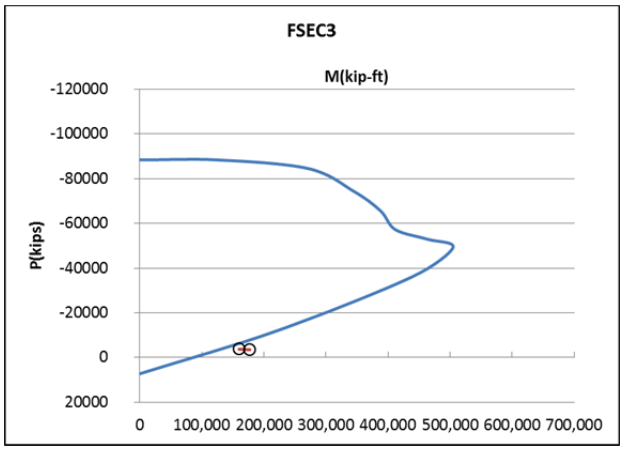

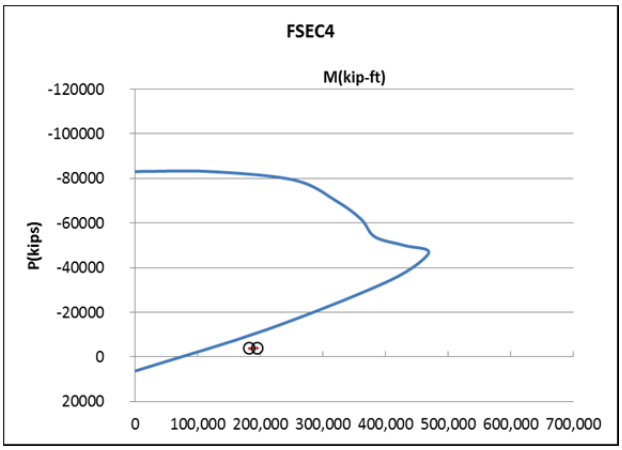

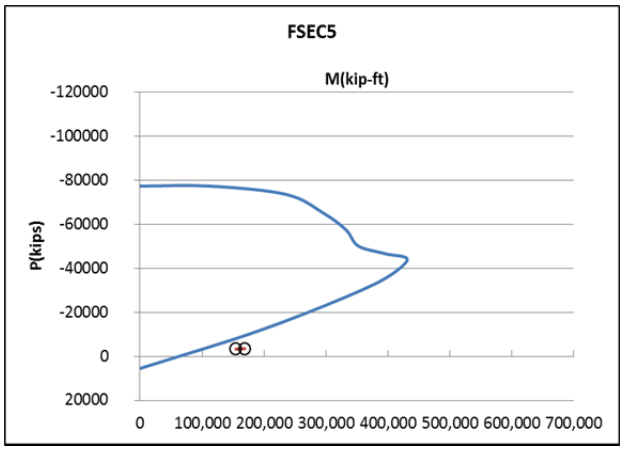

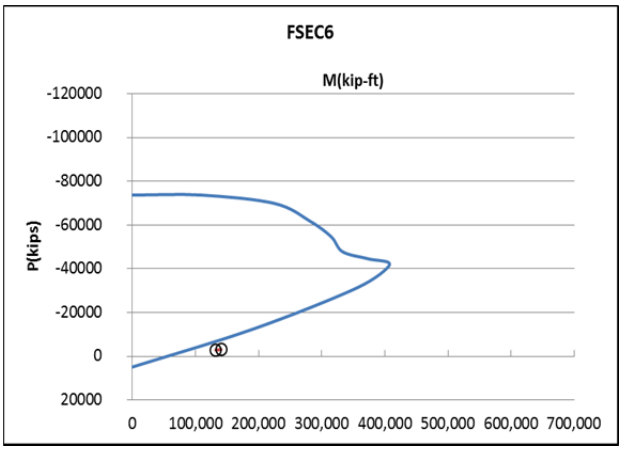

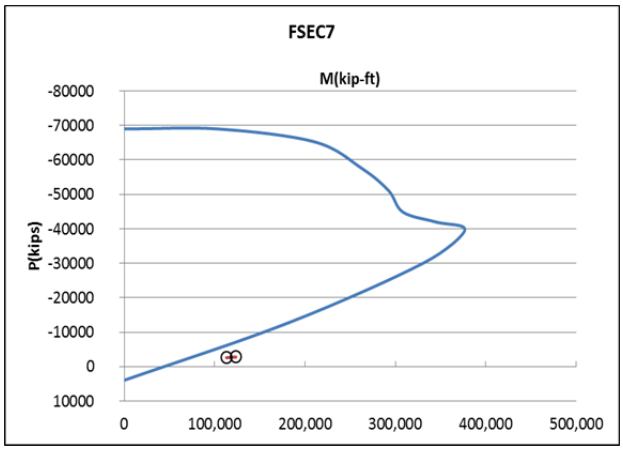
FSEC7
M(kip-ft)
P(kips)
-80000
-70000
-60000
-50000
-40000
-30000
-20000
-10000
0
10000
0
100,000
200,000
300,000
400,000
500,000

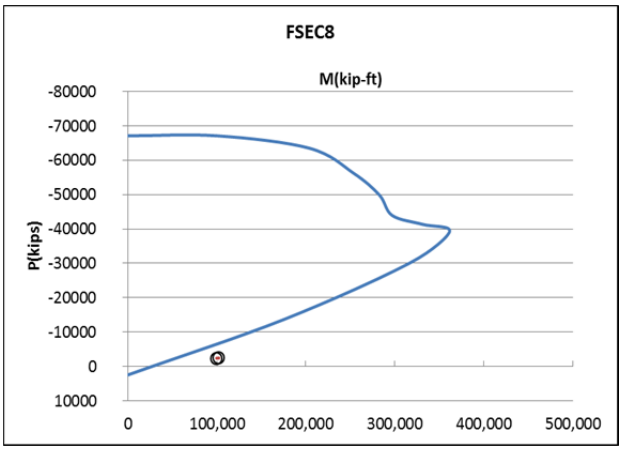
FSEC8
M(kip-ft)
P(kips)
-80000
-70000
-60000
-50000
-40000
-30000
-20000
-10000
0
10000
0
100,000
200,000
300,000
400,000
500,000

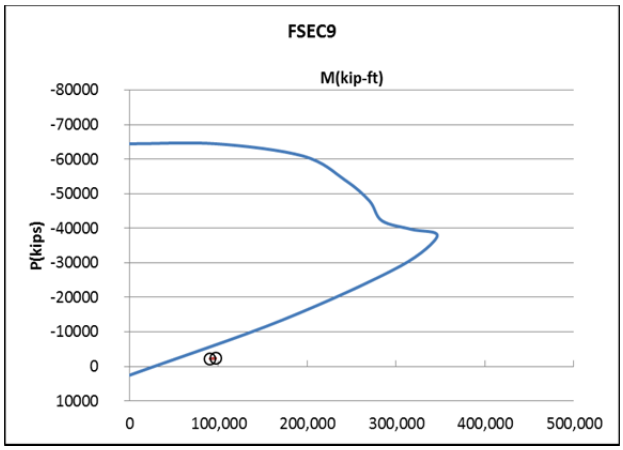
FSEC9
M(kip-ft)
P(kips)
-80000
-70000
-60000
-50000
-40000
-30000
-20000
-10000
0
10000
0
100,000
200,000
300,000
400,000
500,000

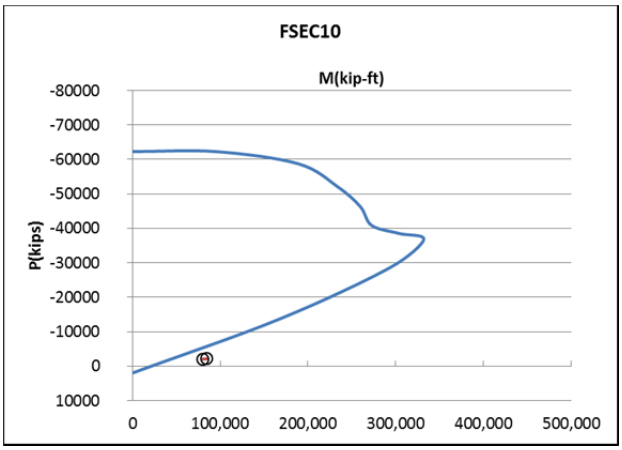
FSEC10
M(kip-ft)
P(kips)
-80000
-70000
-60000
-50000
-40000
-30000
-20000
-10000
0
10000
0
100,000
200,000
300,000
400,000
500,000

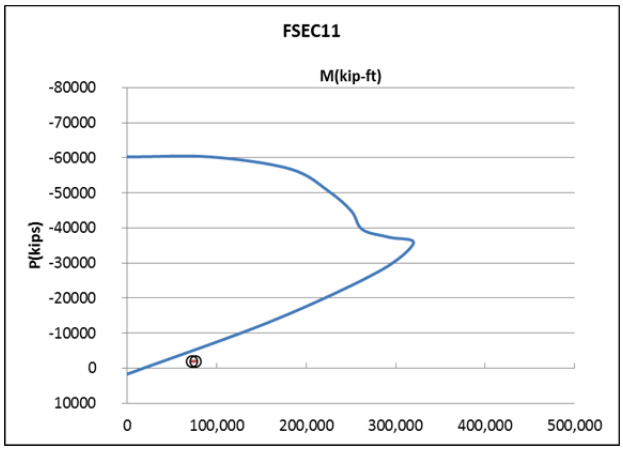
FSEC11
M(kip-ft)
P(kips)
-80000
-70000
-60000
-50000
-40000
-30000
-20000
-10000
0
10000
0
100,000
200,000
300,000
400,000
500,000

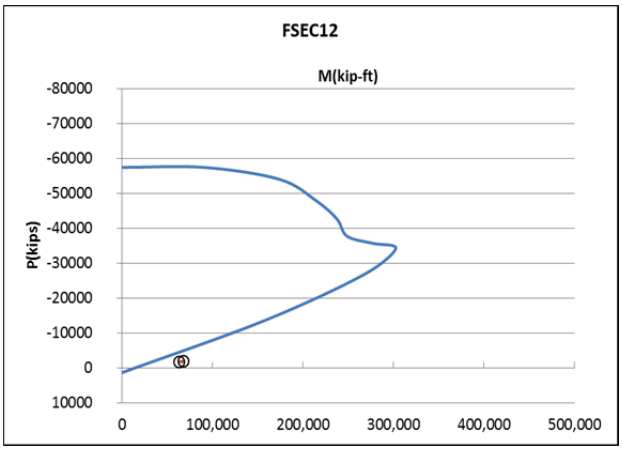
FSEC12
M(kip-ft)
P(kips)
-80000
-70000
-60000
-50000
-40000
-30000
-20000
-10000
0
10000
0
100,000
200,000
300,000
400,000
500,000

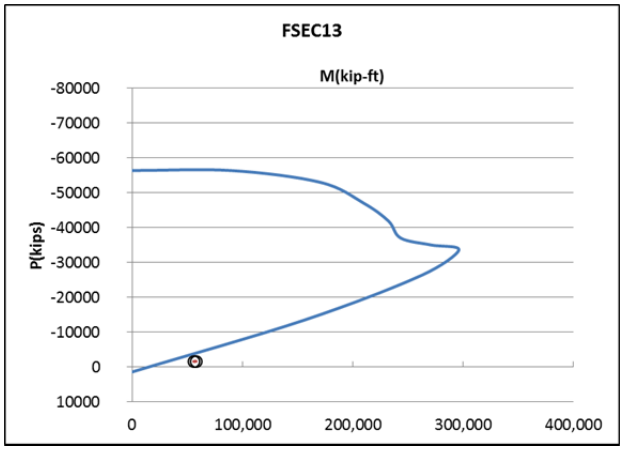
FSEC13
M(kip-ft)
P(kips)
-80000
-70000
-60000
-50000
-40000
-30000
-20000
-10000
0
10000
0
100,000
200,000
300,000
400,000

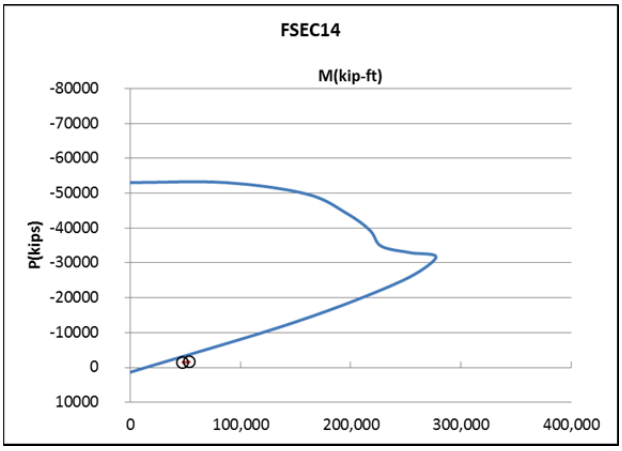
FSEC14
M(kip-ft)
P(kips)
-80000
-70000
-60000
-50000
-40000
-30000
-20000
-10000
0
10000
0
100,000
200,000
300,000
400,000

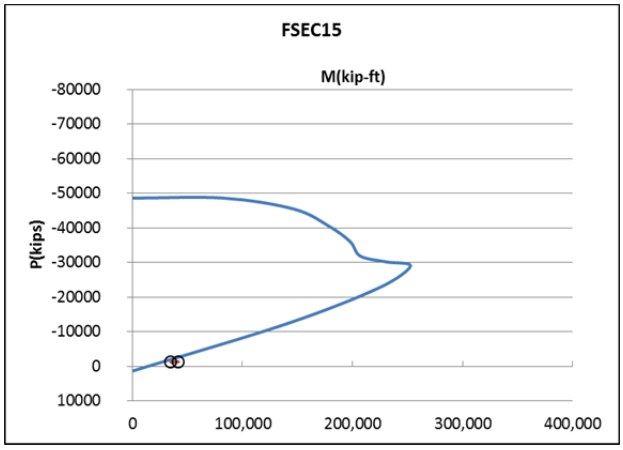
FSEC15
M(kip-ft)
P(kips)
-80000
-70000
-60000
-50000
-40000
-30000
-20000
-10000
0
10000
0
100,000
200,000
300,000
400,000

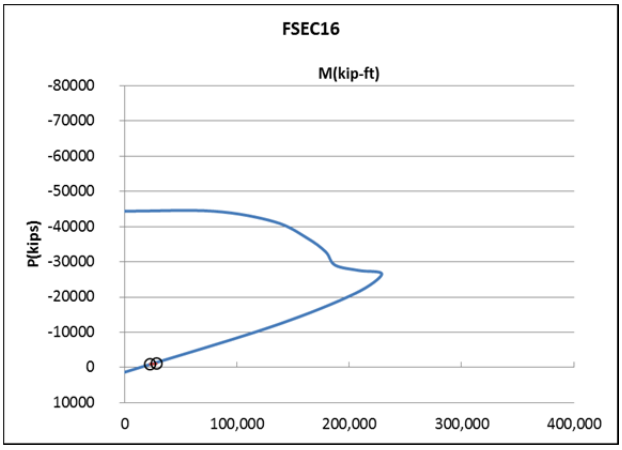
FSEC16
M(kip-ft)
P(kips)
-80000
-70000
-60000
-50000
-40000
-30000
-20000
-10000
0
10000
0
100,000
200,000
300,000
400,000

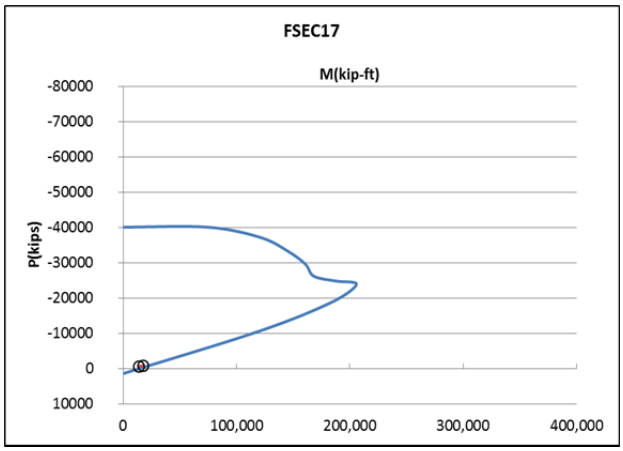
FSEC17
M(kip-ft)
P(kips)
-80000
-70000
-60000
-50000
-40000
-30000
-20000
-10000
0
10000
0
100,000
200,000
300,000
400,000

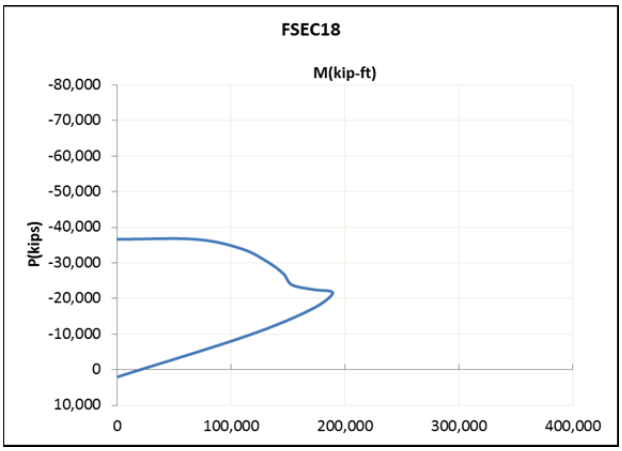
FSEC18
M(kip-ft)
P(kips)
-80,000
-70,000
-60,000
-50,000
-40,000
-30,000
-20,000
-10,000
0
10,000
0
100,000
200,000
300,000
400,000

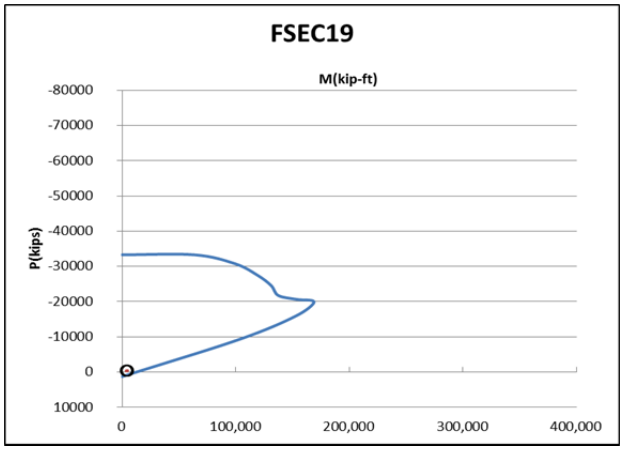
FSEC19
M(kip-ft)
P(kips)
-80000
-70000
-60000
-50000
-40000
-30000
-20000
-10000
0
10000
0
100,000
200,000
300,000
400,000

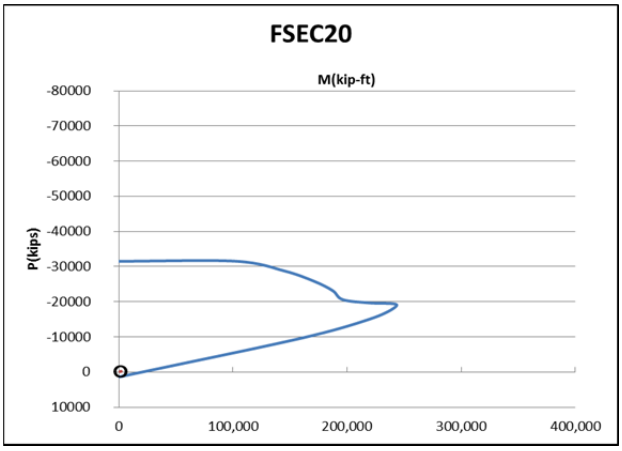
FSEC20
M(kip-ft)
P(kips)
-80000
-70000
-60000
-50000
-40000
-30000
-20000
-10000
0
10000
0
100,000
200,000
300,000
400,000